



Faculty of Health & Life Sciences

Leicester School of Pharmacy

Synthesis and Biological Evaluation of
Chalcone Scaffolds as Potential
Antiangiogenic Agents.

Pharmacology with medicinal chemistry

A thesis submitted in partial fulfilment of the requirements for the
degree of Doctor of Philosophy

By: Aamir Hussain (BSc) Hons

2018

Abstract

Introduction/Aim:

Angiogenesis is an integral part of tumour growth and development. Endothelial cell proliferation, migration and differentiation are the main hallmarks of this physiological process. From this, the use of antiangiogenic therapy have brought about a range of licensed FDA approved agents (that are also used by the NHS), that aim to regress tumour induced angiogenesis. However, issues such as: drug resistance, evasion and poor efficacy have limited the use of antiangiogenic therapy as a main stake in anti-cancer therapy. The need for multi-targeted or combinatorial therapies are ever more needed to enhance the current use of these drugs.

Therefore, in an attempt to identify novel compounds that exhibit antiangiogenic activity, a group of 1-3-diphenylpropenones (chalcones) were designed, synthesised and biologically evaluated using AH1 (2-chloro-2'5'-dihydroxychalcone) as the parent compound.

Methods:

Chalcones were synthesised using variations of the Claisen-Schmidt condensation reaction, to develop a compound library based on AH1 (the parent compound). Thereafter, using HUVECs as an angiogenesis model, the effects of the compounds on HUVEC proliferation and migration were evaluated. This was carried out using the MTT cell proliferation assay and the wound healing "scratch" assay. Therein mechanistic evaluation was carried via gel electrophoresis and chemiluminescence western blot.

Main findings:

Structure activity relationships (SARs) studies identified, that novel compounds AH9 (2-bromo-2'5'-dihydroxychalcone) and AH12 (2-nitro-2'5'-dihydroxychalcone) were shown to exhibit strong anti-proliferative activity along with AH1. Other synthesised derivatives containing different functional groups such as, alkoxy, halogen and methyl did not exhibit similar activities to AH1. The culmination of structure activity relationship suggested that 2'5'-dihydroxy moiety was important to the observed activity only in conjunction with 2-chloro or now 2-bromo substitution on the other phenyl ring. Due to AH9's better drug likeness over AH12, AH9 and AH1 were taken forward as the lead candidates.

Anti-migratory analysis of lead candidates and licensed drug Sorafenib were conducted against HUVECs. AH9 ($p < 0.0007$) was shown to exhibit significantly more potent inhibitory effects on endothelial migration than AH1 ($p = 0.19$) and Sorafenib ($p = 0.41$) over the 8 hour time course study when compared to the untreated control. Mechanistic evaluation identified that AH9 could be exerting its anti-proliferative and potent anti-migratory activity via inhibiting ERK kinase phosphorylation, this was seen at $10\mu\text{M}$ ($p < 0.0001$).

Discussion and conclusion:

To summarise, anti-proliferative and potent anti-migratory activity, towards HUVECs, of a novel molecule AH9 have been identified showing significant effects against two hallmarks of the angiogenesis cascade. AH9 presents a strong case as an agent capable of being developed as an angiogenesis inhibitor for anti-angiogenic therapy.

Communications

Conference and Abstract proceedings

Hussain, A., Fretwell, L., Ruparelia, K., Beresford, K., & Singh, H. (2018). Effects of novel chalcone derivatives on human endothelial cell proliferation and migration. *Cardiovascular Research*, 114(suppl_1), S50–S51. <https://doi.org/10.1093/cvr/cvy060.146>

Hussain, A., Grootveld, M., Arroo, R., Beresford, K., Ruparelia, K., & Fretwell, L. (2016). Effects of novel phenolic chalcone derivatives upon MCF-7 Cell viability. *Planta Medica*, 81(S 01), S1–S381. <https://doi.org/10.1055/s-0036-1596927>

Hussain, A., Wright, J., Ruparelia, K., & Fretwell, L. (2015). Effects of Novel Chalcone Derivatives upon H9c2 and MDCK Cell Viability. *E-Journal British Pharmacological Society*. Retrieved from <http://www.pa2online.org/abstracts/vol13issue3abst163p.pdf>

Poster presentation

Stop cancer? Cut off its blood supply | Graduate School Research Poster Competition
1st Prize winner, De Montfort University

Development of antiangiogenic compounds | School of Allied Health Research conference, Oral presentation 1st prize winner, De Montfort University

Effects of chalcone derivatives on HUVEC proliferation | School of Allied Health Research conference, Poster presentation runner up, De Montfort University

Dual anti-endothelial and anti-cancer effects of novel halogenated chalcones (joint collaboration with Dr H Singh, Dr M Evans and Mr I Alhabib). | Royal Society of Biology East Midlands Branch Postgraduate poster competition, De Montfort University

Acknowledgements

To start with, I would like to express my heartfelt gratitude to my supervisors. I appreciate everything they have done for me to help me develop as a researcher, the guidance in research the help in writing that Dr Fretwell contributed a lot in as by this hidden joke buried in this particular sentence that I am sure she will pick it up on and admire. A big thanks to Dr Harprit Singh for agreeing to come on board to help push the work without him it would have been likely I would have left my PhD. A real appreciation Dr Beresford for his patience with my medicinal chemistry learning and development, I would have severely struggled otherwise. Thank you to Dr Ruparelia for his support over the years even before I started (NMR door knock).

It has been a long journey at DMU as a student, but a life changing one. I could not imagine the amazing people I have met when I first started as an undergraduate to now, both staff colleagues and fellow students. Students AG, Emmanuelle, John, Leo, Pushpa, Bhish, Christina, Bhaskar and Hesham. Special thanks to Jay for all the help setting up the cell culture and teaching me “the ways of the western blot”, also to Simon for all the medicinal chemistry advice! Special mention to Ibrahim and Abid two of my mentors for the past several years I cannot thank them enough for their support, company and advice through the toughest of times.

I would like to thank all the chemistry team in HLS for the help and support, always treating me so well and made me feel part of the family. A mention to Peter Chimkupete for his help early on in my teaching career, it meant a great deal to me. Thank you to Andy Morris for his support on my external projects outside of research.

Finally none of this would have been possible with the lifelong support of my family. I want to take this opportunity to thank my parents who sacrificed so much to raise me, my brothers who have been my guardians since I was born always pulling me up when I needed them the most, my sister in law and her desire to help in any way she can meant so much. This is a testament to everything you all sacrificed to help me – this achievement is as much all of yours as it is mine.

My greatest thanks goes to my mother. You raised me, been patience with me, supportive of me no matter what the circumstance. We made a deal “if you don’t give up I won’t give up” and so I didn’t no matter what. This is for you so you can be proud of the person I have become. I did what many thought was not possible. People laughed at us, now you have three sons who have achieved beyond expectations.

This thesis is dedicated with love to my parents

The late nights in the laboratory, the 70 hour work weeks have all been a part of a huge chapter in my life, which has set up a strong foundation for me to build on. I hope whoever gets a chance to read this can sense the sheer dedication that went into this PhD under the most difficult of situations. I hope it serves as an inspiration for the next generation to have hope on what is truly possible in life.

“We all have a potential that far exceeds what our minds can imagine, what we lack is the belief that we have it and the desire to utilise it”

“Always be grateful for what you have but never be satisfied with what you can achieve”

“PhD: A four-year boxing match. You only get to throw one punch. So wait patiently till the end and make it count”

*“You were never born to just live life,
You were born to change it,
You were never born to just live on this planet
You were born to improve it,”*

Aamir Hussain

Abbreviations

AH1	2-chloro-2'5'-dihydroxychalcone
AH9	2-bromo-2'5'-dihydroxychalcone
Akt	Protein kinase B
AMD	Age-related macular degeneration
AMPK	adenosine monophosphate-activated protein kinase
ANG-1	Angiopoietin 1
ANG-2	Angiopoietin 2
ANOVA	Analysis of variance
ATR	Attenuated total reflectance
Bax	Bcl-2-associated X protein
Bcl-2	B cell lymphoma 2
BDF-1	A cross between female C57BL/6 and male DBA/2.
BF ₃ O	Boron trifluoroetherate
bFGF	basic fibroblast growth factor
Bim	Bcl-2-like protein 11
CAM	Chick Chorioallantoic Membrane
CDCl ₃	Dueterated chloroform

CDK-2	Cyclin-dependent kinase 2
COX-1	Cyclooxygenase-1
COX-2	Cyclooxygenase-2
d6-DMSO	Dueterated dimethyl sulphoxide
DCM	Dichloromethane
DMSO	Dimethyl sulphoxide
DPhP	Diphenylpropen-2-one
DTT	Dithiothreitol
ECL	Enhanced chemiluminescence
EGF	Epidermal growth factor
ERG	Electron releasing group
ERK	Extracellular signal-regulated kinase
EtAc	Ethyl Acetate
EtOH	Ethanol
EWG	Electron withdrawing group
FBS	Foetal bovine serum
FDA	Food and drug administration
FGF	Fibroblast growth factor
FTIR	Fourier transform infrared spectroscopy

HCL	Hydrochloric acid
HMEC-1	Human microvascular endothelial cells
HPLC	High pressure liquid chromatography
HRMS	High resolution mass spectrometry
HUVECs	Human umbilical venous endothelial cells
KOH	Potassium hydroxide
LiOH	Lithium hydroxide
LSGS	Low serum growth supplement
m.p.	Melting point
MEK	Mitogen-activated protein kinase
MeOH	Methanol
MgSO ₄	Magnesium sulphate
MMOA	Molecular mechanism of action
MMP	Matrix metalloproteinases
MOM	Methoxymethyl ether
MS	Mass spectrophotometry
mTOR	mammalian target of rapamycin
MTT	(3-(4,5-Dimethylthiazol-2-yl)-2,5-Diphenyltetrazolium Bromide)
NaOH	Sodium hydroxide

NMR	Nuclear magnetic resonance
NO	Nitric oxide
NSCLC	Non-small cell lung cancer
p-acid	<i>p</i> -toulenesulphonic acid
PAINS	Pan-assay interference compounds
PBS	Phosphate buffer saline
PDGF	Platelet derived growth factor
PF-4	Platelet factor 4
PGI ₂	Prostacyclin
PIGF	Placental growth factor
Ppts	Pyridinium <i>p</i> -toulenesulphonate
Puma	p53 upregulated modulator of apoptosis
Q797	4-hydroxychalcone
QSARs	Quantitative structure activity relationship
RAF	Serine/threonine-specific protein kinase
RB	Retinoblastoma associated protein
ROS	Reactive oxygen species
RTKI	Receptor tyrosine kinase inhibitor
SARs	Structure activity relationships

SEM	Standard error of the mean
s-FLK-1	soluble VEGFR receptor
SOCl ₂	Thionyl Chloride
TBDMS	<i>tert</i> -Butyldimethylsilyl
TBDPS	<i>tert</i> -Butyldiphenylsilyl
THF	Tetrahydrofuran
THP	Tetrahydropyran
Tie-1	Angiopoietin 1 receptor
Tie-2	Angiopoietin 2 receptor
TIMPs	Tissue inhibitors of metalloproteinase
TLC	Thin layer chromatography
TP53	Tumour protein 53
TSP-1	Thrombospondin 1
UV-VIS	Ultraviolet-visible spectrophotometry
VEGF	Vascular endothelial growth factor
VEGFR-2	Vascular endothelial growth factor receptor 2
WHO	World health organisation
WST-1	Water soluble tetrazolium salt 1

XTT

carboxanilide

2,3-Bis(2-methoxy-4-nitro-5-sulfophenyl)-2H-tetrazolium-5-

Contents

Conference and Abstract proceedings.....	4
Poster presentation	4
Chapter 1: Introduction	22
1.1 Cancer.....	23
1.1.1 Hallmarks of Cancer	24
1.2 The Angiogenesis process.....	31
1.2.1 Targeting Angiogenesis	34
1.2.3 VEGF and VEGFRs.....	37
1.2.4 Non-VEGF Modulators of Angiogenesis.....	45
1.3 Antiangiogenic Therapy.....	48
1.3.2 Limitations with Current Licensed Antiangiogenic Agents	51
1.3.3 Antiangiogenic Drug Resistance.....	54
1.4 Preclinical design and development of small molecular anticancer drugs	57
1.4.1 The drug discovery process.....	57
1.4.2 Analogue based drug design and development.....	61
1.5 Chemical Scaffolds as Antiangiogenic Compounds	62
1.5.1 Chalcones	63
1.5.2 Reported Antiangiogenic Activities of Simple Molecular Chalcones	64
Chapter 2: Aims and objectives	69
2. Aims and Objectives:	70
Objectives:.....	71
Chapter 3: Synthesis of chalcone derivatives.....	72
3.1 Introduction.....	73
3.1.1 Synthetic approaches to chalcone synthesis.....	76
3.2 Results and Discussion:	84
3.2.1 Base catalysis for hydroxychalcone synthesis with THP protection step	84
3.2.2 Base catalysis for hydroxychalcone synthesis under pressurised conditions.....	90
3.2.3 Acid catalysis for hydroxychalcone synthesis using thionyl chloride	92
3.2.4 Acid catalysis for hydroxychalcone synthesis using sulphuric acid.	93
3.2.5 Base catalysis for methoxychalcone synthesis.....	95
3.3 Conclusion	97

Chapter 4: Screening and biological evaluation of the synthesised chalcone derivatives	98
4.1 Introduction:	99
4.2 Results and discussion:	102
4.2.1 Anti-proliferative activity:	102
4.2.1.1 Substituent changes of the B ring 2 position to assess the importance of the chlorine group in AH1 (series 1)	103
4.2.1.2 Position changes of the A ring hydroxyl groups to assess the importance of 2'5'-dihydroxy moiety of AH1 (series 2)	106
4.2.1.3 Assessing part derivatives of AH1 to see what substituents are key to the activity observed (series 3)	108
4.2.1.4 Position changes of the halo group on the B ring to further confirm the importance of the halo group at B ring 2 position (series 4)	111
4.2.1.5 Replacement of hydroxyl groups with a methoxy group to assess the importance of hydrogen donation on the A ring (series 5)	113
4.3 Further investigation of AH21 and AH21b (Series 6)	117
4.4 Conclusion:	122
Chapter 5: Anti-migratory analysis of lead candidates AH1 and AH9 against HUVECs	124
5.1 Introduction:	125
5.2 Results and discussion:	128
5.2.1 Endothelial cell migration – wound healing assay	128
5.2.2 Preliminary study to identify optimal concentration for the wound healing assay	129
5.2.3 AH1	131
5.2.4 AH9	135
5.3 Conclusion	138
Chapter 6: Pharmacological evaluation of AH9	140
6.1 Introduction:	141
6.2 Results and Discussion:	143
6.2.1 Experimental design for analysis of protein expression	143
6.2.2 AH9's effects on Erk 1/2 expression and phosphorylation	144
6.2.3 AH9's effects on VEGFR-2 expression stimulated with VEGF	146
6.2.4 Overall discussion on mechanistic studies	148

Chapter 7: Conclusion and Future Directions	151
7.1 Conclusion:	152
7.2 Study limitations	153
7.3 Future directions.....	154
Chapter 8: Experimental	156
8.1 Experimental:	157
8.2 General chemical procedures (Materials & Methods)	157
8.2.1 Reagents	157
8.2.2 Equipment:	157
8.2.3.1 Experimental protocols:	159
8.2.3.2 Chalcone synthesis method 1 (Nam et al, 2003).....	159
8.2.3.3 Chalcone synthesis method 2 (acid catalysis SOCl ₂) modification of (Petrov, Ivanova and Gerova, 2008):.....	168
8.2.3.4 Chalcone synthesis method 3 (acid catalysis H ₂ SO ₄) modification of (Konieczny <i>et al.</i> , 2007).....	169
8.2.3.5 Chalcone synthesis method 4 (Detsi <i>et al.</i> , 2009).....	172
8.3. General biology procedures	178
8.3.1 Materials.....	178
8.3.1.1 Cell culture	178
8.3.1.2 MTT assay.....	178
8.3.2.2 Western blot analysis	178
8.3.2 Methods:.....	181
8.3.2.1 General cell culture:	181
8.3.2.2 Preperation of compound solutions.....	181
8.3.2.3 MTT cell proliferation assay (72 hr).....	181
8.3.2.4 Cell stimulation and lysate preperation.....	182
8.3.2.5 Gel electrophoresis.....	182
8.3.2.6 Transfer of proteins and staining western blotting.....	183
8.3.2.7 Detection	183
8.3.2.8 Scratch assay	184
8.3.2.9 Statistical analysis	184
Chapter 9: References	185

Table of Figures

Figure 1 Current targets in anticancer therapy.....	24
Figure 2 Forms of angiogenesis.	31
Figure 3 Angiogenic stimulators and inhibitors.....	33
Figure 4 the angiogenic switch.	35
Figure 5 Sprouting angiogenesis.....	36
Figure 6 A diagrammatic summary of the RAS RAF ERK pathway.	39
Figure 7 VEGF isoforms and VEGFR receptors.	40
Figure 8 VEGF dependency in stages of tumour growth.....	42
Figure 9 Normal and tumour vasculature.	43
Figure 10 General mechanism of FDA approved antiangiogenic therapies (Folkman, 2007).	48
Figure 11 mechanisms to inhibit VEGF signalling:.....	53
Figure 12 Two modes of resistance seen after exposure to antiangiogenic therapy demonstrating adaptive and non-responsive evasions by tumours adapted (Bergers and Hanahan, 2008).	54
Figure 13 A diagrammatic representation of how a drug discovery cycle encompasses 4 key areas.....	57
Figure 14 A general process in a drug discovery programme.	59
Figure 15 L86-8276 (dechloroflavopiridol) conversion to flavopiridol, adapted form (Hernandes <i>et al.</i> , 2010).....	61
Figure 16 Basic scaffold structures of chalcone. Chemical structure of 1,3-diphenylpropenones.	62
Figure 17 2-chloro-2'5'-dihydroxychalcone.....	65
Figure 18 4-hydroxychalcone (Varinska <i>et al.</i> , 2012)	66
Figure 19 Mono and dihydroxychalcones (Karki <i>et al.</i> , 2012).....	67
Figure 20 2'-hydroxy-4'-methoxychalcone (Y. Lee <i>et al.</i> , 2006).....	67
Figure 21 7-methyl-quinoyl,2'5'-dichlorothienylchalcone (Rizvi <i>et al.</i> , 2012)	68
Figure 22 3-bromo-2'4'-dimethoxychalcone (left) and 2',2,4-trimethoxychalcone (right) (Bertl <i>et al.</i> , 2004)	68

Figure 23 Characteristic two one proton doublets with a large coupling constant (12-18 Hz) found for the trans chalcone configuration	86
Figure 24 (A) AH9 in EtAc solution. (B) UV-vis spectra of AH9 showing lambda max = 308nm. (C) AH9 HPLC spectra conducted at the lambda max 308 gathered by UV-VIS.	87
Figure 25 Chemical structures of the MTT reagent and Formazan product.	100
Figure 26 Chemical structure of AH1 (2-chloro-2'5'-dihydroxychalcone). The parent compound for this study.	101
Figure 27 the effects of all the chalcone derivatives on HUVEC viability.	116
Figure 28 Synthesisg analogues of AH21 and AH21b to form 2'4'-dimethoxy derivatives AH22 and AH22a.	117
Figure 29 LD ₅₀ plots of AH1 AH9 and Sorafenib showing their anti-proliferative activity against HUVECs after 72 hour exposure.	121
Figure 30 Chemical structures of lead chalcones AH1 and AH9.	125
Figure 31 A abstract diagrammatic representation of wound closure in a wound healing assay over 8 hours.	128
Figure 32 The effects of AH1 on HUVEC migration:	130
Figure 33	132
Figure 34 Figure Effects of AH1 on HUVEC migration across 8 hours.	134
Figure 35 Effects of AH9 on HUVEC migration across 8hrs.	137
Figure 36 Chemical structures of AH1 and AH9.	138
Figure 37 Effects of AH1, AH9 and Sorafenib (3 μM) on HUVEC migration, over 8 hours.	139
Figure 38 membrane captures of AH9's effect on ERK phosphorylation.	144
Figure 39 effects of AH9 on ERK phosphorylation.	145
Figure 40 membrane captures of AH9's effect on VEGFR-2 expression.	146
Figure 41 effects of AH9 on VEGFR-2 expression.	147
Figure 42 preliminary mechanism of action of AH9.	150

Table of Tables

Table 1 Possible molecular mechanisms for the adverse drug reactions of angiogenesis inhibition. (Adapted from (Verheul and Pinedo, 2007)).....	52
Table 2 Possible solutions to counteract antiangiogenic drug resistance and evasion. ..	56
Table 3: 2'5'-dihydroxychalcones EC ₅₀ values against cancer cell lines and HUVECs. .	65
Table 4 Brief rationales as to the compounds designs for this study	75
Table 5 Compounds synthesised via method 1	88
Table 6 Compounds synthesised via method 1 continued	88
Table 7 Compound synthesised via the acid catalysis route using thionyl chloride.....	92
Table 8 Compounds synthesised via the acid catalysis route using sulphuric acid.	94
Table 9 Compounds synthesised via the base catalysis route using either NaOH, LiOH or Ba(OH) ₂	95
Table 10 Summary of structure and biological activity for Series 1	105
Table 11 Summary of structure and biological activity for Series 2	107
Table 12 Summary of structure and biological activity for Series 3	110
Table 13 Summary of structure and biological activity for Series 4	112
Table 14 Summary of structure and biological activity for Series 4	115
Table 15 Summary of structure and biological activity for Series 6	119
Table 16 LD ₅₀ values of AH1 AH9 and Sorafenib, determined using HillSlope's nonlinear regression.	120
Table 17 Showing the average width of wounds (µm) for each gathered from three independent experiments (untreated control, AH1 3µM, 1µM and Sorafenib 3µM) with time points ± SEM. * = p < 0.05 vs time matched untreated control (statistical analysis carried out by one way –ANOVA followed by Tukey-Kramer post hoc t test for multiple comparisons).	133
Table 18 showing the % migration of the untreated control, AH1 (3µM) and Sorafenib (3µM) after 8hrs of incubation.....	133
Table 19 showing the average width of wounds (µm) for each gathered from three independent experiments (untreated control, AH9 3 µM, 1 µM and Sorafenib 3 µM) with time points ± SEM; * = p < 0.05 vs time matched untreated control (statistical analysis	

carried out by one way –ANOVA followed by Tukey-Kramer post hoc t test for multiple comparisons).	136
Table 20 showing the % migration of the untreated control, AH9 (3 μ M) and Sorafenib (3 μ M) after 8hrs of incubation.....	136
Table 21 Buffers and solutions	179
Table 22 ECL solution	179
Table 23 Antibodies	180

Table of Schemes

Scheme 1 Different chalcone synthesis routes:.....	76
Scheme 2 Base catalysed Claisen-Schmidt reaction mechanism.....	78
Scheme 3 Acid catalysed Claisen-Schmidt reaction mechanism.....	81
Scheme 4 Method 1 of synthesising dihydroxychalcones (Nam et al., 2003)	84
Scheme 5 Cyclisation of the 2'5'-dihydroxychalcone to a hydroxyl-dihydroflavone if left to react further under the KOH/EtOH reaction conditions in a sealed tube (Stoyanov <i>et al.</i> , 2002).	90
Scheme 6 Method 2 of synthesising dihydroxychalcones (Konieczny <i>et al.</i> , 2007)	93
Scheme 7 Method to synthesise dimethoxychalcone (Detsi <i>et al.</i> , 2009).....	95

Chapter 1: Introduction

1.1 Cancer

Cancer was the second leading cause of death worldwide (8.8 million) in 2015 (WHO, 2018). Based on the current trends of the major cancers worldwide, prevalence of new cases will increase to 23.6 million by 2030, an increase of 68% compared to 2012 (Bray *et al.*, 2012; Ferlay *et al.*, 2015). According to a study by Laudicella and colleagues in 2010, cost of the four main cancers on the NHS was £1.5 billion (Laudicella *et al.*, 2016).

Cancer or tumours are defined as “abnormal cells dividing in an uncontrollable fashion” (Yu and Jove, 2004). Tumours are the result of uncontrolled cell proliferation. They can arise as a result of tumour suppressor genes being inactivated or tumour growth genes being overexpressed. These mutations can be the result of inherited or environmental conditions. Only 5-10% of cancer are the result of an inherited genetic defect (Anand *et al.*, 2008; Roukos, 2009). The remaining 90-95% can be the consequence of several environmental triggers such as: smoking, diet, lifestyle, stress, infections, radiations and pollutants (Anand *et al.*, 2008). The Knudson two hit hypothesis (Knudson, 2001) is a model that proposes that two “hits” are required for tumour development. The “first hit” is a genetic predisposition to develop a particular type of cancer, but, to trigger tumourigenesis, the “second hit” is needed and can arise from an environmental factor whether acute or chronic (Knudson, 2001).

Significant amounts of research have gone into better understanding tumour development from a molecular biological standpoint (Vander Heiden and DeBerardinis, 2017). Many views have been put forward on the key components needed for tumour development such as: causes, molecular environments, key signalling molecules, mutations and many more (Cooper, 2000; Hanahan and Weinberg, 2011). It is because of this type of research that more targeted anti-cancer therapies have been developed (Weinstein and Joe, 2006).

1.1.1 Hallmarks of Cancer

The hallmarks of cancer are a list of fundamental steps in cancer development. They provide therapeutic targets for anti-cancer drugs, as illustrated in Figure 1.

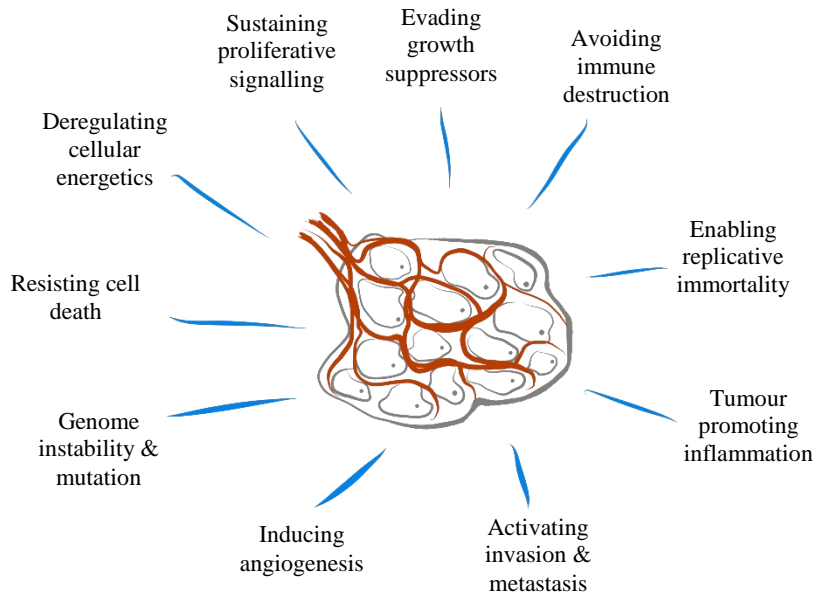


Figure 1 Current targets in anticancer therapy.

The 10 hallmarks illustrated above provide a key set of targets on which anti-cancer agents have been modelled from. These hallmarks enable the use of different form of anti-cancer studies *i.e.* anti-mitotic to anti-angiogenic agents. Adapted from (Hanahan and Weinberg, 2011).

1.1.1.1 Sustaining Proliferative Signalling

Sustained chronic proliferation is an integral part of tumour survival (Feitelson *et al.*, 2015). The body maintains homeostasis of growth signals to ensure normal regulated tissue growth. When this is deregulated in tumours, uncontrolled proliferation can occur. Tumour cells can also release elevated levels of growth factors, causing autocrine proliferative stimulation (Heldin, 2012).

1.1.1.2 Evading Cell Growth Suppressors

Under normal conditions, tumour suppressor genes control cell growth (Vogelstein and Kinzler, 2004). Two suppressor genes, that encode RB (retinoblastoma-associated) and TP53 (tumour protein 53) proteins control cell growth functions, whether it is proliferation, activating senescence or triggering apoptosis (Hanahan and Weinberg, 2011). Both proteins operate in different ways to maintain normal cell division; RB protein transduces extracellular signals that inhibit growth, whereas TP53 protein responds to intracellular signals stemming from cell stress or abnormalities (Sherr and McCormick, 2002).

1.1.1.3 Resisting Cell death

Programmed cell death by apoptosis is a well-established natural defence against tumour development (Evan and Littlewood, 1998; Lowe, Cepero and Evan, 2004; Adams and Cory, 2007). The mechanism of apoptosis is governed by upstream regulators and downstream effectors (Adams and Cory, 2007). These regulators can be further categorised into receiving and transmitting extracellular and intracellular signals. Together or independently these pathways activate proteases, usually caspases that cause a cell wide cascade of proteolysis and ultimately cell death. Adams and Cory (2007) also stated that the “apoptotic trigger” that relays the signals between the regulators and effectors is controlled by neutralising pro and antiapoptotic proteins belonging to the Bcl-2 family (Lindsten *et al.*, 2000). Bcl-2 and similar proteins like Bcl-x and Bcl-w are inhibitors of apoptosis, they work mostly by suppressing Bax and Bak proapoptotic proteins (Adams and Cory, 2007).

Tumour cells can evolve to evade these regulatory mechanisms, *i.e.* avoiding programmed cell death, most commonly through the loss of TP53 tumour suppressor function (Hanahan 2011). Other possible routes of evasion include increasing the expression of antiapoptotic regulators like Bcl-2 and surviving signals (Igf1/2), or decreasing proapoptotic controllers such as Bax, Bim, Puma (Hanahan and Weinberg, 2011). Autophagy is another physiological process that can both facilitate and suppress tumour growth (White, 2012). It is a physiological “housekeeping” mechanism that maintains organelle function and minimises build-up of toxic cellular waste. Autophagy can support tumour growth through intracellular recycling of the cellular waste, suppression of p53 protein and upregulation of mitochondrial function (White, 2015).

1.1.1.4 Enabling Replicative Immortality

It is a widely accepted notion that normal functioning cells have a limited number of continuous cell cycles (Shay and Bacchetti, 1997; Naasani, Seimiya and Tsuruo, 1998; Rudolph *et al.*, 1999; Harley, 2008; Hainaut and Plymoth, 2013; Yaswen *et al.*, 2015). There are two physiological processes that ultimately prevent unlimited replication. These are cell senescence, a permanent state of non-proliferative viability and crisis which ultimately involves cell death. The general process dictates that as numerous cell cycles occur, a point comes where senescence is triggered and thereafter any cells that remain proliferative enter the crisis phase where most cells die. Similar to the growth of antibiotic-resistant bacteria, a small population of cells survive this two part process. Therefore by evading cell senescence and crisis tumour cells can become immortalised (Hanahan and Weinberg, 2000, 2011).

Several reports (Counter ' *et al.*, 1992; Hemann *et al.*, 2001; Bailey and Murnane, 2006) support the concept that telomeres, which progressively become shorter over cycles, lose their ability to stabilise chromosomal DNA. Telomeres, are protective caps at the end of DNA strands. Hanahan and Weinberg (2011) argued the degree and rate of “telomere shortening” could be viewed as a biological clock device to assess the lifespan of cells (Hanahan and Weinberg, 2011). Telomerase, a specific DNA polymerase, can catalyse the process of adding telomeric segments to the ends of telomeric DNA. This is a crucial process to maintain cell viability over continuous cell cycles (Harley, 2008). A mechanism for maintaining telemetric DNA at high enough levels to avoid triggering cell senescence or crisis is via upregulating the amount of telomerase available (Hanahan and Weinberg, 2011). Therefore inhibiting telomerase activity could be seen as a potential anti-cancer avenue (Harley, 2008)

1.1.1.5 Activating Invasion and Metastasis

In tumours, invasion and metastases can be viewed as a multistep process referred to as the invasion- metastasis cascade (Talmadge and Fidler, 2010). As tumour cell develop, cell to cell adhesion molecules can be disrupted allowing clusters of tumour cells to dissociate from the primary tumour into nearby capillaries or lymphatic vessels. This can increase the likelihood of metastasis (Martin *et al.*, 2013). E-cadherin, a key adhesion molecule, has been shown to be an antagonist to invasion and metastasis, leading to reports of it being downregulated in human carcinomas (Cavallaro and Christofori, 2004; Berx and van Roy, 2009).

1.1.1.6 Inducing Angiogenesis

Angiogenesis is the formation of new blood vessels from pre-existing vasculature, it is vital in normal physiological processes such as healing of wounds, reproduction, growth and development (Folkman, 1995). It has been recognised that angiogenesis is a major factor in many severe and debilitating diseases from stroke and cardiovascular disease, to age related macular degeneration (AMD) and cancer (Carmeliet and Jain, 2000). Angiogenesis is regulated by precise balance between angiogenic stimulatory and inhibitory factors (Li *et al.*, 2012). Disruption of this balance can contribute to tumour development through proliferation of tumour vasculature (Vasudev and Reynolds, 2014). This section will be further expanded on later (see Section 1.2 onwards).

1.1.1.7 Emerging hallmarks and characteristics

There are several core developments in cancer biology that have gained attention as targets for anti-cancer therapy. In turn these developments lead to qualities the tumour can then possess. Hanahan and Weinberg (2011) highlighted the following developments (Hanahan and Weinberg, 2011).

Spontaneous mutations

Due to the maintenance system that governs repairing faulty DNA in cells, spontaneous mutations occur rarely. But when they do occur, these mutations do not just affect cell proliferation directly but also energy metabolism. The factors that affect fuelling cells can be reprogrammed via these function-altering mutations to essentially accelerate tumour cell division (Korkola and Gray, 2010).

Immunoediting

Immunoediting is one the key ways in which tumours evade the immune system (Vinay *et al.*, 2015) Other forms of evasion include, tumours presenting weak antigens on the cell surface to avoid immune recognition, or increasing the expression of immunoregulatory molecules to develop an immunosuppressive tumour environment (Muenst *et al.*, 2016).

Tumour promoting inflammation

It has been readily known that much of the inflammation occurring in a tumour environment contributes to tumour progression, from a preliminary neoplastic tissue to a fully formed malignant tumour (Visser, Eichten and Coussens, 2006; Qian and Pollard, 2010). This ability of immune cells, in particular innate immune cells to enhance tumour

progression can contribute to tumours evading immune destruction. Chronic inflammation contributes to tumour progression by causing DNA damage. NF- κ B has been known to be a key tumour promoter in chronic inflammatory environment by inhibiting apoptosis of cells destined to be tumourigenic (Karin and Greten, 2005).

1.2 The Angiogenesis process

There are two known types of angiogenesis, sprouting and intussusceptive (Adair and Montani, 2010). Although both occur in nearly all tissues types, sprouting angiogenesis is more readily occurring (Hillen and Griffioen, 2007). Intussusceptive angiogenesis, also known as splitting angiogenesis tends to occur quite rapidly. It differs to sprouting angiogenesis as it is more about reorganisation of existing vasculature (splitting blood vessels into two) as opposed to endothelial cell migration and proliferation (Kurz, Burri and Djonov, 2003).

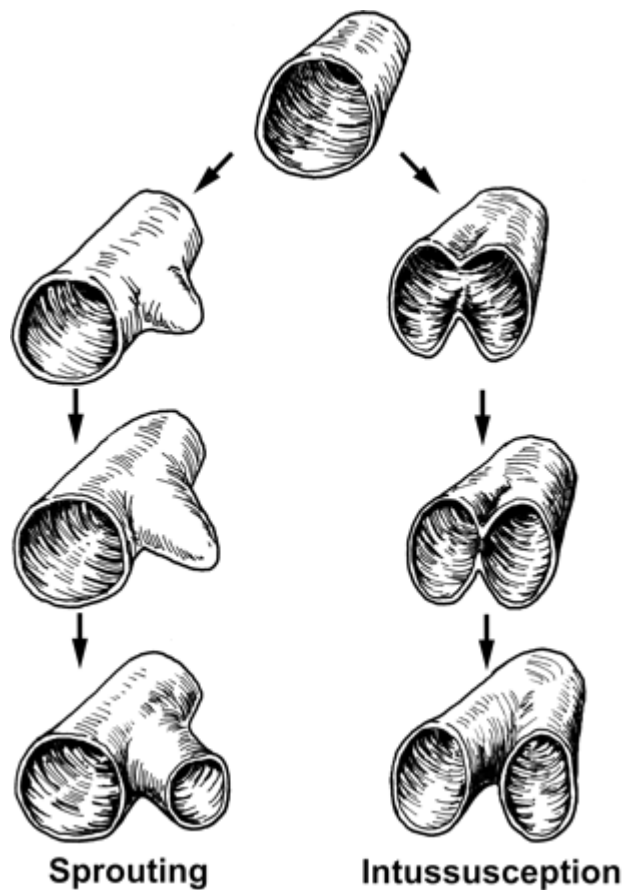


Figure 2 Forms of angiogenesis.

A representation showing the difference between sprouting and intussusceptive angiogenesis. Sprouting angiogenesis shows the new sprouting vessel maturing and developing from the original vessel similar to a branch extending from a tree. Intussusceptive angiogenesis looks at forming two blood vessels by splitting one vessel into two. Figure adapted from (Prior, Yang and Terjung, 2004)

Upon stimulation by a pro-angiogenic signalling mediator (*e.g.* VEGF), endothelial cell: sprouting, proliferation, migration and differentiation can occur as described below (Klagsbrun and Moses, 1999; Tan *et al.*, 2003; Adams and Alitalo, 2007).

1) Tip cell selection from successful sprouting cells

Sprouting cells exposed to the highest concentrations of VEGF become the tip cell to lead the angiogenesis process.

2) Activated endothelial cells secrete matrix metalloproteinase (MMPs)

Basement membrane degradation occurs via MMPs and other extracellular proteinases to provide space for the angiogenic vessel to migrate.

3) Endothelial cell migration towards the angiogenic stimulus

A tip cell guides the developing capillary sprout through the extracellular matrix towards the angiogenic stimulus *e.g.* VEGF.

4) Endothelial cell proliferation and sprouting into the stromal space

Stalk cells proliferate and elongate to extend the developing vessel towards the angiogenic stimulus.

5) Formation of tight junctions and the establishment of a new basement membrane

Cell to cell adhesion molecules are recruited to form blood vessel loops that transform the premature vessel into a fully formed blood vessel.

6) Endothelial cell organisation and oxygenation

Tip cells fuse together forming a continuous lumen to allow oxygenation. Once cells are oxygenated VEGF levels return to a quiescent state.

7) Pericytes recruitment to stabilise newly formed blood vessel.

Pericytes are gathered to stabilise and mature the vessel. New basement membrane is deposited and blood flow is initiated (Hanahan and Folkman, 1996).

Figure 3 highlights the many molecules involved in the highly regulated angiogenic process.

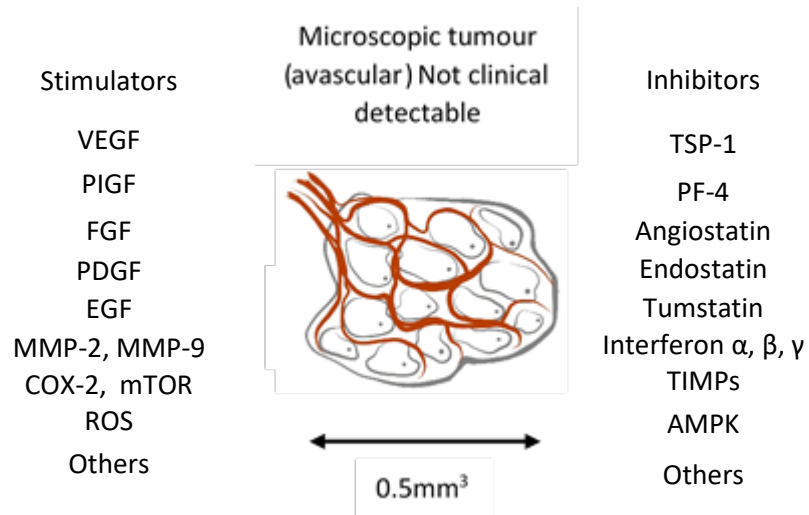


Figure 3 Angiogenic stimulators and inhibitors.

In a microscopic tumour there are many angiogenic stimulators and inhibitors (adapted from Albini *et al.* 2012) .

1.2.1 Targeting Angiogenesis

Different forms of angiogenesis exist, physiological angiogenesis, lymphangiogenesis and pathological angiogenesis (Jussila and Alitalo, 2002). Folkman (2007) described how pathological angiogenesis can persist for years, leading to the rationale of “angiogenesis-dependent diseases” (Folkman, 2007). This term explains how angiogenesis can contribute to disease progression in several diseases, including AMD, cancer, rheumatoid arthritis and atherosclerosis. As a result, angiogenesis has become a target for clinical intervention (Folkman, 1995). It was proposed by Folkman (2007) that due to angiogenesis being an integral part of a range of diseases, it could be deemed as an organising principle for disease treatment as a whole (Folkman, 2007).

For tumours, angiogenesis has a fundamental role in its growth and development, which is why this process has been targeted for anti-cancer research. Over the years many have hypothesised ways to disrupt angiogenesis in hope to starve the tumour of its blood supply and bring neoplastic cell proliferation to a halt (Ferrara and Kerbel, 2005; Folkman, 2006; Mahar *et al.*, 2009; Gotink and Verheul, 2010; Ebos and Kerbel, 2011; Vasudev and Reynolds, 2014). Weidner *et al.* (1991), found that the greater the degree of angiogenesis detected in a primary tumour, the worse the prognosis, essentially establishing a direct correlation between angiogenesis and tumour prognosis. In tumours, the balance of angiogenic stimulators and inhibitors is altered. Thus, the “angiogenic switch” is turned on (Figure 4) and the level of stimulators considerably exceeds the level of inhibitors, this is commonly seen in a tumour environment.

Bergers *et al.* (2003) highlighted that the angiogenic switch is largely seen as a rate limiting phase in the multi-stage process of carcinogenesis (Bergers and Hanahan,

2008a). VEGF overexpression is one of many ways that can shift the balance of angiogenic factors leading to tumour induced angiogenesis (Hanrahan *et al.*, 2003). This consequently causes the development of a complex arrangement of capillaries in close proximity to tumour cells (Nagy *et al.*, 2009). As a result, this allows sustainable transportation of oxygen and nutrients to increase cell growth as well as waste removal. Figure 5 highlights some of the mediators involved in tumour induced angiogenesis.

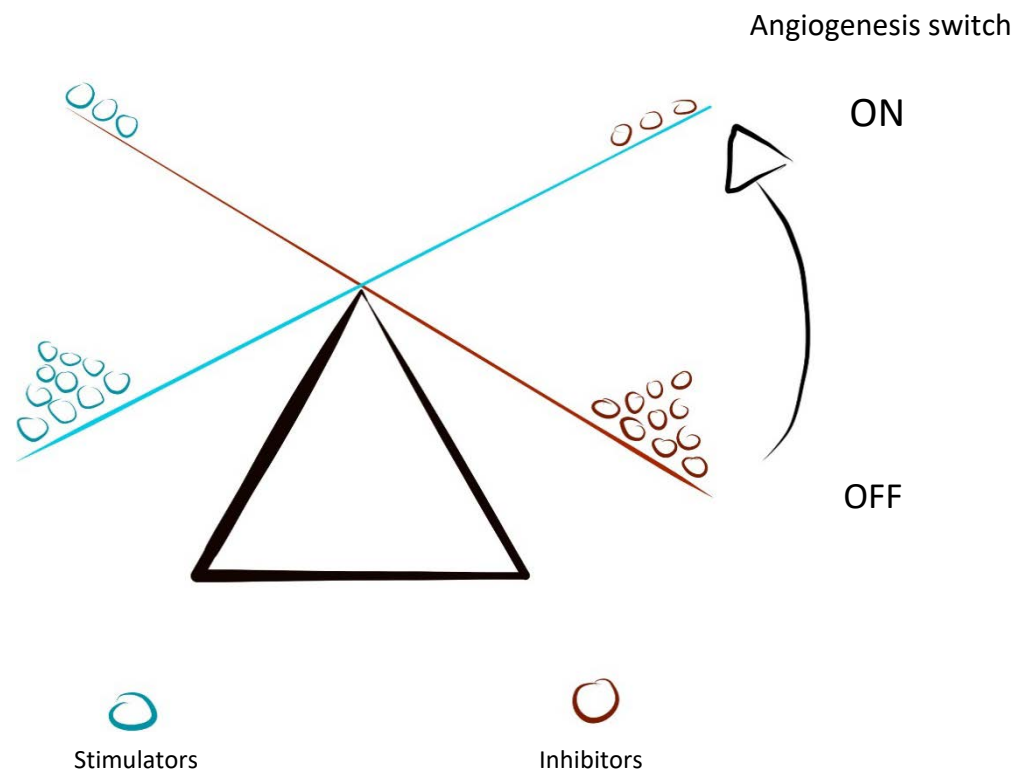


Figure 4 the angiogenic switch.

The angiogenic switch refers to when the amount of angiogenesis activators outweigh the effects of angiogenic inhibitors (Bergers and Benjamin, 2003).

Tumour induced angiogenesis can ultimately lead to an increase in the probability of tumour cells entering the bloodstream, contributed by an increased interstitial pressure causing “leaky vessels” (Jain, 2005). Factors such as, irregular shaped cells and weak cell to cell junctions also play a role in the cause of leaky vasculature. This in turn can lead to possible wide spread metastasis and poor prognosis (Ferrara and Kerbel, 2005).

Consequently, this links back to the direct correlation first discovered by Weidner *et al.* (1991) between increased angiogenesis and poor prognosis. Due to metastasis, as a result of unsuccessful clinical intervention (Plank and Sleeman, 2003), other studies have also suggested a link between angiogenesis and tumour lethality (Kim *et al.*, 1993; Bikfalvi, 1995; Bielenberg and Zetter, 2015).

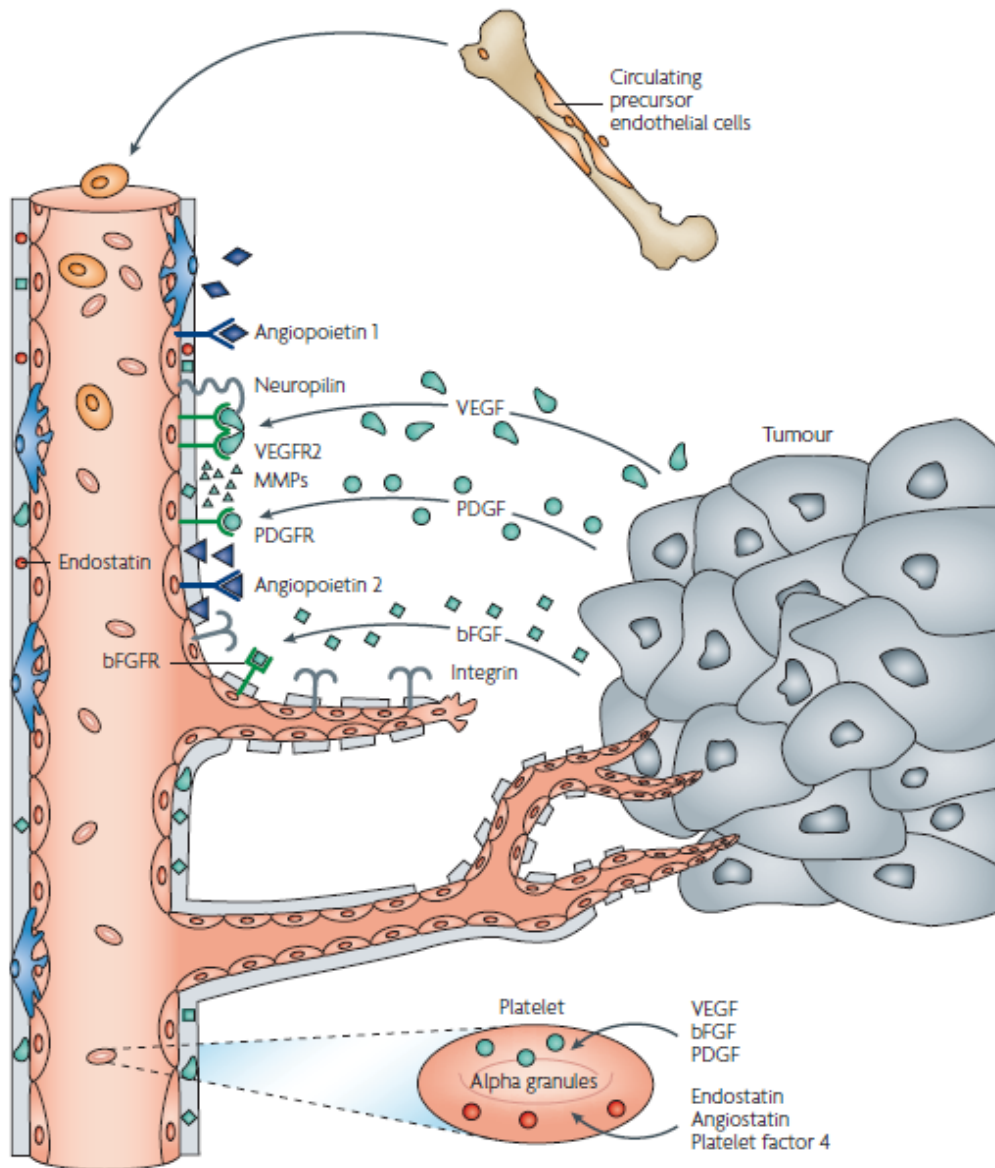


Figure 5 Sprouting angiogenesis.

In sprouting angiogenesis there are several key mediators (VEGF, PDGF, bFGF) that are released from a tumour, activating the angiogenesis process via receptor binding on an endothelial cell surface. Extracellular matrix proteinases are released by activated endothelial cells to breakdown the existing extracellular matrix to provide space for the sprouting blood vessel (Folkman, 2007).

1.2.3 VEGF and VEGFRs

Amongst the many angiogenic factors seen in Figure 3, the most potent proangiogenic factor is vascular endothelial growth factor (VEGF) (Olsson *et al.*, 2006). The VEGF family comprises of several glycoproteins known as VEGF-A, VEGF-B, VEGF-C, VEGF-D and VEGF-E. VEGF-A is more commonly referred to as VEGF, and is the centre of attention in terms of its direct importance and efficacy in stimulating VEGFR signalling pathways (Hicklin and Ellis, 2005, Rapisarda and Melillo, 2012). VEGF ligands exert their angiogenic effects by binding to VEGF receptors (VEGFRs), with three VEGFRs known to date, VEGFR-1, VEGFR-2 and VEGFR-3. These are predominantly found on endothelial cell surfaces (Neufeld *et al.*, 1999). VEGFRs are receptor tyrosine kinase (RTK) and are activated upon ligand-mediated dimerisation. The difference RTKs have to G protein couple receptors (GPCR) are that multiple cellular responses can occur from one dimerisation event of a RTK dimer, whereas only one cellular response can occur from a GPCR dimer. This is due to the multiple tyrosine molecules on the intracellular domain of a RTK (Shibuya, 2011). VEGF signalling induces migration, differentiation and increased vascular permeability of endothelial cells; these are all vital processes in angiogenesis. Figure 6 illustrates the VEGF-VEGFR-2 pathway highlighting specifically the MAPK/ERK pathway. ERK 1/2 kinases are key mediators in the signalling cascade to trigger endothelial cell proliferation and migration. The MAPK/ERK pathway contributes to a whole host of cellular processes such as: regulating T cell activation, phosphorylation of the p53 transcription factor, activation of phospholipase A2 (PLA2) in mast cells and more (Shaul and Seger, 2007). Regulation of this pathway is key to prevent tumourigenesis, as overexpression of ERK 1/2 can lead to

inhibition of apoptosis. In turn this can lead to over proliferation of cells and as a result tumour development.

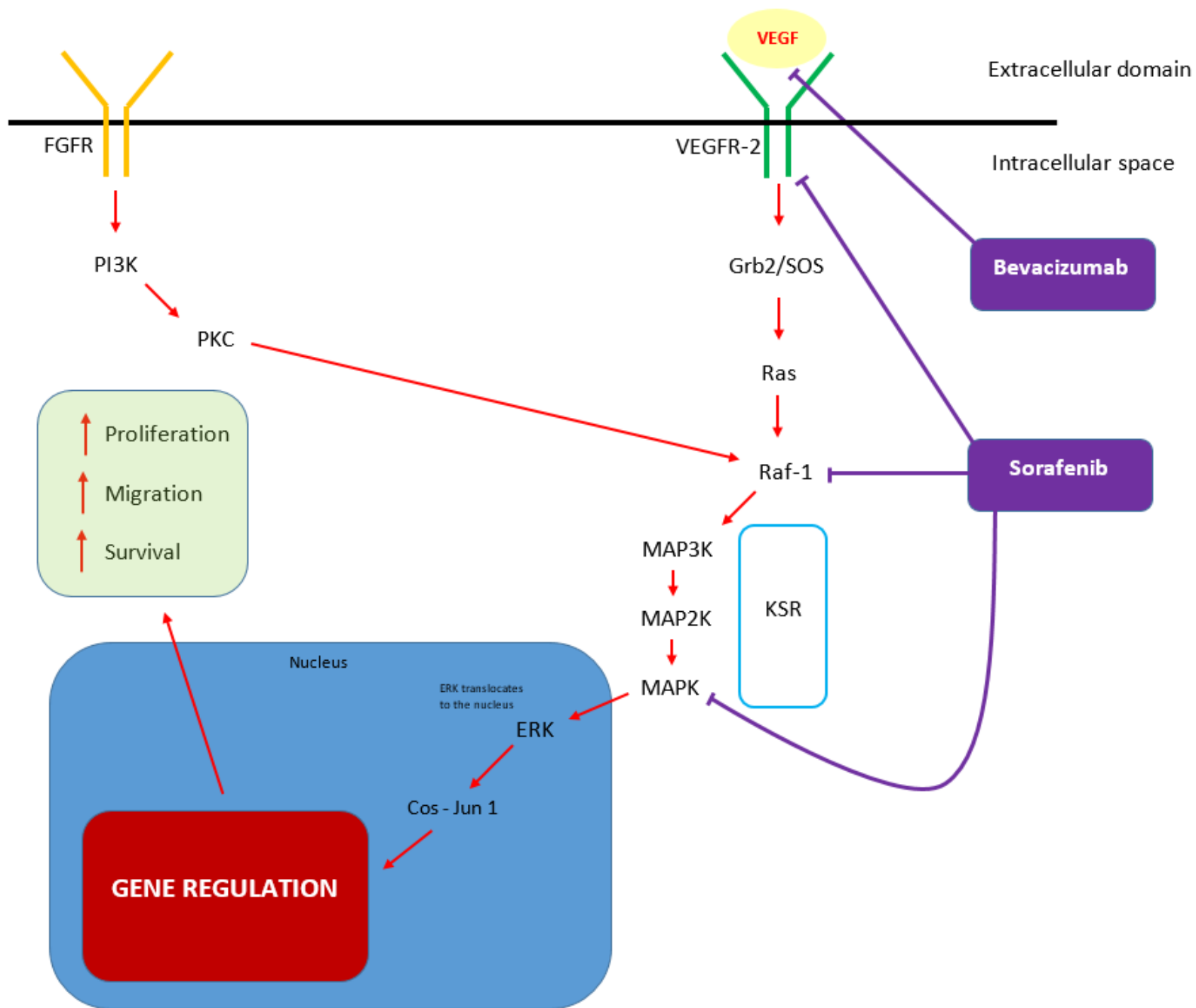


Figure 6 A diagrammatic summary of the RAS RAF ERK pathway.

The diagram illustrated the MAPK phosphorylation cascade as a result of VEGFR-2 activation by VEGF. Kinase suppressor of RAF (KSR) is used as a scaffold protein to help facilitate the phosphorylation cascade. Once complete, ERK activates the transcription factors Cos and Jun-1 which target the AP-1 promoter gene region, this in turns helps to facilitate proteomic changes to increase proliferation, migration and survival. Bevacizumab and Sorafenib represent two current antiangiogenic therapies, target the growth factor VEGF or key receptors and mediators. Raf-1 holds great importance in this pathway as it can be stimulated by both VEGFR-2 and FGFR, hence it has been a target for drug intervention (Sorafenib). (Maitland *et al.*, 2010)

VEGFR-1, is commonly expressed on endothelial cells and macrophages in adulthood (Shibuya, 2006). Amongst the three VEGFRs, VEGFR-1 is unique as it expresses two types of mRNA, a RTK and a soluble free circulating truncated protein referred to as sVEGFR-1 (s-Flk-1) (Laird *et al.*, 2002; Shibuya, 2006). Both VEGFR-1 and s-Flk-1 have been viewed as decoy receptors to VEGFR-2 essentially trapping VEGF, this notion has been exploited as an antiangiogenic approach by increasing the amount of free circulating VEGFR via the use of aptamers (this is further described in section 1.3). Although VEGFR-1 is largely a receptor for VEGF, it has the ability to allow the binding of VEGF-B and placental growth factor (PLGF), another proangiogenic factor (Malik *et al.*, 2006). This ability has been heavily targeted for anti-VEGF therapy, as inhibiting this receptor could lead to several pro-angiogenic signalling pathways being halted. Figure 7 illustrates the different VEGF to VEGFR binding interactions.

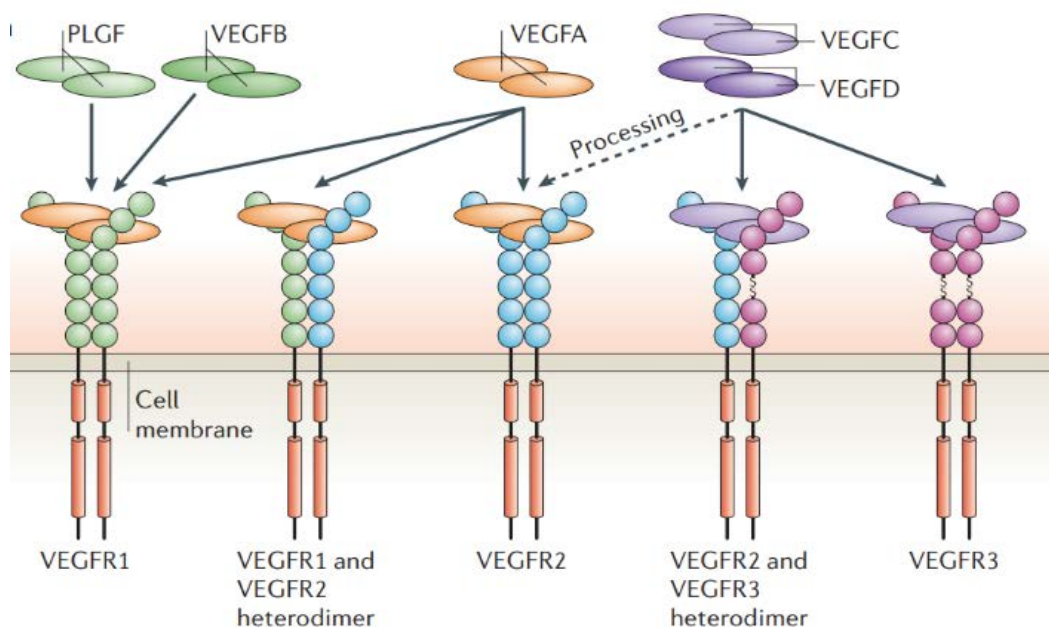


Figure 7 VEGF isoforms and VEGFR receptors.

Schematic diagram of VEGFA VEGFB VEGFC VEGFD isoforms and PLGF binding to VEGF receptors. The diagram displays how VEGF B binds to VEGFR-1 but how the most abundant isoform VEGFA can bind to both VEGFR-1 and VEGFR-2. It also illustrates how VEGFC and VEGFD are mostly associated with VEGFR-3 found on lymphatic vessels. Diagram adapted from (Olsson *et al.*, 2006).

In relation to VEGF, VEGFR-2 is the main pro-angiogenic receptor in angiogenesis. VEGFR-2 mediates the downstream effects of VEGF in angiogenesis specifically its role in micro vascular permeability, endothelial cell proliferation, invasion, migration and cell survival. Activation of VEGFR-2 has shown potent endothelial cell activity both in *in vitro* and *in vivo* models, heavily supporting the concept of angiogenesis activation via VEGFR-2 alone (Yancopoulos *et al.*, 2000; Hicklin and Ellis, 2005).

VEGFR-3 is most commonly found in lymphatic endothelial cells (Witmer *et al.*, 2001). Lymphangiogenesis refers to the formation of new lymphatic vessels and is essential in physiological processes such as homeostasis, metabolism and immunity (Maby-El Hajjami and Petrova, 2008; Stacker and Achen, 2009). It is most active during embryonic development and less so postnatal. As a result it is seen in adults under pathological conditions such as inflammation and tumour growth (Christiansen and Detmar, 2011). Therefore antiangiogenic approaches could help combat neoplastic cells metastasising via the lymphatic system to lymph nodes.

VEGF plays a vital role in the progressive stages of tumour growth along with the increasing induction of many other angiogenic factors. The change from high VEGF dependency in early stages, to an array of proangiogenic factors in advanced stages, could be further investigated for antiangiogenic therapy (See Figure 8).

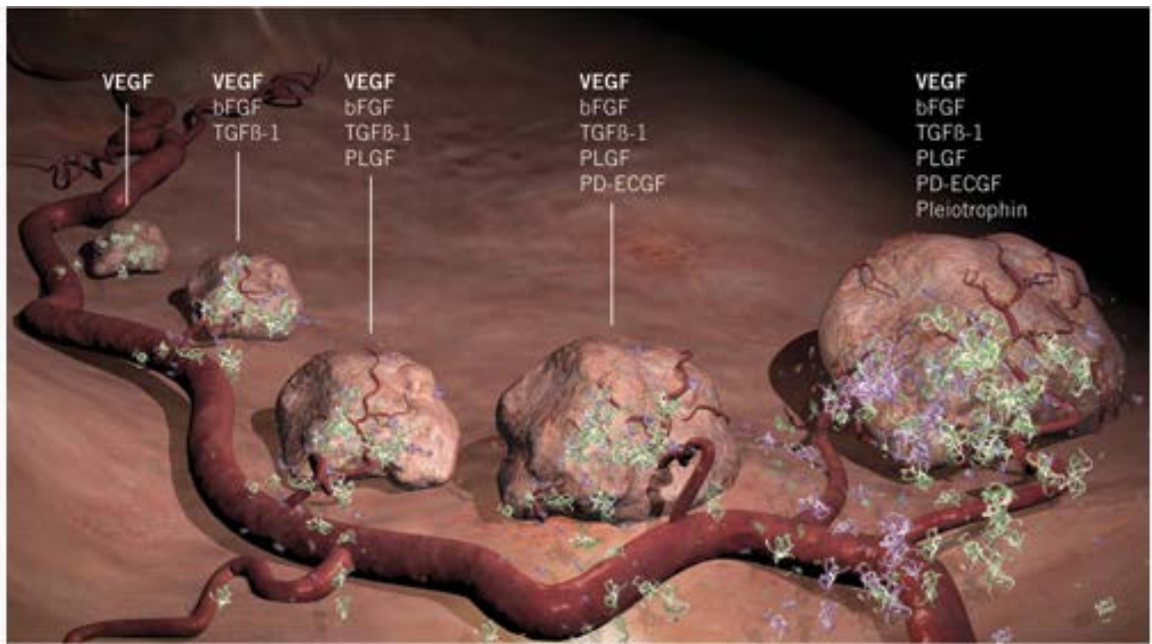


Figure 8 VEGF dependency in stages of tumour growth.

As the tumour becomes more vascularised the dependency on VEGF signalling is reduced and other non-VEGF angiogenic stimulators are utilised to further the development of the tumour, adapted from (DeVita, Hellman and Rosenberg, 2005).

VEGF induces the secretion of multiple enzymes and proteins vital for degradation of the extracellular matrix, *e.g.* matrix metalloproteinases, metalloproteinase interstitial collagenase and serine proteases such as tissue-type plasminogen activator. The extracellular matrix is the non-cellular part found in all tissue types. It provides the essential scaffolding to support the cellular components of tissues and initiates key biological cascades important in tissue morphogenesis and differentiation (Frantz *et al.*, 2010). The activation of these compounds causes the endothelial cells to form sprouts from the existing blood vessel, starting the angiogenic process. What is key is that the absence, or inhibition, of VEGF can cause the extracellular matrix to undergo apoptosis and trigger vessel regression, *i.e.* cause an antiangiogenic episode (Plank and Sleeman, 2003).

Angiogenesis is essential to provide a supply of blood and oxygen to nearby tissues; in tumours this enables growth. However pathological angiogenesis produces more dysfunctional vessels as seen in Figure 9. Specifically, it is the overexpression of VEGF that can result in a hyperperfused, hyperpermeable neovasculature, which is often complex, leaky and irregular compared to normal vasculature.

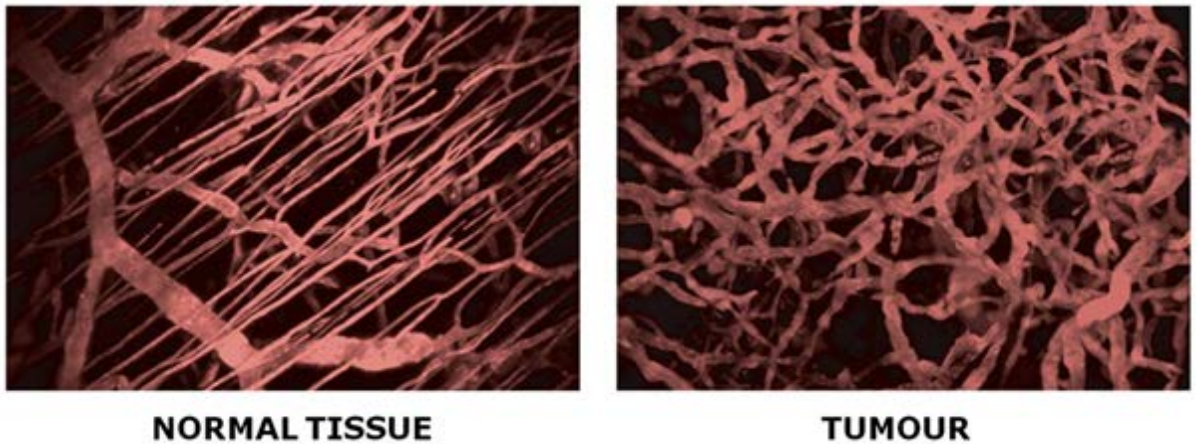


Figure 9 Normal and tumour vasculature.

The difference in vasculature between normal and tumour environments is that tumour vasculature is often irregular and hyperpermeable whereas the normal physiological vasculature is more uniform and tightly regulated (Weinberg, 2013)

Although the original concept behind antiangiogenic therapy was to starve tumours of oxygen, studies have revealed a concept termed tumour vascular normalisation (Jain, 2005). It was initially seen as an unexpected property of antiangiogenic therapy, but further studies were able to clarify how bringing the tumour vascular to a more controlled state *i.e.* by inhibiting the overexpression of VEGF, was linked to the normalisation observed (Huang *et al.*, 2013; Shi, Chen and Huang, 2013). Therefore, it has now become a key concept behind antiangiogenic therapy because the normalised vasculature allows for an increase in chemotherapeutic drug delivery and consequently drug efficacy (Carmeliet and Jain, 2011).

Longo *et al.* (2002) recognised that expression of VEGF in normal adult vasculature was independent of survival, stability and normal function (Longo *et al.*, 2002). Whereas in tumour vessels, VEGF was seen as a key survival factor (Longo *et al.*, 2002). It is arguably the most potent proangiogenic factor as many studies such as one by Ferrara and Kerbel (2005) observed that the majority of tumours analysed in his study showed elevated levels of VEGF (Ferrara and Kerbel, 2005; Jain *et al.*, 2005; Olsson *et al.*, 2006a; Shibuya, 2011; Rapisarda and Melillo, 2012).

1.2.4 Non-VEGF Modulators of Angiogenesis

Non-VEGF pathways appeared to gain importance when VEGF is inhibited. Growth factors like the fibroblast growth factor (FGF) family are deemed as key mediators of angiogenesis (Lieu *et al.*, 2011). They have shown similar and, in rare cases, superior effects to VEGF (Pepper *et al.*, 1992; Turner and Grose, 2010). In an attempt to better understand the importance of FGF in tumour angiogenesis, Compagni and colleagues (2000) used adenoviral sFlk-1 (AdsFlt) and sFGF (adsFGFR) receptors to interfere with VEGFR-1 and FGFR (Compagni *et al.*, 2000). They found that adsFlt predominantly impaired initiation of tumour angiogenesis, whereby adsFGFR disrupted the maintenance of tumour angiogenesis (Compagni *et al.*, 2000).

Angiopoietins are a family of vascular growth factors that are part of the ANGPT-TIE2 pathway (Little, 2015). This pathway is crucial in the angiogenesis process (Saharinen, Eklund and Alitalo, 2017). Studies have shown that the pathway is critical in triggering and supporting tumour induced angiogenesis (Ferrara and Kerbel, 2005; Pouyssegur, Dayan and Mazure, 2006; Huang *et al.*, 2010). Angiopoietin 1 (ANGPT1) is considered to be responsible for blood vessel maturation and stability (Saharinen, Eklund and Alitalo, 2017). Angiopoietin 2 (ANGPT2) binds to the TIE-2 receptor and acts as an antagonist to ANGPT1 (Little, 2016). It is also upregulated in hypoxic and inflamed environments (Blumenkranz *et al.*, 2013). In a tumour setting, evidence has shown that increased ANGPT2 expression in tumours results in poor prognosis for patients (Loges *et al.*, 2005; Hou *et al.*, 2008; Koenecke *et al.*, 2010). ANGPT2 has been identified in melanomas, glioblastomas, breast cancer, colorectal cancer and renal cell carcinoma (Sfiligoi *et al.*, 2003; Helfrich *et al.*, 2009; Goede *et al.*, 2010; Wang *et al.*, 2014; Scholz *et al.*, 2016). Whereas increased ANGPT1 levels, responsible for increasing vessel stability, has shown

to normalise tumour vasculature enabling better drug delivery (Winkler *et al.*, 2004; Falcón *et al.*, 2009; Coxon *et al.*, 2010).

Matrix metalloproteinases (MMP) are a group of proteinases that play an important role in tumour growth (Egeblad and Werb, 2002). Their function of extracellular matrix degradation via collagen breakdown are critical in the angiogenesis process (Foda and Zucker, 2001). Studies have revealed particular MMPs and their involvement in tumour induced angiogenesis (Bergers *et al.*, 2000). Iurlaro *et al.* (1999) identified that increased levels of MMP-2 and MMP-9 resulted in enhanced angiogenesis and tumour invasiveness (Iurlaro *et al.*, 1999). In a murine study, cancer colonies in lungs were reduced by the downregulation of MMP-9 (Itoh *et al.*, 1998, 1999). MMP-7, 9 and 12 overexpression has also been identified in squamous cell carcinoma (Impola *et al.*, 2004).

Cyclooxygenase (COX) enzymes, in particular COX-2, have a well understood role in inflammation (Ricciotti and FitzGerald, 2011). They are responsible for catalysing the formation of prostanoids (Smyth *et al.*, 2009). But they also play an important role in activating angiogenesis, as they are expressed on many tumour cells as well as endothelial cells (Gately and Li, 2004). The proangiogenic effects are as a result of arachidonic acid metabolism forming metabolites specifically epoxyeicosatrienoic acids (EETs) that are angiogenic (Masferrer *et al.*, 2000; Rand *et al.*, 2017). Furthermore, COX-2 is expressed by tumour endothelium in various tumours types such as human colon and prostate cancer whereas in normal quiescent endothelial cells only COX-1 is found (Leahy *et al.*, 2002).

It is evident that non-VEGF growth factors play a pivotal role not only in angiogenesis itself but also in anti-VEGF drug resistance. Preclinical models have revealed how non-VEGF growth factors support the development of tumour induced angiogenesis (Plate *et*

al., 1992; Kim *et al.*, 1993). One study revealed FGF-2 levels increase with VEGF-axis inhibition (Casanovas *et al.*, 2005). While blockade of FGF2 in anti-VEGF resistant tumour models *in vivo* caused reduction in tumour growth (Allen, Walters and Hanahan, 2011). Another study identified upregulation of FGF-2 in RIP-TAG tumours after treatment with a VEGFR-2 inhibitor (Casanovas *et al.*, 2005) Several other studies have reported high levels of PDGF-BB expression in highly vascularised malignant glioblastoma; as well as elevated FGF-2 levels in advanced vascularised tumours (Cao and Pettersson, 1990; Soutter *et al.*, 1993; Malek *et al.*, 1997; Auguste, Javerzat and Bikfalvi, 2003; Heldin, 2004; Ostman and Heldin, 2007). Both of these non-VEGF angiogenic factors (FGF-2 and PDGF) have been linked to tumour progression and metastasis (Soutter *et al.*, 1993; Nguyen *et al.*, 1994).

These findings support the notion that multi targeted receptor (RTKIs) inhibitors such as sunitinib, sorafenib and regorafenib (described in 1.3.1) are needed to minimise escape mechanisms, for instance, non-VEGF mediated angiogenesis.

1.3 Antiangiogenic Therapy

Antiangiogenic therapies are based on preventing, disrupting or regressing neo vascular formation (Samant and Shevde, 2011; Al-Abd *et al.*, 2017). Approaches to antiangiogenic therapy are conducted via three methods highlighted in Figure 10.

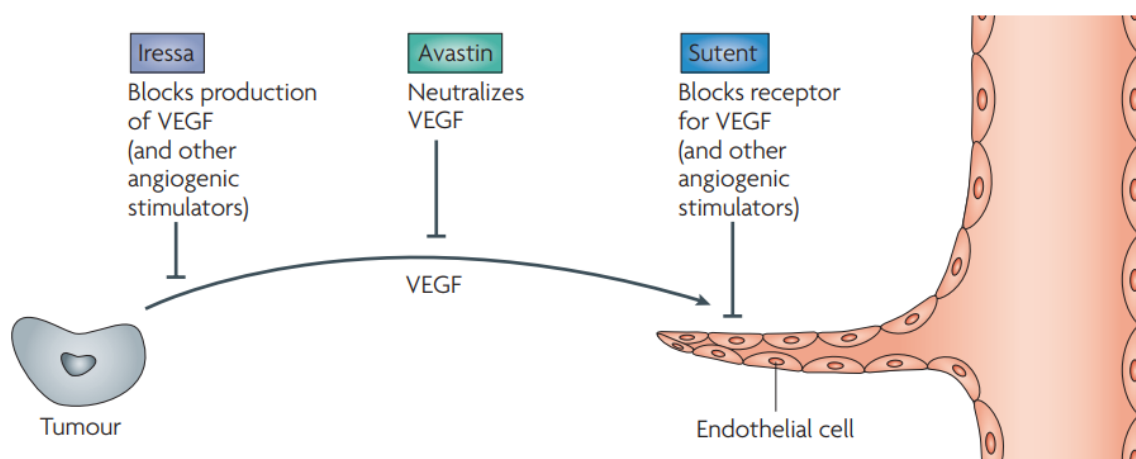


Figure 10 General mechanism of FDA approved antiangiogenic therapies (Folkman, 2007).

There are therapies that block angiogenic receptors (Sutent), neutralise VEGF ligands (Avastin) or inhibition the production of VEGF and other key angiogenic stimulators (Iressa).

The first approved treatment was Avastin (bevacizumab) in 2004, a monoclonal antibody that binds to VEGF preventing it binding to a VEGFR (Ferrara and Kerbel, 2005; Kamba and McDonald, 2007). Originally it was licensed to be used in conjunction with intravenous 5-fluorouracil based chemotherapy as a first or second treatment for colorectal carcinoma. Two years later it was approved in combination with anti-mitotic agent paclitaxel and anti-neoplastic agent carboplatin for first line treatment against various forms of non-small cell lung cancer (NSCLC), (Sandler *et al.*, 2006). As of 2014, the FDA approved its use against metastatic cervical cancer with paclitaxel and cisplatin.

Ranibizumab and aflibercept are two licensed drugs that work in similar ways to bevacizumab, *i.e.* agents that bind to VEGF. Ranibizumab is a monoclonal antibody fragment derived from the same mouse antibody as bevacizumab (CATT Research Group *et al.*, 2011). Although it has similar modes of action to bevacizumab its price per single dose is considerably higher, as a single dose costs around £1450 whereas bevacizumab costs £35 (CATT Research Group *et al.*, 2011). Aflibercept acts as decoy receptor to bind to circulating plasma VEGF as “VEGF trap”, it is composed of domains from VEGFR-1 and VEGFR-2. It also has the ability to bind to PLGF and VEGF-B (Saharinen, Eklund and Alitalo, 2017).

Aptamers such as pegaptanib also neutralise VEGF but via a different approach. Aptamers are DNA or RNA oligonucleotide strands that can specifically bind to selective VEGF-isoforms in particular VEGF-165; which is the most abundant splice variant of VEGF-A (Enseleit, Michels and Ruschitzka, 2010).

Receptor tyrosine kinase inhibitors (RTKIs) are a group of drugs that target a broad range of pro-angiogenic tyrosine kinase receptors (VEGFR, FGFR, PDGFR) (Ferrara and Kerbel, 2005), these have largely been the common focus of antiangiogenic drug discovery for many years (Morin, 2000). As of July 2015, 28 small molecular RTKI's have been FDA approved for use against several types of cancer (Wu, Nielsen and Clausen, 2016). Many analogues and derivatives have been developed that either are: tyrosine kinase inhibitors, serine/threonine kinase inhibitors, dual protein kinase inhibitors or lipid kinase inhibitors. However, the overwhelming majority are tyrosine kinase inhibitors (Wu, Nielsen and Clausen, 2016). The most widely used RTKI is sunitinib, also known as sunitinib, it predominantly targets VEGFRs and PDGFRs (Abrams, Lee, *et al.*, 2003; Abrams, Murray, *et al.*, 2003).

Currently, two dual specificity kinase inhibitors have been approved, sorafenib and regorafenib. Dual specificity kinase inhibitors bind to receptors found on separate signalling pathways. Sorafenib has the ability to target the RAF/MEK/ERK pathway in tumour cells and VEGFR/PDGFR tyrosine kinase receptors in the surrounding vasculature (Adnane *et al.*, 2006), regorafenib targets the VEGFR-2 and Tie-2 receptors (Saharinen, Eklund and Alitalo, 2017).

1.3.2 Limitations with Current Licensed Antiangiogenic Agents

Inducing an antiangiogenic response with antibodies or tyrosine kinase inhibitors is effective for treating malignancy (Abdollahi and Folkman, 2010). Initial findings from phase III clinical trials have revealed improved survival with the use of multi targeted RTKI monotherapy, such as sunitinib and sorafenib, in gastrointestinal and renal tumours (Jain *et al.*, 2005). However, there is room for improvement in terms of efficacy and long term use (Fan *et al.*, 2006). Jain and colleagues in 2005 expressed that optimised treatments are needed to prevent tumour escape and extend patient survival past 5 months (Jain *et al.*, 2005).

The rationale as to antiangiogenic therapies only showing efficacy towards some tumour cell types and not others is unknown, but the difference in the biological composition between tumour types may contribute (Vasudev and Reynolds, 2014).

However antiangiogenic therapies are accompanied by various side effects. The most common side effect seen in nearly all drugs that inhibit anti-VEGF activity is hypertension. In clinical studies the first VEGF inhibitor, bevacizumab, was shown to have an overall hypertensive incidence of 32%, however, only 1% of patients developed a life threatening hypertensive crisis (Hurwitz *et al.*, 2004; Kabbinavar *et al.*, 2005). Hypertension is direct cause of VEGF inhibition, by reducing vasodilation via inhibition of nitric oxide production (Kamba and McDonald, 2007; Robinson *et al.*, 2010). Therefore it has been viewed as a potential biomarker to monitor the desired effects of anti-VEGF therapies (Mir *et al.*, 2009; Robinson *et al.*, 2010). Other reported adverse effects include gastrointestinal perforation, haemorrhage, thromboses and in rare occurrences congestive heart failure (Kamba and McDonald, 2007). In another study with

bevacizumab against unresectable hepatocellular carcinoma, serious bleeding complications were apparent in 11% of patients (Siegel *et al.*, 2008).

Similarly to bevacizumab, small molecule RTKIs create adverse effects. Common adverse reactions range from hypertension and mild bleeding, to infrequent but life threatening haemorrhages and ischaemic conditions (Kamba and McDonald, 2007). One study by Lee *et al.* (2009) identified significant cutaneous toxicities in patients receiving sunitinib or sorafenib, with hand and foot skin reaction seen as the most common effect (Lee *et al.*, 2009). This was observed in 48% of patients treated with sorafenib (52 out of 109 patients) and 36% of those treated with sunitinib (39 out of 119 patients) (Lee *et al.*, 2009). Verheul and Pinedo (2007) formulated a concise table (table 1) of the potential mechanisms underlying antiangiogenic therapy induced side effects (Verheul and Pinedo, 2007). It was evident that the toxicities were varied, affecting a whole host of physiological processes. However, the research concluded that short term toxicities are generally manageable in clinical trials (Verheul and Pinedo, 2007).

Table 1 Possible molecular mechanisms for the adverse drug reactions of angiogenesis inhibition. (Adapted from (Verheul and Pinedo, 2007)).

<i>Adverse drug reactions</i>	<i>Possible underlying mechanism</i>
Bleeding, impaired wound healing	Platelet dysfunction; decreased expression of endothelial tissue factor
Hypertension	Decreased NO and/or PGI ₂ production; inappropriate density vessels; vascular stiffness; disturbed endothelin function
Hypothyroidism	Disturbed thyroid cell function; reduced vascularity of thyroid
Proteinuria and oedema	Podocyte dysfunction owing to VEGF blockade; hypertension
Dizziness, nausea, vomiting and diarrhoea	Mucosa disturbance
Skin toxicity including rash and hand-foot syndrome	Epidermal cell apoptosis

Reformation of dysfunctional tumour vasculature is often seen when anti-VEGF therapies are stopped, and the re-emergence of endothelial cells and microvasculature occurs (Vosseler *et al.*, 2005). Thus, the long-term capabilities of anti-VEGF therapies are vital in sustaining the antiangiogenic activity, and possibly preventing the angiogenic switch. Long term use of anti-VEGF therapies in itself can be problematic due to acquired resistance, poor drug delivery or long-term side effects. Therefore, this drawback could pave the way for the need of other long term non-VEGF alternatives. Figure 11 illustrates the current mechanism of action to inhibit VEGF signalling. Optimal combinations such as multi-drug approaches specific for antiangiogenic therapy, are still overlooked, especially with drug resistance and escape mechanisms identified with anti-VEGF therapy (Fan *et al.*, 2006; Folkman, 2007; Loges, Schmidt and Carmeliet, 2010; Vasudev and Reynolds, 2014). Further investigations will help to identify the positive or negative consequences of antiangiogenic therapy in relation to the tumour, its growth and metastatic potential (Ebos and Kerbel, 2011).

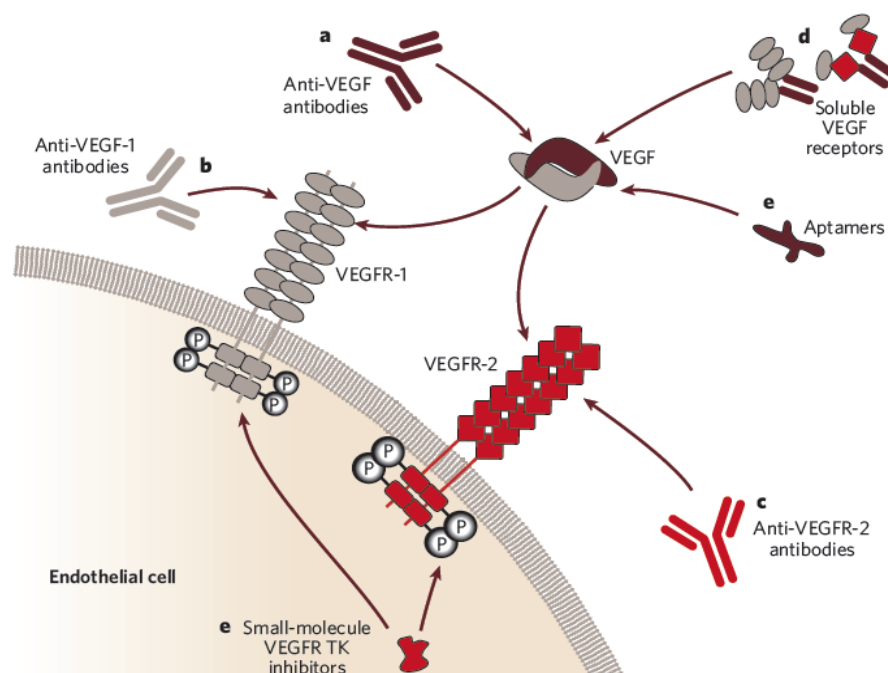


Figure 11 mechanisms to inhibit VEGF signalling:

There are different mechanisms of which to inhibit VEGF signalling: a) binding to the VEGF b) binding to VEGFR-1 c) binding to VEGFR-2 d) introducing free soluble VEGF receptors e) utilising small-molecular intracellular and extracellular or intracellular RTKIs (Ferrara and Kerbel, 2005).

1.3.3 Antiangiogenic Drug Resistance

Although anti-VEGF monotherapy has been shown to increase survival in patients with specific cancers, Jain and colleagues (2005) identified there has been noticeable tumour resistance and evasion against anti-VEGF therapies (Jain *et al.*, 2005). In 2006, the founder of antiangiogenic studies, Judah Folkman, postulated the stubborn nature of tumours in response to mono-antiangiogenic therapy targeting a single protein, *e.g.* VEGF (Folkman, 2006, 2007). This anti-VEGF resistance has resulted in non-VEGF reactivation of angiogenesis via the FGF family (Casanovas *et al.*, 2005). To add, anti-VEGF therapies can cause increased amounts of plasma VEGF leading to increased VEGFR activation once the inhibitor is removed (Dreves *et al.*, 2005; Motzer *et al.*, 2006; Verheul and Pinedo, 2007).

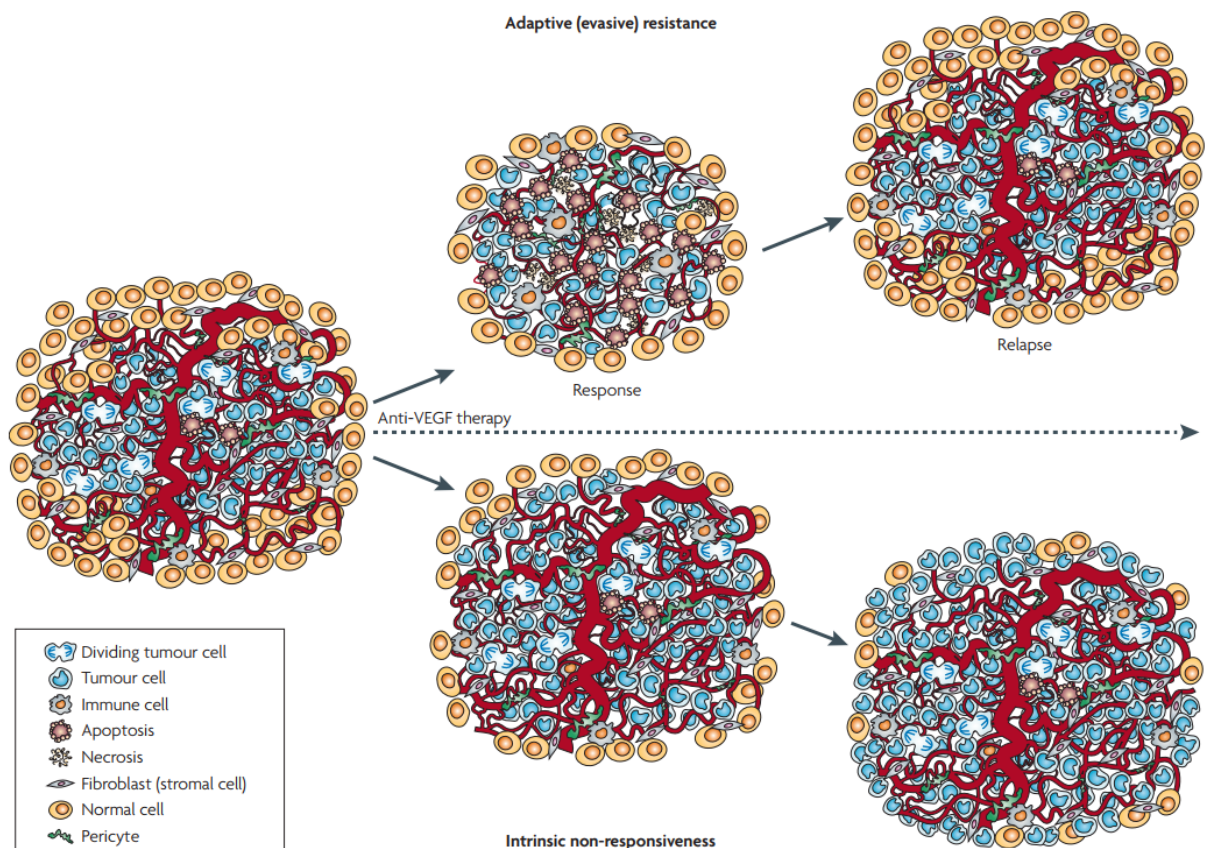


Figure 12 Two modes of resistance seen after exposure to antiangiogenic therapy demonstrating adaptive and non-responsive evasions by tumours adapted (Bergers and Hanahan, 2008).

Adaptive resistance represents a tumour's ability to adapt after initial exposure to angiogenic inhibitors. Non-responsive resistances refer to a pre-existing attribute a tumour has, causing antiangiogenic therapy to be redundant in its effects.

According to Bergers and Hanahan (2008), emerging data suggests that antiangiogenic drug resistance falls into two categories, evasive and intrinsic as illustrated in Figure 12 (Bergers and Hanahan, 2008). Evasive resistance refers to a tumour's ability to adapt after an initial exposure to angiogenesis inhibitors in an attempt to evade the therapy and continue tumour growth (Loges, Schmidt and Carmeliet, 2010). Whereas intrinsic, also known as non-responsive, resistance describes a latent pre-existing condition within the tumour, rendering the antiangiogenic therapy ineffective (Bergers and Hanahan, 2008).

Table 2 highlights the potential solutions that need to be developed to overcome tumours escaping or evading antiangiogenic therapy (Jain *et al.*, 2005; Loges, Schmidt and Carmeliet, 2010). Using novel chemical scaffolds that target alternative pathways is a potential solution going forward. Chemical scaffolds such as chalcones have shown to exhibit antiangiogenic activity via downregulation of VEGFR-2 and signalling mediators *e.g.* ERK 1/2 and Akt (Mojzis *et al.*, 2008; Lee *et al.*, 2012; Mahapatra, Bharti and Asati, 2015). This will be further expanded on in chapter 1.5. Development of inhibitors targeting alternative proangiogenic factors could supplement current antiangiogenic therapies as a combinatorial or synergistic approach (Loges, Schmidt and Carmeliet, 2010; Ebos and Kerbel, 2011).

Table 2 Possible solutions to counteract antiangiogenic drug resistance and evasion.

Target alternative pathways, using combinatorial approaches or modifying drug dosage (adapted from Jain *et al.*, 2005).

<i>Possible mechanisms</i>	Tumour does not respond to VEGF-blockade	Ineffective or no cytotoxic therapy	Inefficient vasculature Acquired resistance to the antiangiogenic or cytotoxic agents
<i>Potential solution</i>	Use antiangiogenic agents that target alternative pathways	Combine the antiangiogenic agent with effective cytotoxic	Modify the dose/schedule of the antiangiogenic agent Use alternative antiangiogenic or cytotoxic agents

1.4 Preclinical design and development of small molecular anticancer drugs

1.4.1 The drug discovery process

The discovery of general anti-cancer drugs is a long-term process comprising of preclinical and clinical development. From target identification to a marketable drug, the process encompasses core fields of medicinal chemistry and pharmacology. Pharmacodynamics is often carried out in the early parts of drug discovery to identify a compound exhibiting a targeted activity. It is defined as the branch of pharmacology that focuses on the effects drugs on an organism and their mechanism of action. Whereas pharmacokinetics (focused on the effects of drug movement in an organism) is recognised in the latter stages to improve the qualities of drug likeness and effectiveness. All fields and parts of the process are interchangeable to form more of a drug discovery cycle as opposed to a rigid one way process. Figure 13 demonstrates the different stages that encompass the general drug discovery cycle.

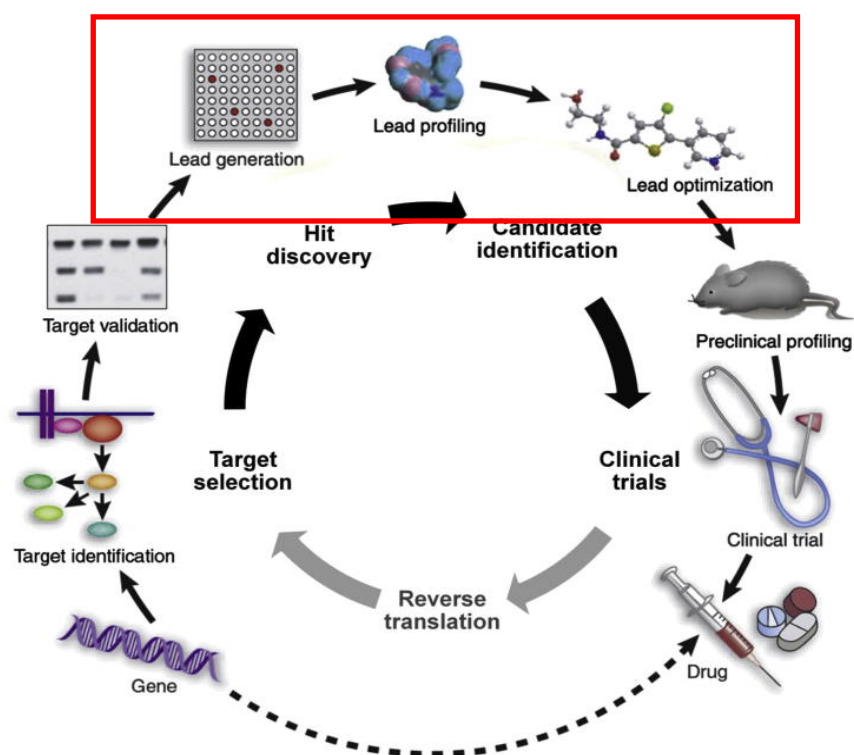


Figure 13 A diagrammatic representation of how a drug discovery cycle encompasses 4 key areas.

Target selection, Hit discovery, candidate identification and clinical trials. The red box highlights the areas involved in this study (Hoelder, Clarke and Workman, 2012).

The hallmarks of cancer provide a useful guide for the development of a drug target. Once a target is selected, the “hit generation” phase occurs where “hit” compounds with preliminary biological activity must be generated. There are several routes for hit generation which are used independently or in combination. These approaches consist of: high-throughput screening, fragment screening, virtual screening, molecular docking design, nuclear magnetic resonance (NMR) screening, computer aided drug design, knowledge based design, ligand or structure based design and analogue based drug design (Hughes *et al.*, 2011; Hoelder, Clarke and Workman, 2012). For this to occur via an analogue based approach parent compound(s) must be chosen (see chapter 3).

Once Hit compounds are identified, secondary or confirmatory assays like dose response curves and counter screens are conducted to confirm the compounds preliminary activity (Deprez-Poulain and Deprez, 2004). Therein different routes are exploited, the hit compounds can undergo assays assessing bioavailability, toxicity and metabolism to hone in on improved hit compounds. Or the hit compounds can be investigated through a structure-activity relationships (SARs) approach to understand and define the key functional groups or regions to help a hit-to-lead optimisation phase (Katsuno *et al.*, 2015; Patrick, 2017). Figure 14 provides a generic overview to the common drug discovery cascade from target validation to clinical drug candidate.

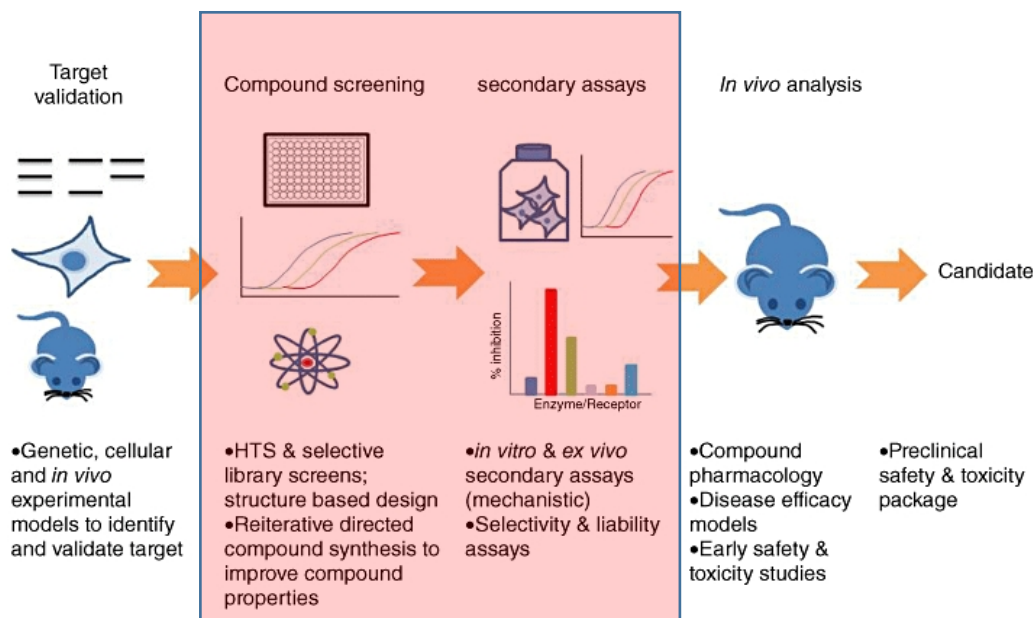


Figure 14 A general process in a drug discovery programme.

Within each stage key experimental procedures are conducted. Compound screening and secondary assays highlighted in red iterate the areas focused on in this research taken from (Hughes *et al.*, 2011)

At this stage there are certain characteristics that hit compounds should possess before the development of lead candidates from them. Such characteristics are as follows

(Hughes *et al.*, 2011; Yusof *et al.*, 2014; Katsuno *et al.*, 2015):

- The chemical structure of a hit should be confirmed by identification (for natural products) re-synthesis or re-purification.
- Preliminary knowledge of the structure-activity relationship of a hit is desirable.
- A Hi should exhibit a significant *in vitro* response with a typical IC/EC₅₀ value between 5 µM-100 nM.
- Hits should meet basic drug like profiles such as the pan-assay interference filters (PAINS) to prevent hits that lack target specificity. Or comply with drug likeness models such as the Lipinski Rule of five.
- Counter screens should be conducted on the hit for further confirmation of its activity.
- A 10-fold selective activity for cytotoxicity against the desired cell line vs normal mammalian cell line should be met.
- Compounds should ideally be synthesised in fewer than five steps with no major synthesis or formulation issues and have an acceptable yield
- Compounds should have suitable water/organic solubility *e.g.* clogp values between 2-3 considered optimal for a balance between cell membrane permeability and first pass clearance.

Lead optimisation is where lead compounds are generated with improved potency, reduced off target effects and enhanced pharmacokinetic properties (Bleicher *et al.*, 2003; Keseru and Makara, 2006). This is carried out by modifying the existing hit compounds from the SAR studies. This cycle of “Hit to lead” optimisation can continue as described in Figure 13 until a promising lead candidate is identified (Hoelder, Clarke and Workman, 2012). Approaches within this phase are varied, as some cycles can be focused on enhancing the pharmacodynamics whereas others can be improving druglikeness via refining the ADMET (Absorption, Distribution, Metabolism, Excretion and Toxicology) properties of the lead compounds. Drug design models like the Lipinski rule of five can be incorporated to identify the pre-clinical drug candidate (Lipinski, 2004). If successful, these lead candidate(s) can undergo clinical development and evaluation via phase trials to finally produce a licensed drug (Bleicher *et al.*, 2003; Lipinski, 2004; Katsuno *et al.*, 2015).

1.4.2 Analogue based drug design and development

Analogue drug design aims to improve the pharmacological properties of existing drugs or compounds. This approach is one of the most common methods used in drug discovery (Kuntz, 1992; Shu, 1998; Sharma *et al.*, 2009; Ghorab *et al.*, 2016). Flavopiridol is a key example in showing the success of using an analogue based drug design approach (Hernandes *et al.*, 2010). Flavopiridol is a CDK2 inhibitor used to treat acute myeloid leukaemia. Its hit to lead conversion from an analogue demonstrates the use of functional group addition in improving the observed activity. L86-8276, also known as dechloroflavopiridol, seen in Figure 15 contains a phenyl ring next to the flavone ring. This particular dechlorinated analogue generates 10 van der Waals interactions within the ATP binding pocket of CDK2. However, Flavopiridol which contains a chlorophenyl caused an increase in kinase inhibition by six fold. The most likely reason for this was that the inclusion of the chlorine caused new binding contacts within the ATP binding pocket, raising the number of drug to target interactions from 10 to 61 (Hernandes *et al.*, 2010). By replacing the phenyl with a chlorophenyl to increase binding interactions, Flavopiridol showed greater kinase inhibition.

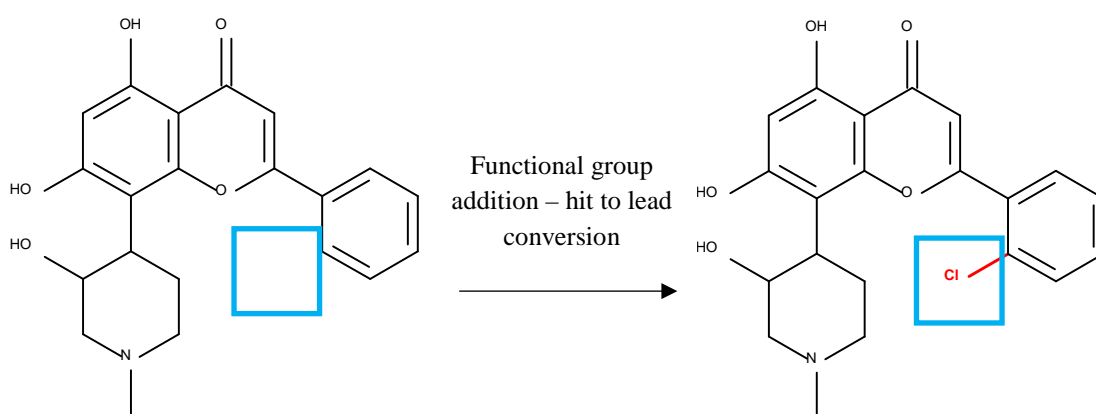


Figure 15 L86-8276 (dechloroflavopiridol) conversion to flavopiridol, adapted from (Hernandes *et al.*, 2010)

1.5 Chemical Scaffolds as Antiangiogenic Compounds

Mojzis *et al.* (2008) explained that much effort has been dedicated to identifying compounds, specifically novel chemical scaffolds, that exhibit antiangiogenic activity (Mojzis *et al.*, 2008). Therein many studies have been focused on drugs that block extracellular matrix degradation, target endothelial cells specifically, block stimulators of angiogenesis, or downregulate a variety of angiogenic signalling mediators (Mojzis *et al.*, 2008).

Chemical scaffolds like chalcones have been a cornerstone of drug discovery studies for several decades (Anto *et al.*, 1995; Li *et al.*, 1995; Torres-Santos *et al.*, 1999; Balunas and Kinghorn, 2005; Koehn and Carter, 2005; K. Sahu *et al.*, 2012; Zhang *et al.*, 2013). Many licensed drugs to treat various conditions have been modelled from naturally derived chemical scaffolds (de Sá Alves, Barreiro and Fraga, 2009; Mishra and Tiwari, 2011; Brown, Lister and May-Dracka, 2014; Rodrigues *et al.*, 2016). In 2005, 11 out of the 22 FDA approved licensed antiangiogenic agents were either a natural product or were modelled from a natural product parent (El Sayed, 2005). Collectively, chalcones as well as similar structures like stilbenes and flavanoids are amongst several extensively studied compounds (Ratty and Das, 1988; Woods *et al.*, 1995; Bertelli *et al.*, 1999; Zheng and Ramirez, 1999; Zhishen, Mengcheng and Jianming, 1999; Tan *et al.*, 2003; Albin *et al.*, 2006; Kimura, Sumiyoshi and Baba, 2008; Mojzis *et al.*, 2008; Chahar *et al.*, 2011; Martí-Centelles *et al.*, 2013; Sirerol *et al.*, 2016).

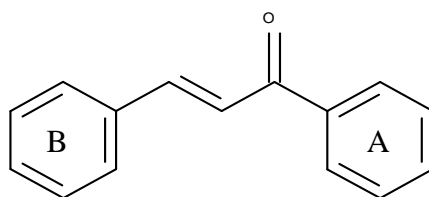


Figure 16 Basic scaffold structures of chalcone.
Chemical structure of 1,3-diphenylpropenones.

1.5.1 Chalcones

Chalcones are a class of naturally derived compounds that are found in plants. All chalcones, whether natural or synthetic, consist of a 1, 3-diaryl-2-propen-1-one scaffold, which has been found to exhibit an array of pharmacological properties, from anti-microbial activities to anti-proliferative applications on leukaemic or cancer cell lines (Mojzis *et al.*, 2008; Pilatova *et al.*, 2010; Mahapatra, Bharti and Asati, 2015). The enone refers to the alpha beta unsaturated carbonyl region between the two phenyl rings (see Figure 16). Variations in functional groups and substituent positions on the aromatic rings have together produces hundreds of chalcone analogs. Thus, it was stated by Mahapatra et al (2015) that with the knowledge of molecular targets and (SARs), further phases of new synthesis will produce chalcones with increased efficacy and minimal toxicity (Mahapatra, Bharti and Asati, 2015).

Polyphenolic chalcones are found in abundance in a range of plants, these plant extracts have been tested to uncover pharmacological properties (Ngameni, 2006; Detsi *et al.*, 2009; Batovska and Todorova, 2010; Huang, Cai and Zhang, 2010) . Within the extracts the active component has been the phenolic chalcone scaffold, and as a result they have been the initial parent design of drug discovery studies (Yang *et al.*, 2001; Huang, Cai and Zhang, 2010).

On top of this, the utilisation of synthetic methoxy based analogs have brought a variety of biological activities (Ethiraj, Aranjani and Khan, 2013). In 2010, Bandgar and colleagues reported anti-cancer, anti-inflammatory and anti-oxidant activities of simple synthetic methoxy based chalcones (Bandgar *et al.*, 2010).

1.5.2 Reported Antiangiogenic Activities of Simple Molecular Chalcones

In 2012, Lee and colleagues investigated several types of synthetic phenylpropenones derivatives, of which some derivatives contained heterocyclic furan or thiophene rings (Lee *et al.*, 2012). Out of four derivatives the chalcone with no altered phenyl rings displayed the most effective inhibitory activity against VEGF-induced angiogenesis of HUVECs. RTK studies identified the chalcone's ability to inhibit several RTKs including VEGFR-2, Tie-2, EGF, FGF and IGF-1. Mechanistic studies revealed significant inhibition of ERK phosphorylation and NF- κ B activation. Functional analysis via a HT29 colon cancer cell inoculated CAM assay showed substantial inhibition of both tumour growth and tumour induced angiogenesis at 10 μ g/ml (Lee *et al.*, 2012).

Lee and colleagues (2012) compared the antiangiogenic activity of diphenylpropenone (DPhP) with furan-2-yl-3-pyridin-2-ylpropenone (a COX-2 inhibitor reported in their previous studies, (E.-S. Lee *et al.*, 2006)). Furan-2-yl-3-pyridin-2-ylpropenone (FPP-3) was put forward as a possible antiangiogenic drug due to its cyclooxygenase-2 selectivity, however in this study it was found that the diphenylpropenone could possess superior antiangiogenic activity than FPP-3 due to its greater inhibition of VEGFR. Another supporting factor was DPhP significantly higher inhibition of angiogenesis *in vivo* of 70% at 5 μ g/CAM than FPP-3 42% at a dose of 20 μ g/chick chorioallantoic membrane (CAM). Overall they concluded that the diphenylpropenone with no substituted phenyl rings was a promising candidate for further development as an antiangiogenic agent (Lee *et al.*, 2012).

Synthesised 2'5'-dihydroxychalcones by Nam and colleagues in 2003, with electron withdrawing group (EWG) substituents, showed overall greater cytotoxicity against various tumour cell lines than the same compounds with electron releasing groups (ERG). It was noted that the position of the EWG and the charge of the β carbon of the $\alpha\beta$ unsaturated region of the chalcone were pivotal in the compounds activities. In particular, out of the several EWG compounds, 2-chloro-2'5'-dihydroxychalcone exhibited the highest selective cytotoxicity against HUVECs (table 3). The compound also displayed strong inhibitory effects in *an vitro* model of HUVEC tube formation. In an *in vivo* study with BDF1 mice bearing Lewis lung carcinoma cells at 50 mg/kg/day the compound was found to inhibit tumour growth by 60.5% (Nam *et al.*, 2003).

Table 3: 2'5'-dihydroxychalcones EC₅₀ values against cancer cell lines and HUVECs

With 2-chloro-2'5'-dihydroxychalcone (highlighted in yellow) showing the most selective potency towards HUVECs (Nam *et al.*, 2003).

<i>B ring</i>	Cell Line			
	B16	HCT116	A431	HUVEC
<i>H</i>	2.25	3.29	2.44	1.89
<i>2-F</i>	1.78	1.99	1.11	1.02
<i>2-Cl</i>	1.34	1.83	0.09	0.03
<i>3-Cl</i>	1.39	1.81	1.97	1.71
<i>4-Cl</i>	2.18	3.62	2.16	2.01

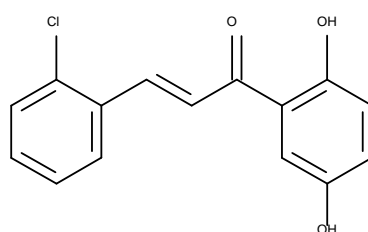


Figure 17 2-chloro-2'5'-dihydroxychalcone.

Referred to AH1 the parent compound for the purpose of this study (Nam *et al.*, 2003)

In 2012, Varinska *et al.*, assessed the anti-angiogenic properties of 4-hydroxychalcone with no additional EWG or ERG groups (Varinska *et al.*, 2012). Selective activity was found on different cell lines to those used by Nam *et al.* (2003), including human epithelial tumour cell line (HeLa) and activated endothelial cells (A549) (Varinska *et al.*, 2012). In mechanistic studies, 4-hydroxychalcone displayed moderate activity for both VEGF and bFGF (Varinska *et al.*, 2012). Induced phosphorylation by extracellular signal kinase (ERK)-1/2 and Akt kinase was seen. However it did not affect tumour necrotic factor alpha stimulated endothelial cells. Collectively this indicated that the inhibition of *in vitro* angiogenic activity was as a result of a suppression of growth factor pathways (Varinska *et al.*, 2012). Results from the chick chorioallantoic membrane (CAM) assay also showed that 4-hydroxychalcone had inhibitory effects on bFGF driven neovascularisation (Varinska *et al.*, 2012).

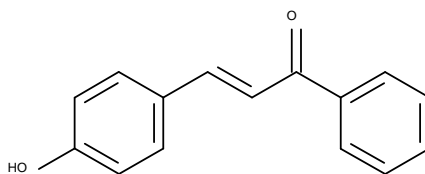


Figure 18 4-hydroxychalcone (Varinska *et al.*, 2012)

Various hydroxyl based chalcones have shown promise in exhibiting antiangiogenic activity; in 2012, Karki synthesised 15 different hydroxychalcones with activity against VEGF induced angiogenesis *in vivo*, assessed via the CAM assay (Karki *et al.*, 2012). Hydroxyl groups were in several ortho, meta and para positions on both A and B phenyl rings. Structure activity relationships revealed that amongst the compounds bearing a single hydroxyl group on the B ring, the hydroxyl group at the para position exhibited the highest anti angiogenic activity of 66% at 1 μ g/CAM, however only slightly more than

the basic chalcone scaffold itself (64%). Looking into hydroxyl groups on the A ring (see Figure 19), 1 exerted the highest inhibition of 89% compared with dihydroxychalcones 3 (87%) and 4 (80%) (Karki *et al.*, 2012). This indicates that the hydroxyl group on the A ring resulted in superior activity than that of the B ring and the chalcone scaffold itself.

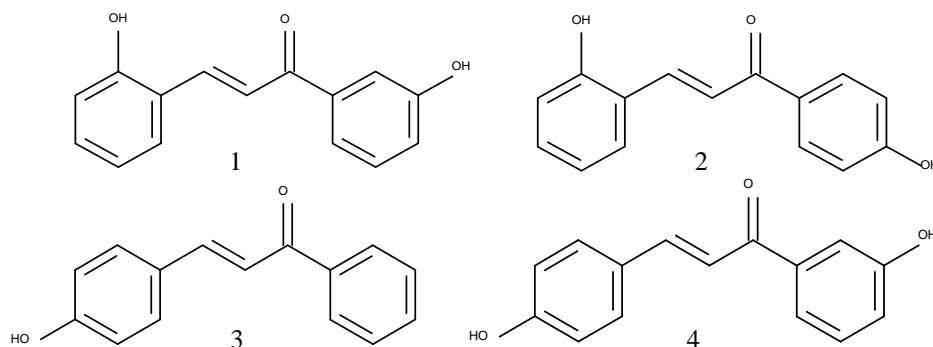


Figure 19 Mono and dihydroxychalcones (Karki *et al.*, 2012)

2'-Hydroxy-4'-methoxychalcone displayed antiangiogenic activities in studies conducted by Lee *et al.* in 2006 (Y. Lee *et al.*, 2006). The authors identified that this chalcone decreased angiogenesis in both CAM assay and the mouse matrigel plug assay (Y. Lee *et al.*, 2006). Upon subcutaneous administration (30mg/kg, 20 days) to mice implanted with murine Lewis lung carcinoma, tumour volume was reduced by 27.2% (Y. Lee *et al.*, 2006).

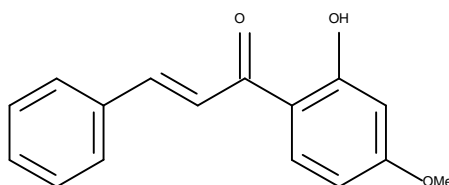


Figure 20 2'-hydroxy-4'-methoxychalcone (Y. Lee *et al.*, 2006)

Cell cycle studies showed that, E-2-(4'-methoxybenzylidene)-1-benzosuberone, a synthetic chalcone, has anti-proliferative effects via the reduced expression of anti-apoptotic gene in both Jurkat and HeLa cells (Pilatova *et al.*, 2010). Additionally, at non-

toxic concentrations the chalcone was able to inhibit VEGF-induced migration of HUVECs (Pilatova *et al.*, 2010). Furthermore, decreased secretion of both MMP (predominantly MMP-9) and VEGF were observed (Pilatova *et al.*, 2010).

Molecular docking of VEGFR with quinoyl-thienyl based chalcones in one study by Rizvi *et al.* (2012), revealed that amongst their extensive series of chalcones, those with substituted chlorine groups at the 2 or 5 position on the thienyl ring, showed deeper interaction into the VEGFR ATP binding pocket, with 7-methyl-quinoyl-2'5'-dichlorothierylchalcone (figure 21) the most potent for HUVEC cytotoxicity (Rizvi *et al.*, 2012). It was also identified that all bromine derivatives were less potent, and that those with iodine components were deemed inactive, possibly due to the larger size compared to other halogens affecting their fit into the ATP binding pocket. (Rizvi *et al.*, 2012)

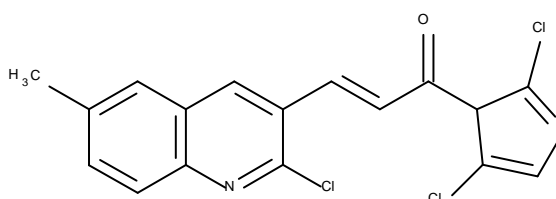


Figure 21 7-methyl-quinoyl,2'5'-dichlorothierylchalcone (Rizvi *et al.*, 2012)

In addition to the reported activities of hydroxylated chalcones, some methoxy derivatives have shown promise in inhibiting endothelial cell proliferation; for example, Bertl *et al.* (2004) identified that 2',2,4-trimethoxychalcone and 3-bromo-2'4'-dimethoxychalcone exhibited selective effects towards endothelial cell line HMEC-1, (0.15 $\mu\text{g/ml}$ and 0.10 $\mu\text{g/ml}$) and HCT116 (0.56 $\mu\text{g/ml}$ and 0.38 $\mu\text{g/ml}$) (Bertl *et al.*, 2004).

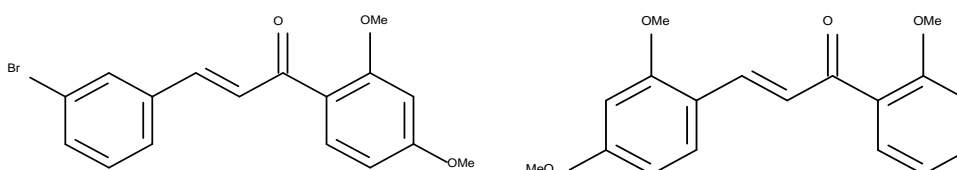


Figure 22 3-bromo-2'4'-dimethoxychalcone (left) and 2',2,4-trimethoxychalcone (right) (Bertl *et al.*, 2004)

Chapter 2: Aims and objectives

2. Aims and Objectives:

Aims:

Nam *et al.* (2003) reported 2-chloro-2'5'-dihydroxychalcone had an IC₅₀ value of 109 nM against HUVEC cell proliferation across 3 days. This simple molecular chalcone displayed selectivity towards endothelial cells compared to HCT116 (colon cancer) and B16 (murine melanoma) cells and brought about promising antiangiogenic activity, yet its analogues 3 and 4-chloro-2'5'-dihydroxychalcone were inactive in comparison (Nam *et al.*, 2003). It raised the question as to why this particular decoration pattern produced antiangiogenic activity compared to other analogues. Therefore, the **aims of this research were to design, synthesise and biological evaluate novel classes of hydroxyl-derivatives with 2-chloro-2'5'-dihydroxychalcone as the parent compound** to:

- better understand what components of the molecule were contributing to the activity observed, through structure activity relationship analyses.
- investigate antiangiogenic activity of the hydroxyl-lead candidates via *in vitro* and mechanistic studies.

Hypothesis:

Change in the decoration pattern of 2-chloro-2'5'-dihydroxychalcone will alter the effects on endothelial cell proliferation and migration, compared to the parent compound.

Null hypothesis:

Change in the decoration patterns of 2-chloro-2'5'-dihydroxychalcone **will not** alter the effects on endothelial cell proliferation and migration.

Objectives:

To achieve this overall aim, the following objectives were put in place.

- 1) Design and synthesise derivatives of 2-chloro-2'5'-dihydroxychalcone as novel antiangiogenic agents, using variations of the Claisen-Schmidt cross aldol condensation.
- 2) Understand SAR of the new compounds via their effects on endothelial cell proliferation. This will add to the previously reported SARs to collectively give a better understanding of the optimal features required on a chalcone scaffold to exhibit anti-endothelial activity. In turn these SARs will help to identify lead compounds from the new analogues.
- 3) Investigate the *in vitro* antiangiogenic functionality of the lead compounds via endothelial migration by using the wound healing assay.
- 4) To perform mechanistic studies on the final lead compounds to delineate their interaction, if any, with the VEGF/VEGFR signalling pathway.

Chapter 3: Synthesis of chalcone derivatives

3.1 Introduction

Manipulation of substituents for lead optimisation has been a widely used method, for fine tuning intermolecular drug-target binding interactions, in hope to increase pharmacological activity (Patrick, 2017). Different approaches are used to improve specific characteristics, for instance phenolic groups can be used to interact with binding sites on protein receptor surfaces via hydrogen bonding.

In general, functional group modifications are vital in understanding the relevance of specific groups on a lead compound. Analogues are made with added or removed groups to determine whether the specific activity is affected by such a change (Patrick, 2017). Of the many, halogen incorporation into the drug scaffold is very commonly used. One of the first uses of halogens in medicinal chemistry were to act as bulk groups in binding sites due to their steric effects (Hernandes *et al.*, 2010). Now, halogens have been used to stabilise protein-ligand complexes as the halogen bond can be viewed as a form of intermolecular interaction. This is why halogens are favourable for binding in protein-protein interactions (Patrick, 2013). Halogenation is also a pre-requisite for compounds designed to pass blood the brain barrier or reach the central nervous system (Gentry *et al.*, 1999; Gerebtzoff *et al.*, 2004)

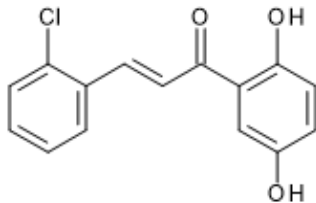
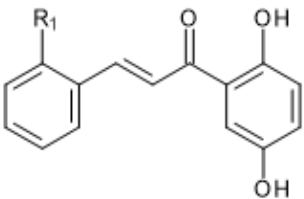
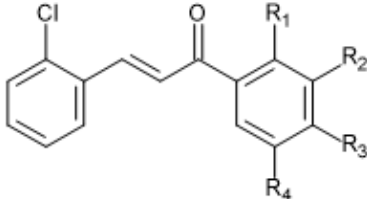
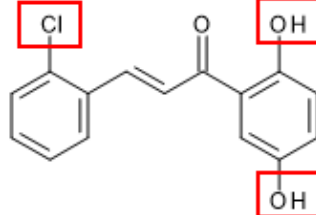
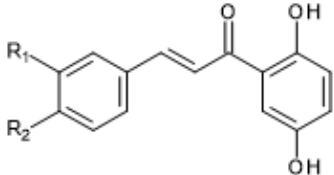
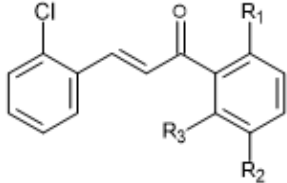
As discussed in chapter 1 Flavopiridol and 2-chloro-2'5'-dihydroxychalcone were key examples of structural modification that significantly increased the desired activity. This formed the basis for the five series of compounds that were synthesised and tested.

This chapter will focus on the synthesis of the compounds. The following chapter (Chapter 4) will discuss in more detail about the rationales of the design and anti-

proliferative activity against HUVECs. A brief rationale as to the design of compounds is described in Table 4

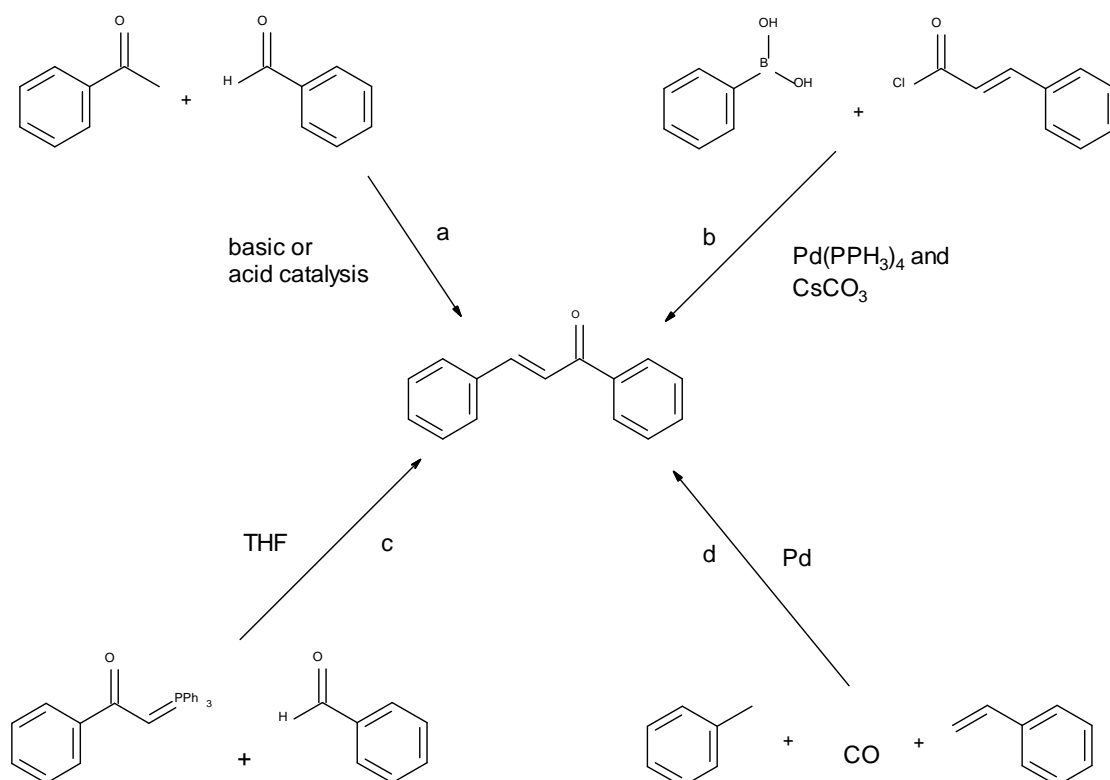
Table 4 Brief rationales as to the compounds designs for this study

Series 1 looks at replacing the chlorine group on the B ring with different functional groups. Series 2 looks at repositioning the hydroxyl groups on the A ring. Series 3 focuses on synthesising part derivatives of the AH1 molecule. Series 4 centres around moving halogen group on the B ring to the 3 and 4 positions. Series 5 is based on synthesising methoxychalcone derivatives equivalent to the hydroxychalcones.

Parent compound AH1 – 2-chloro-2'5'-dihydroxychalcone				
				
Series 1	Series 2	Series 3	Series 4	Series 5
				
Assessing the B ring 2 ortho position by synthesising different ortho substituted dihydroxychalcones	Looking at the importance of the 2'5'-dihydroxy A ring by synthesising 2-chloro chalcones with hydroxyl groups in different positions on the A ring.	Focusing on the parent compound AH1 and assessing what happens when certain components of the molecule are removed. This was done by synthesising "part derivatives" e.g. 2-chlorochalcone and no hydroxyl groups or the 2'5'-dihydroxychalcone without the chlorine group on the B ring.	Re confirming the findings of Nam et al by looking at 3 and 4 positioned halogenated dihydroxychalcones to see the influence of resonance and inductive effects at the 2 and 4 positioned.	Looking at the importance of hydrogen donating vs hydrogen accepting ability of the hydroxyl groups on the A ring. This was done by synthesising methoxy chalcones equivalent (which are only hydrogen accepting ability).

3.1.1 Synthetic approaches to chalcone synthesis

Chalcones are known to exhibit a wide range of pharmacological properties (as discussed in Chapter 1). Therefore, it is not surprising that there are numerous approaches to synthesising this scaffold. Prominent examples include Suzuki Miyaura reaction, Claisen Schmidt condensation, Carbonylative Heck Coupling reaction and Wittig reaction (Climent *et al.*, 1995; Reddy *et al.*, 2001; Eddarir *et al.*, 2003). These are illustrated in Scheme 1. The predominant and most favoured route used out of these is the Claisen Schmidt condensation (Climent *et al.*, 1995). The reasons are that substituted starting materials (benzaldehydes and acetophenones) are readily available to order and saves synthesising them (minimising reaction steps). The route also uses mild conditions without the need of harsh or anhydrous reagents.

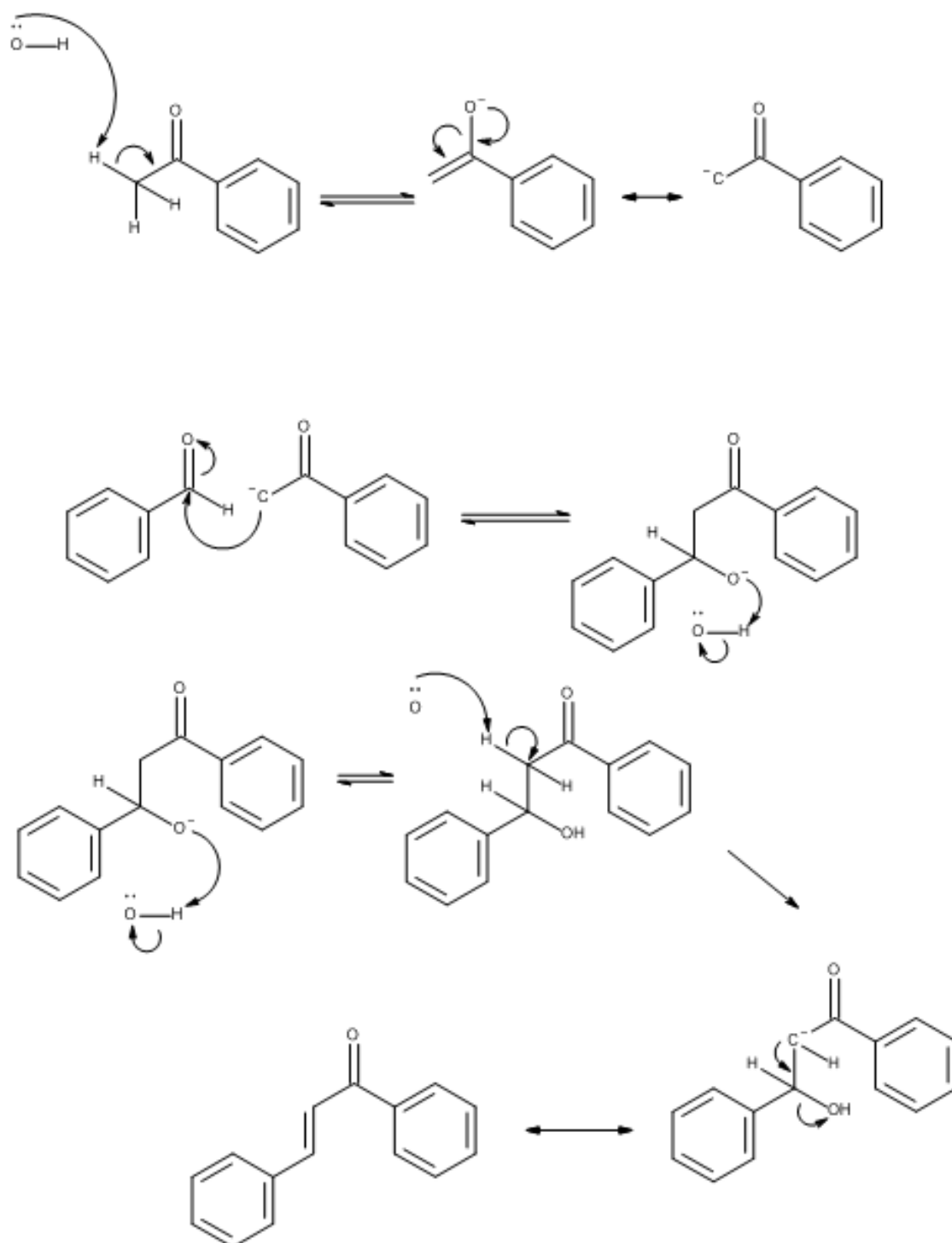


Scheme 1 Different chalcone synthesis routes:

a) Claisen-Schmidt condensation, (Smith and March, 2007); b) Suzuki-Miyaura reaction, (Selepe and Van Heerden, 2013); c) Wittig reaction, (Xu, Chen and Huang, 1995); d) Carbonylative Heck coupling reaction, (Wu *et al.*, 2010).

The Claisen Schmidt condensation is a cross aldol addition-condensation reaction that generally uses equimolar amounts of a benzaldehyde and an acetophenone in the presence of a base or acid catalyst (Wang, 2009). Reaction times and conditions vary depending on route employed and type of chalcone to be synthesised.

For base catalysed reactions, general conditions are mostly room temperature with a short chain alcohol as a solvent (preferably methanol or ethanol) but addition of heat via classical heating or microwave irradiation can be used to drive reactions forward (Wang, 2009). A mechanism for the base catalysed approach is shown in Scheme 2.



Scheme 2 Base catalysed Claisen-Schmidt reaction mechanism

The first step starts off with with deprotonation of the acetophenone to form an enolate, although in equilibrium, it favours the enolate enough to drive the reaction forward. Nucleophilic attack of the enolate on the benzaldehyde's carbonyl group occurs, forming the β -hydroxyketone (aldol). At this stage this intermediate compound can be isolated, but if left to react further, the hydroxide induced elimination of water occurs in a stereoselective manner to form the *trans* alpha beta unsaturated carbonyl compound.

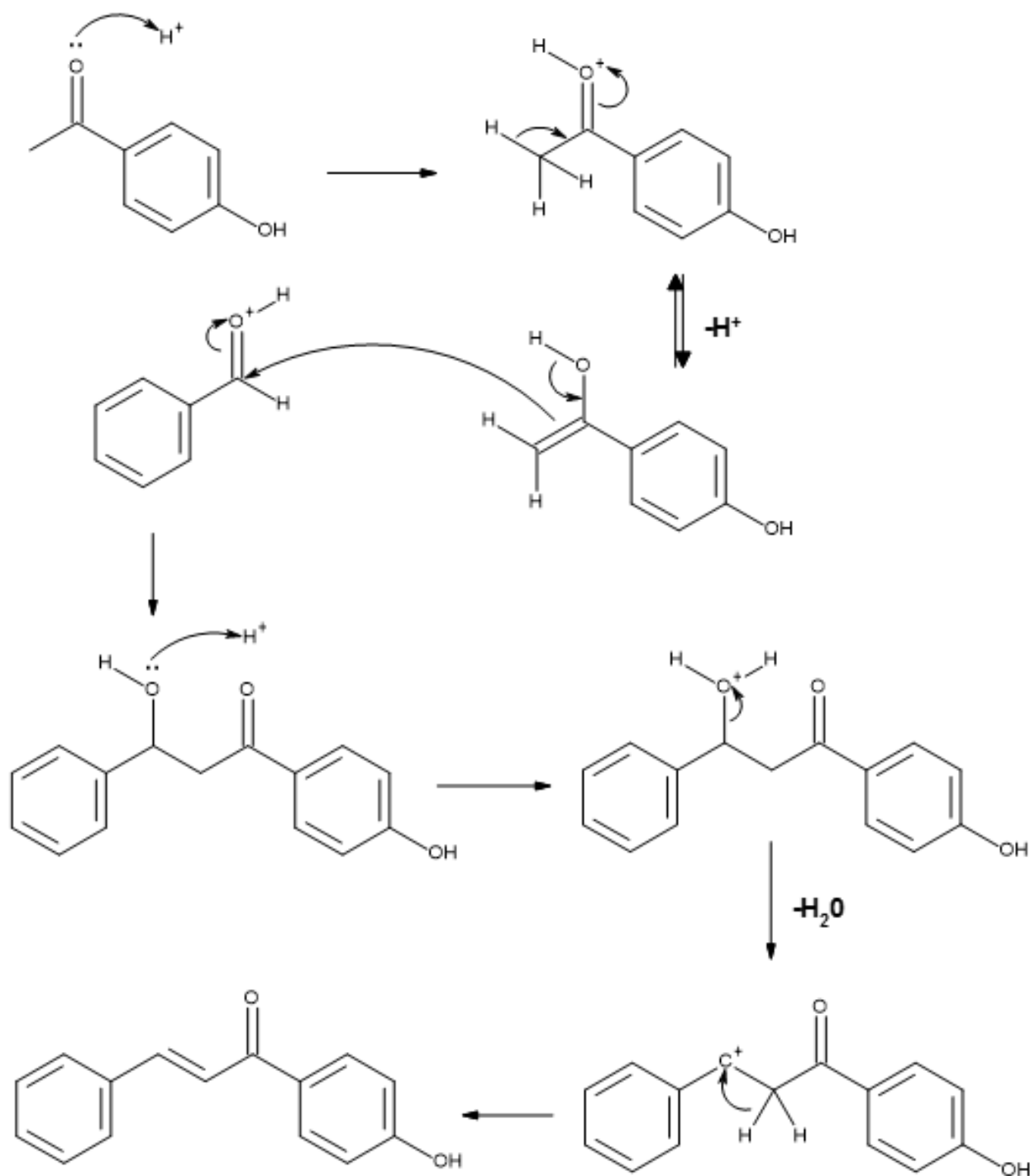
There are many different variations of the base catalysed Claisen Schmidt reaction. Typically, sodium and potassium hydroxide are used and methanol or ethanol the solvent of choice. But lithium hydroxide with ethanol has been successfully used to form a variety of chalcone structure via a dual activation route (Bhagat *et al.*, 2006). In which, the LiOH firstly provides a hydroxide source to form the enolate. Secondly, the Li⁺ cation combines with the oxygen of the aldehyde carbonyl group to form a six-membered cyclic transition ring. This ring causes an increase in the electrophilicity of the aldehyde carbonyl group making it more susceptible to nucleophilic attack by the enolate ion.

Barium hydroxide has been used in several studies to synthesise hydroxyl-based chalcones (Hsieh *et al.*, 2000; Nam *et al.*, 2003; Kumar, Lamba and Makrandi, 2008). Phenolic groups under basic conditions interfere with the formation of the enolate. As a result there are protecting groups like tetrahydropyranyl (THP) ethers and methoxymethyl (MOM) also an ether, are used to mask the phenolic groups during chalcone formation (Wuts, 2014). Other ether based protecting groups like *tert*-butyldiphenylsilyl (TBDPS) and *tert*-butyldimethylsilyl (TBDMS) have also been used, but their instability under strong aqueous base (pH > 12) conditions requires the use organolithium reagents as a base with anhydrous solvents like tetrahydrofuran (THF).

Other approaches vary in the method and conditions used as, Stoyanov et al in 2002 identified that microwave assisted reactions using potassium hydroxide and ethanol yielded a variety of different substituted chalcones in high yields. Including nitro and phenolic substituents without the use of protection groups (Stoyanov *et al.*, 2002). Conducting these reactions in a sealed tube allows the reactions to reach temperatures higher than the boiling point of the solvent. These heat assisted reactions can improve reaction times considerably and remove the need for protective groups or anhydrous conditions.

Solid state or solventless approaches have successfully yielded chalcone compounds, as Kumar et al in 2008 used barium hydroxide with equimolar amounts of benzaldehyde and acetophenone grinded in a pestle and mortar for 2-5 minutes. This was followed by ice cold quenching to precipitate out the chalcone. Filtration of the precipitate and subsequent recrystallisation via ethanol produced the desired product in yields up to 92% (Kumar, Lamba and Makrandi, 2008).

For acid catalysed reactions sulphuric acid has been used as a proton source (Konieczny *et al.*, 2007). *In situ* approaches to generate the proton source have also been looked at with thionyl chloride (SOCl₂), as thionyl chloride reacts with ethanol to generate an ethanolic solution of hydrogen chloride. Another avenue has been to use boron trifluoride etherate (BF₃.OEt₂) that functions as a Lewis acid to catalyse the reactions (Narender and Papi Reddy, 2007; Karki *et al.*, 2012). A mechanism of the acid catalysed approach is shown in Scheme 3.



Scheme 3 Acid catalysed Claisen-Schmidt reaction mechanism

The enol tautomer of the acetophenone attacks the protonated carbonyl group of the benzaldehyde to generate an intermediate aldol. Protonation of the beta hydroxyl group of the aldol is followed by elimination of water via an E1 mechanism to generate the chalcone.

Acid catalysed reactions are not as extensively used when compared with base catalysis for chalcone synthesis. But there are still several routes that successfully yield a variety of chalcones. Phenolic chalcones are heavily investigated for their pharmacological properties and this approach can be very useful for synthesising them, as under these conditions protecting groups of phenolic substituents are not required and reduces the need for additional steps in the overall reaction (Batovska and Todorova, 2010; Orlikova *et al.*, 2011).

The use of boron trifluoride etherate ($\text{BF}_3 \cdot \text{OEt}_2$) with 1,4-dioxane has yielded many types of which bear hydroxyl, nitro, halo and methoxy substituents (Narender and Papi Reddy, 2007; Karki *et al.*, 2012). However, as $\text{BF}_3 \cdot \text{O}$ readily reacts with water in the air, reactions must be carried out under anhydrous conditions.

Chalcones synthesised using thionyl chloride approach can be carried out without the need of an inert atmosphere and has also successfully produced different substituted chalcones, including hydroxyl and nitro groups. These are generally difficult to synthesise under basic conditions (Petrov, Ivanova and Gerova, 2008).

Sulphuric acid as a proton source has been used to yield chalcone derivatives. A combination of sulphuric acid with acetic acid as a solvent has been used to produce oxathiolone fused chalcones (Konieczny *et al.*, 2007). The oxathiolone ring was deemed

more favourable due to its flexibility than Konieczny (2007) and colleagues previous work on aurone derivatives, which are fixed in a flat planar configuration.

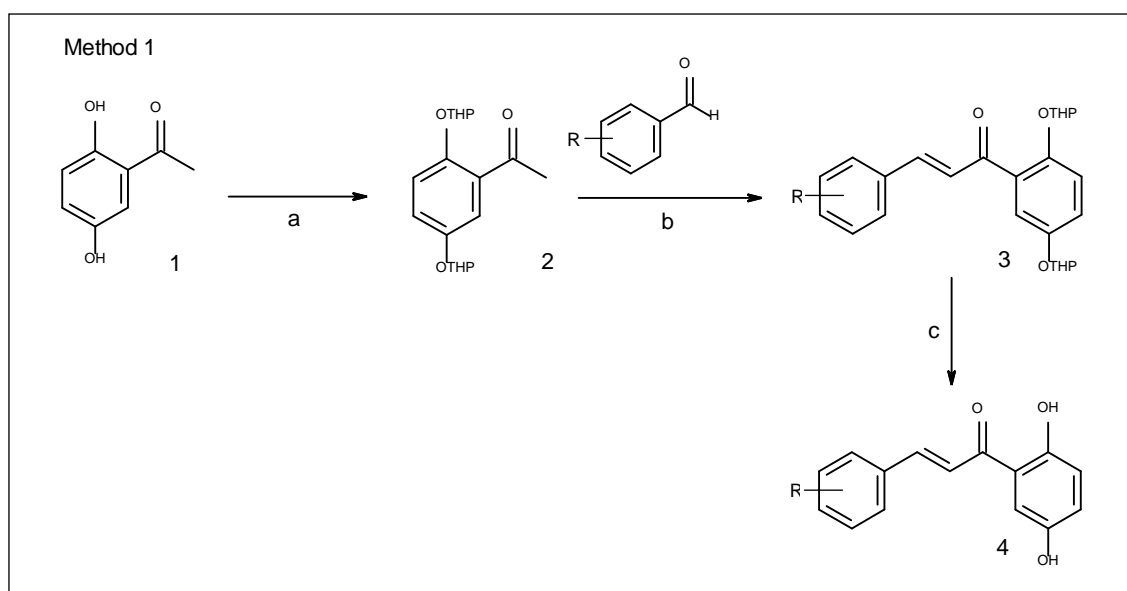
All the chalcones synthesised in this project were carried out using variations of the Claisen Schmidt condensation. Reactions were carried out and chalcones were verified using NMR, MS, FTIR-ATR instruments.

3.2 Results and Discussion:

The code AH was used as a prefix to code each compound synthesised e.g. AH1.

3.2.1 Base catalysis for hydroxychalcone synthesis with THP protection step

For hydroxyl based chalcones, the Claisen Schmidt base catalysed reaction with THP protection was the initial route of choice, as polyphenolic groups hinder enolate formation under normal basic conditions. This was the same route used by Nam et al (2003) to synthesise their 2'5'-dihydroxychalcones (Nam *et al.*, 2003). The scheme of how the THP group is used is shown in Scheme 4 below.



Scheme 4 Method 1 of synthesising dihydroxychalcones (Nam et al., 2003)

Reagents and conditions: (a) pyridinium-*p*-toulenesulphonate, 3-4-dihydro-2H-pyran, anhydrous DCM, r.t. (b) aryl aldehyde, barium hydroxide octahydrate, MeOH, 18hr, r.t. (c) pyridinium-*p*-toulenesulphonic acid, MeOH, 2hr, r.t.

The general procedure for this route was as follows. The dihydroxyacetophenone **1** was dissolved in DCM with pyridinium-*p*-toluene sulfonate (ppts) followed by 3-4-dihydro-2H-pyran. The residue yielded crude protected-acetophenone **2**. The crude protected-acetophenone **2**, barium hydroxide octahydrate and benzaldehyde were dissolved in

methanol and left to stir for 24 hours. This yielded crude protected hydroxychalcone. The protected chalcone **3** and *p*-toluenesulfonic acid were dissolved in methanol for 4 hours. This yielded the crude deprotected chalcone **4** which was purified by recrystallisation from ethanol or propan-2-ol or by flash column chromatography.

AH9, **AH10**, **AH11**, **AH15** and **AH19** were synthesised using the above procedure and verified using NMR, FTIR, MS and HPLC (see Table 5).

Coupling constants of the alkene protons via NMR provides a way to distinguish between *cis* and *trans* configurations, as *trans* give slightly higher values of 12-18Hz compared to 5-14Hz of *cis*. The *trans*-chalcone configuration was confirmed by the larger coupling constants (between 15-18 Hz) see experimental section 8.2.3.2. This was seen as a characteristic two one proton doublets (see figure 23). Secondly the deshielded phenolic protons were seen far downfield (11-15ppm).

For FTIR-ATR, hydrogen bonding of the carbonyl group with phenolic group in A ring ortho position resulted in lower frequency absorption via reduction in double bond behaviour (Williams and Fleming, 1995). This was seen with many of the phenolic chalcones IR spectras bearing A ring 2-position hydroxy groups as the carbonyl peak values were between 1639-1643cm⁻¹ (only **AH12** showing a higher value of 1647 cm⁻¹) which is collectively lower than the standard αβ unsaturated carbonyl peak value between 1685-1665cm⁻¹.

Purity of each compound was validated using HPLC. All compounds showed purity above 95% which was an agreed pre-requisite in order for them to be biologically tested *in vitro*. Figure 24 shows an example of a dihydroxychalcone in MeOH solution ready for UV-VIS analysis, in order to obtain the lambda max needed to run the sample via

HPLC (using a UV-VIS detector). HPLC spectra of **AH9** illustrates the “one peak” representing the one pure compound in the sample.

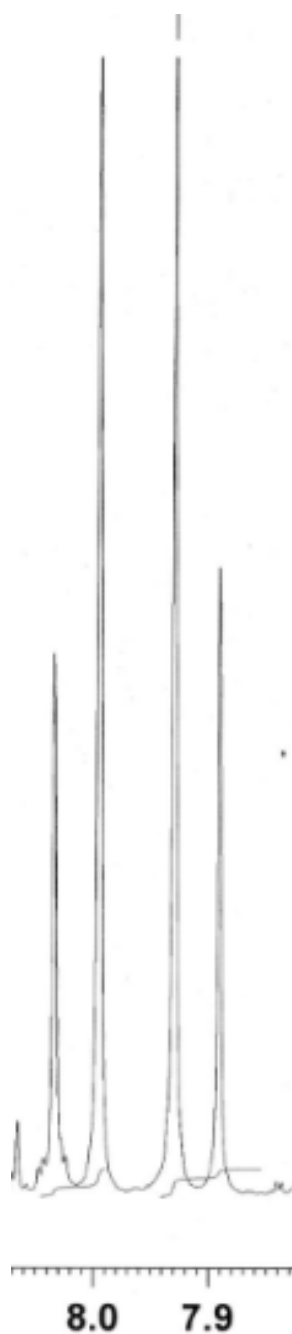
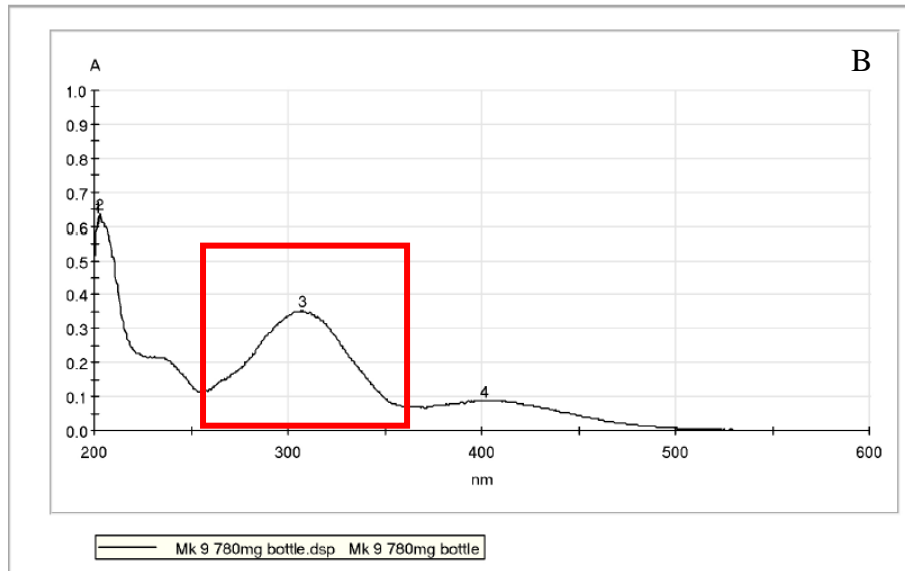


Figure 23 Characteristic two one proton doublets with a large coupling constant (12-18 Hz) found for the trans chalcone configuration



Mk 9 780mg bottle.dsp		Mk 9 780mg bottle	
Maxima	Threshold: 0.01 A		
1 202.0 nm;	0.629 A	2 203.0 nm;	0.637 A
4 401.5 nm;	0.088 A	3 307.5 nm;	0.352 A

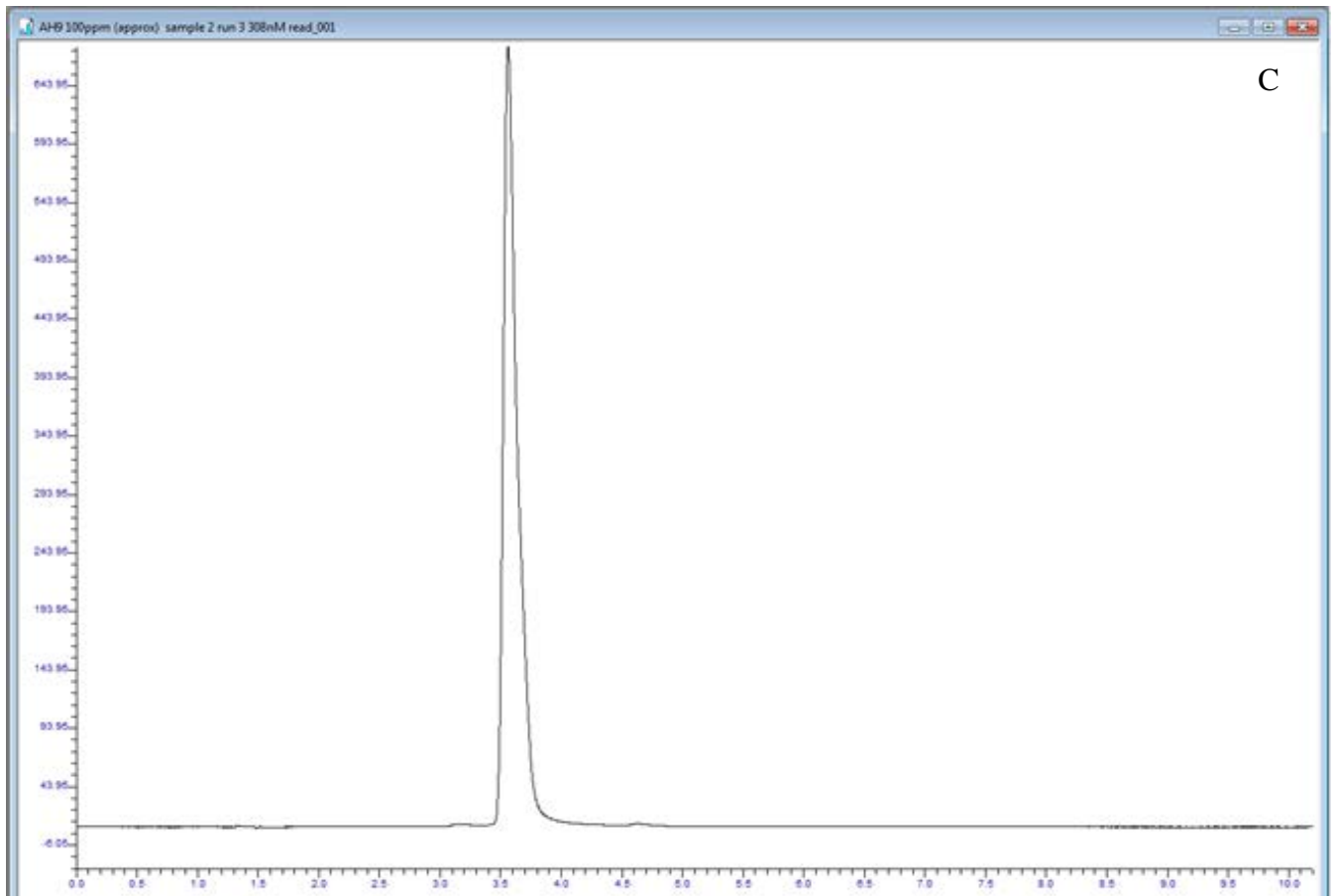


Figure 24 (A) AH9 in EtAc solution. (B) UV-vis spectra of AH9 showing lambda max = 308nm. (C) AH9 HPLC spectra conducted at the lambda max 308 gathered by UV-VIS.

Table 5 Compounds synthesised via method 1

These compounds were purified via recrystallisation from ethanol.

Compound	Ar (B-ring)	Ar' (A-ring)	Yield (%)	m.p (°C)
AH9	2-Br-C ₆ H ₄	2,5-(OH) ₂ C ₆ H ₃	35	177-179
AH10	2-(CH ₃)C ₆ H ₄	2,5-(OH) ₂ C ₆ H ₃	26	174-179
AH15	2-Cl-C ₆ H ₄	2,4-(OH) ₂ C ₆ H ₃		127-130
AH11	2-F-C ₆ H ₄	2,5-(OH) ₂ C ₆ H ₃	26	192-194

AH1, **AH8** and **AH13** were also synthesised via this procedure but did not recrystallise out from flash column chromatography was used (see Table 6). TLC analysis of the final crude mixture for these reactions showed multiple similar polarity spots. Staining the TLC plate with 2-4-diphenylhydrazine to visualise the spots containing a carbonyl groups but it was the visible yellow colour of the chalcone (due to conjugation) that allowed us to identify it amongst the others. Comparing the TLC plates of the protected chalcone mixture vs the deprotected mixture showed that separating out the protected chalcone would be more appropriate given the gap in R_f values between the chalcone, benzaldehyde and aldol. Therefore the protected chalcone was isolated via column chromatography leaving deprotection to yield pure hydroxychalcone.

Table 6 Compounds synthesised via method 1 continued

These compounds were purified via flash column chromatography.

Compound	Ar (B-ring)	Ar' (A-ring)	Yield (%)	m.p (°C)
AH1	2-Cl-C ₆ H ₄	2,5-(OH) ₂ C ₆ H ₃	21	187-189
AH8	2-(OC ₂ H ₅)C ₆ H ₄	2,5-(OH) ₂ C ₆ H ₃	60	89-91
AH13	2-(OCH ₃)C ₆ H ₄	2,5-(OH) ₂ C ₆ H ₃	14	146-149
AH2	3-Cl-C ₆ H ₄	2,5-(OH) ₂ C ₆ H ₃	52	168-170
AH3	4-Cl-C ₆ H ₄	2,5-(OH) ₂ C ₆ H ₃	22	187-188
AH4	3-Br-C ₆ H ₄	2,5-(OH) ₂ C ₆ H ₃	42	152-144
AH5	4-Br-C ₆ H ₄	2,5-(OH) ₂ C ₆ H ₃	17	188-189

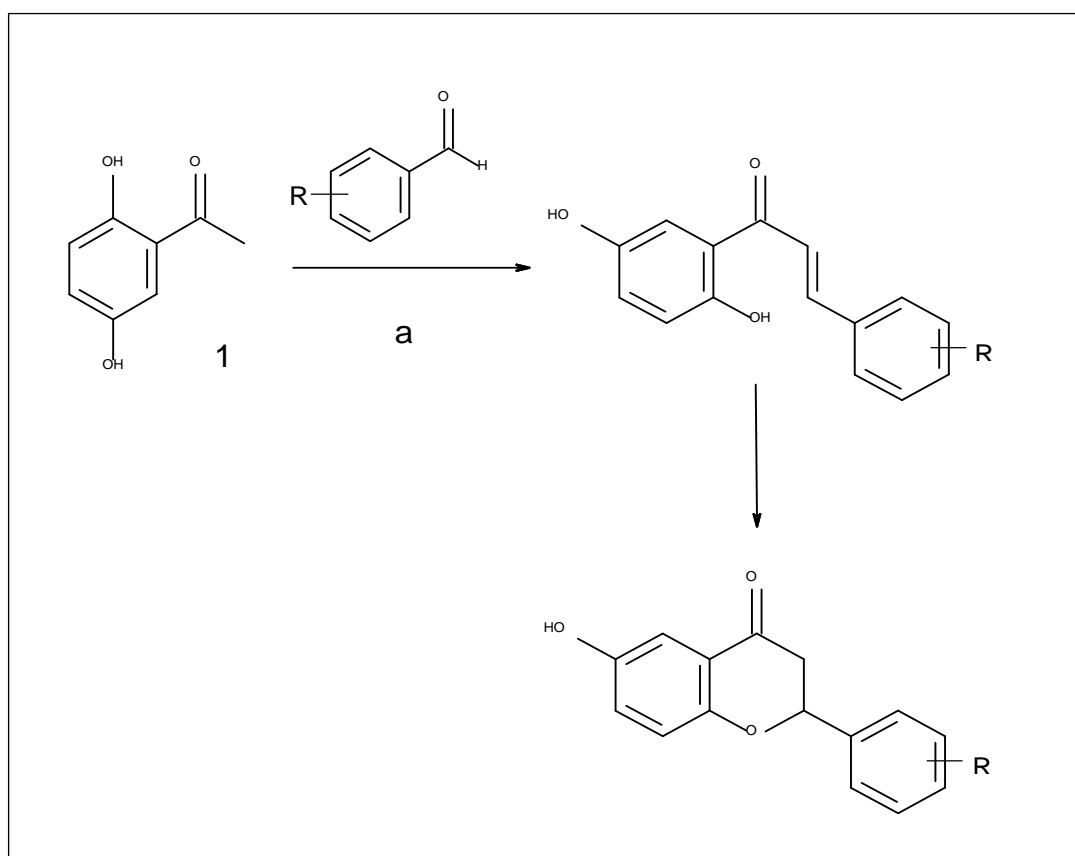
NMR analysis of both **AH8** and **AH13** confirmed the presence of the compound with very similar spectras in the aromatic regions. Both possess an alkoxy group on the B ring ortho positions thus proton splitting patterns were similar. The marked difference was that with **AH8** the CH₃ protons of the ethoxy group contributed to the triplet seen in the aliphatic region of 1.44ppm. The CH₂ protons contributed to the quartet which was seen more downfield (4.17ppm) in comparison due to the neighbouring electronegative oxygen group. Whereas for **AH13**, a singlet was seen at 3.92 ppm corresponding to the CH₃ having no neighbouring protons.

Synthesis of **AH12** (2-nitro-2'5'-dihydroxychalcone) was attempted via this route, but TLC analysis during the chalcone reaction stage revealed no product formation and only the presence of the two starting materials. This agreed with the findings of Nam et al in 2003, as they could not synthesise a nitro-dihydroxychalcone via this route due to the strong electron withdrawing nature of the nitro group hindering aldol formation (Nam *et al.*, 2003). Therefore the reaction was abandoned and another approach was used.

3.2.2 Base catalysis for hydroxychalcone synthesis under pressurised conditions

In an attempt to improve yields of the compounds synthesised (via the THP route) and to minimise the steps required, different conditions were looked at.

This sets of conditions utilised a conventional base catalysed reaction (KOH) and ethanol but in a sealed tube heated up to 132°C for several minutes in an oil bath (Stoyanov *et al.*, 2002). Stoyanov (2002) reported 3 minutes was enough to ensure reaction completion and any further would have caused cyclisation to the dihydroflavone, which is illustrated in scheme 5 below (Stoyanov *et al.*, 2002). AH9 was used as a model reaction.



Scheme 5 Cyclisation of the 2',5'-dihydroxychalcone to a hydroxyl-dihydroflavone if left to react further under the KOH/EtOH reaction conditions in a sealed tube (Stoyanov *et al.*, 2002).

Reagents and conditions: (a) KOH, EtOH - μ W or 132°C

Several reactions were carried out at with different reaction times to assess at what time flavone formation occurs. Despite Stoyanov and colleagues stating that no flavone would be produced after 3 minutes, the TLC analysis showed both chalcone and potential flavone formation. Shorter times showed starting materials and longer durations showed decomposition and minimal chalcone formation. Some chalcone was isolated but only afforded enough for proton NMR analysis.

Therefore due to the breath of resources (silica and solvents) required to just afford enough 4-5mg the reaction was deemed unfeasible for multiple chalcone syntheses and thus other avenues were explored.

3.2.3 Acid catalysis for hydroxychalcone synthesis using thionyl chloride

This acid catalysis route consisted an ethanolic solution of hydrogen chloride generated from thionyl chloride and ethanol. Initially, investigation into the synthesis of a monohydroxy analogue was first looked at to see if this could be synthesised, as Petrov (2008) reported successful synthesis of 4-hydroxychalcone (Petrov, Ivanova and Gerova, 2008). **AH16** (2-chloro-4'-hydroxychalcone) was reacted using the following protocol. Equimolar quantities of the acetophenone and benzaldehyde were dissolved in ethanol followed by dropwise addition of thionyl chloride (1.6eq) and allowed to react overnight. Quenching with water induced a precipitate. TLC analysis confirmed chalcone formation which was further verified by NMR and MS.

Table 7 Compound synthesised via the acid catalysis route using thionyl chloride

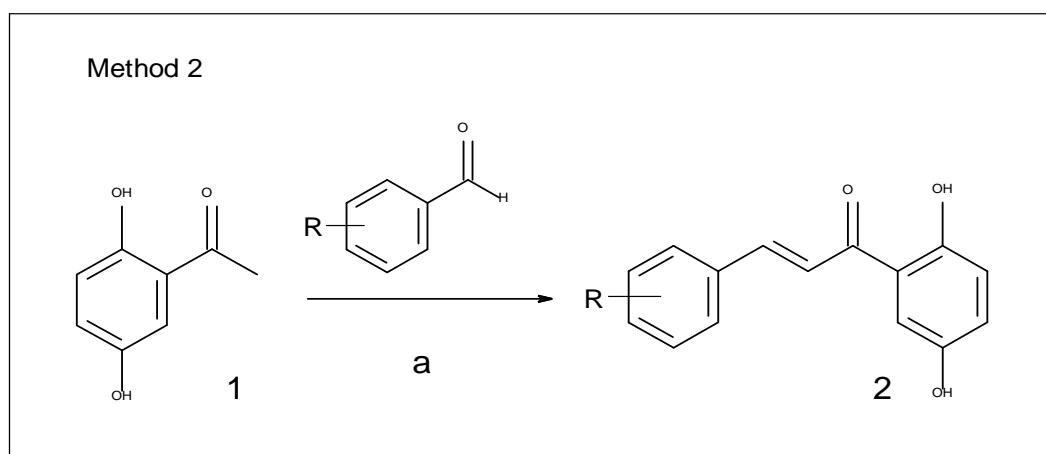
This compound were purified via recrystallisation by ethanol.

Compound	Ar (B-ring)	Ar' (A-ring)	Yield (%)	m.p (°C)
AH16	2-ClC ₆ H ₄	4-(OH)C ₆ H ₃	25	167-169

This route synthesised **AH16** and yielded 25%. The route was then used to try and synthesise **AH12**. Sticky residue was apparent after quenching, TLC analysis showed baseline decomposition and no indication of any chalcone formation. Repeating the reaction with 10x the amount of thionyl chloride was attempted but no improvement in reaction progression was seen. As a result, this approach was stopped and another route was considered.

3.2.4 Acid catalysis for hydroxychalcone synthesis using sulphuric acid.

As the thionyl chloride or pressurised routes did not successfully yield dihydroxychalcones another route was looked at. The route involved the use of sulphuric acid as the proton source coupled with acetic acid as the solvent (Konieczny *et al.*, 2007).



Scheme 6 Method 2 of synthesising dihydroxychalcones (Konieczny *et al.*, 2007)

Reagents and conditions: (a) CH₃COOH, H₂SO₄, 80°C, 18hr.

The general procedure is as follows. Equimolar quantities of the acetophenone and benzaldehyde were dissolved in acetic acid followed by dropwise addition of conc sulphuric acid. The reaction was stirred at 80°C until reaction completion. **AH12** was attempted via this route, TLC analysis after several hours of reacting showed presence of the chalcone but that it was co running with the acetophenone in the mixture. After allowing the reaction to occur for several days, no improvement in furthering the reaction was seen. The co-running spots would cause difficulty in purification, therefore repeating the reaction with a slight modification was carried out. This reaction used a slight excess of benzaldehyde (1:1.1 ratio) to ensure that all the acetophenone would be used up. After 24 hours of reacting TLC analysis showed only chalcone formation and benzaldehyde but no acetophenone. On top of this solid precipitate was formed, recrystallisation from

ethanol afforded the chalcone with 27% yield. Monohydroxychalcones (AH17 and AH17a) was also successfully synthesised via this route.

This route was used to synthesise a nitro-dihydroxychalcone without the use of protecting steps or anhydrous/aprotic conditions in a one pot synthesis approach. For structure determination of AH12, FTIR-ATR identified NO₂ peaks at 1345 and 1517 cm⁻¹ along with the C=O (1647 cm⁻¹) and OH (3396 cm⁻¹) peaks.

Due to the success of this route of reaction, AH1 was resynthesised via this route in an attempt to improve the yield of the parent compound without using additional protection steps. Only a slight improvement in yield was seen.

Table 8 Compounds synthesised via the acid catalysis route using sulphuric acid.

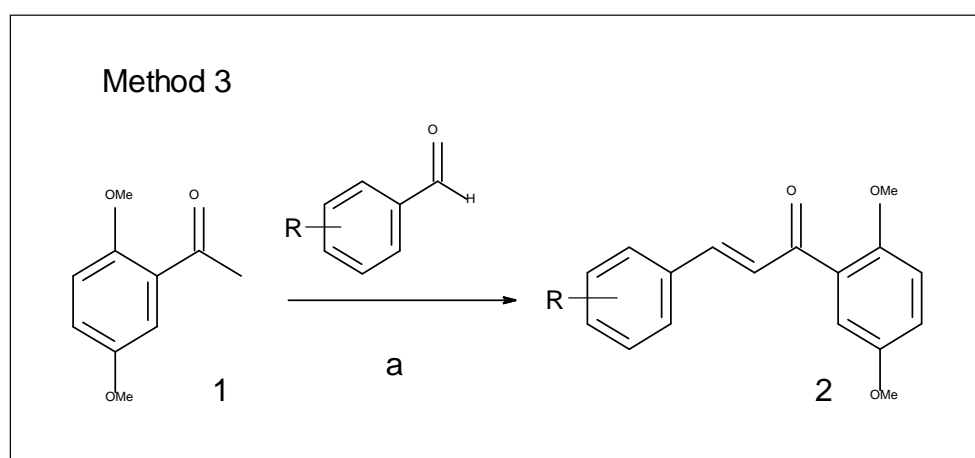
These compounds were purified via recrystallisation by ethanol.

Compound	Ar (B-ring)	Ar' (A-ring)	Yield (%)	m.p (°C)
AH12	2-NO ₂ -C ₆ H ₄	4-(OH)C ₆ H ₃	25	190-192
AH1	2-Cl-C ₆ H ₄	2,5-(OH) ₂ C ₆ H ₃	29	187-189
AH17a	2-Cl-C ₆ H ₄	2-(OH)C ₆ H ₃	18	77-81
AH17	2-Cl-C ₆ H ₄	3-(OH)C ₆ H ₃	20	112-115

To add, resynthesis of AH8 and AH13 via this route were unsuccessful. This suggested that the route is favourable to certain substituted dihydroxychalcones. But further testing is required to explore this hypothesis.

3.2.5 Base catalysis for methoxychalcone synthesis

A base catalysed Claisen-Schmidt condensation was used to yield the non-hydroxyl based chalcones. A few different combinations of base with MeOH or EtOH were attempted, for instance 50% aq NaOH with MeOH, 10eqv Ba(OH)₂ with MeOH and LiOH with EtOH (Bhagat *et al.*, 2006; Kumar, Lamba and Makrandi, 2008). But the most efficient route with the highest yields was using 20% aq KOH with EtOH for these halogenated dimethoxy derivatives (Detsi *et al.*, 2009).



Scheme 7 Method to synthesise dimethoxychalcone (Detsi *et al.*, 2009)

Reagents and conditions: (a) EtOH, 20% KOH (aq), RT, 18hr.

Table 9 Compounds synthesised via the base catalysis route using either NaOH, LiOH or Ba(OH)₂.

These compounds were purified via recrystallisation by ethanol. * = 2nd standard compound from (Bertl *et al.*, 2004).

Compound	Ar (B-ring)	Ar' (A-ring)	Yield (%)	m.p (°C)
AH21	2-Cl-C ₆ H ₄	2,5-(OCH ₃) ₂ C ₆ H ₃	55	88-92
AH21a	2-Cl-C ₆ H ₄	2,6-(OCH ₃) ₂ C ₆ H ₃	56	132-139
AH21b	2-Br-C ₆ H ₄	2,5-(OCH ₃) ₂ C ₆ H ₃	88	100-102
AH21c	2-Br-C ₆ H ₄	2,6-(OCH ₃) ₂ C ₆ H ₃	61	159-160
AH22	2-Cl-C ₆ H ₄	2,4-(OCH ₃) ₂ C ₆ H ₃	67	112-115
AH22a	2-Br-C ₆ H ₄	2,4-(OCH ₃) ₂ C ₆ H ₃	81	123-125
AH22b	3-Cl-C ₆ H ₄	2,4-(OCH ₃) ₂ C ₆ H ₃	81	123-125
AH22s2*	3-Br-C ₆ H ₄	2,4-(OCH ₃) ₂ C ₆ H ₃	80	89-90
AHXRS1	2-Cl-C ₆ H ₄	C ₆ H ₃	91	52-54

Structure determination by NMR confirmed the chalcones were synthesised. As along with the characteristic alkene protons and aromatics between 6-8ppm, the methoxy protons were apparent as singlets around 3.9ppm just after the water peak (3.4ppm) of the deuterated DMSO solvent.

3.3 Conclusion

Dihydroxychalcone derivatives (**AH1**, **AH2**, **AH3**, **AH4**, **AH5**, **AH8**, **AH9**, **AH10**, **AH11**, **AH13** and **AH15**) were synthesised successfully using the base catalysed Claisen-Schmidt condensation with THP protection step. **AH12** could not be synthesised via this route, due to the strong EWG nature of the nitro group hindering enolate formation. Different base catalysed conditions were looked at including: heating the reaction to 132°C in a sealed tube and grinding the starting materials in a pestle and mortar. Both reaction methods were unsuccessful in yielding **AH12**.

Acid catalysed routes were also looked at. At first, *in situ* formation of the proton source via thionyl chloride and EtOH was attempted, **AH16** a monohydroxy derivative was synthesised successfully (yield 25%) but in this study dihydroxychalcones synthesis via this route were all unsuccessful despite reports of this in literature (Jayapal, Sreenivasa Prasad and Sreedhar, 2010). The use of sulphuric acid as an acid catalyst with acetic acid as a solvent successfully yielded a nitro-dihydroxychalcone (**AH12**, 25%) in a one pot procedure. This was otherwise unable to be made with the conventional THP protection base catalyse route. **AH1** was also made via this route and yielded a slightly more than the THP protection route (29 % to 21%). However given that multiple steps were needed for the protection route, when compared to the one pot synthesis via sulphuric acid/acetic acid route, the reduction in synthetic steps could be seen as an improvement in the synthesis of **AH1**.

Chapter 4: Screening and biological
evaluation of the synthesised
chalcone derivatives

4.1 Introduction:

Proliferation assays conducted on endothelial cells are a common way to screen compounds to identify lead candidates with possible antiangiogenic activity (Nam *et al.*, 2003). A cell-based screening process was carried out against the synthesised chalcone derivatives to assess anti-proliferative activity of the compounds towards HUVECs as well as understanding how changes in substitution patterns affect the anti-endothelial activity observed. The main aim of this piece of work was to identify lead compounds of interest to further test from.

HUVECs are seen as one of the common endothelial cell models to assess angiogenesis due its primary origin and ease of cell isolation (Staton, Lewis and Bicknell, 2007), as a result they are a widely accepted model (Morales *et al.*, 1995; Tsujii *et al.*, 1998; Ridgway *et al.*, 2006; Zhong *et al.*, 2012; Su *et al.*, 2016).

Several types of proliferation assays are used to assess drug induced cytotoxicity. Some use variations of tetrazolium salts like WST-1, XTT and commonly used MTT. The MTT assay measures the colourmetric conversion of a yellow water soluble dye to an insoluble purple formazan product which is catalysed by mitochondrial dehydrogenases in viable cells, this is demonstrated in figure 25 (Denizot and Lang, 1986). The MTT reagent is positively charged and can easily penetrate cells, whereas the WST-1 and XTT are negatively charged and require an intermediate electron acceptor in order to penetrate cells (Riss *et al.*, 2004). This is one the reasons why the MTT assay is more commonly used. The absorbance measured (560nm) via spectrophotometry is proportional to the number of living cells present (Denizot and Lang, 1986). Therefore this assay can be used for assessment of both endothelial cell viability and cell proliferation, as a result it was

the assay of choice for this study (Mosmann, 1983; Denizot and Lang, 1986). The preliminary screening process comprises of using one concentration of each drug, allowing for quick identification of potential lead candidates for further pharmacological analysis.

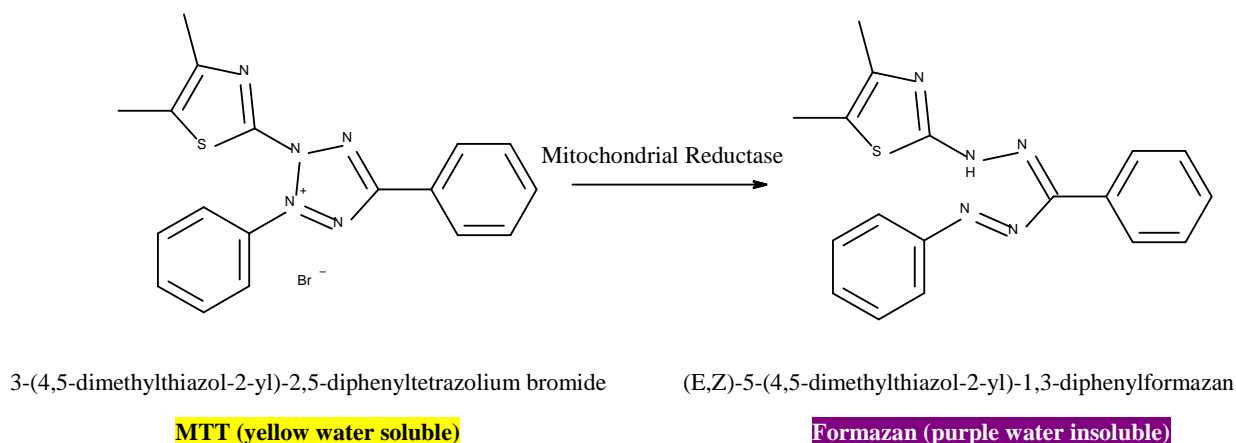


Figure 25 Chemical structures of the MTT reagent and Formazan product.

The MTT reagent is reduced by the mitochondrial reductase to form the purple formazan product. This can only be carried out by living cells and therefore is used as a measure to assess cell viability and cell proliferation.

Several drug discovery studies have used this approach of a single concentration screen.

Cabrera and colleagues (2007) adopted a one concentration method to screen a group of chalcones, flavones and flavanones. A 10 μM screen was utilised by Bandgar et al 2010 to elucidate lead candidates from a library of simple methoxylated chalcones. (Cabrera *et al.*, 2007; Bandgar *et al.*, 2010; Dias *et al.*, 2013). To identify lead compounds from a library of chalcones and flavanols, Dias and colleagues (2013) used a 15 μM screen.

Early screening assays generally use concentrations within 1-10 μM to identify possible lead candidates (Hughes *et al.*, 2011). The lead compounds EC_{50} concentrations usually fall within the range of 100 nM - 5 μM (Hughes *et al.*, 2011; Yusof *et al.*, 2014). This is one of the “HIT” criteria mentioned in Chapter 1.4.1. As discussed in Chapter 3, AH1 (2-

chloro-2'5'-dihydroxychalcone) was the parent compound used for this study of which the synthesised compounds have been modelled from (Figure 26).

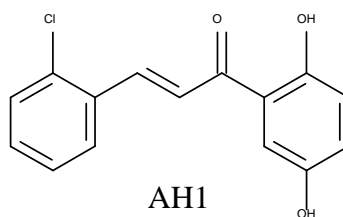


Figure 26 Chemical structure of AH1 (2-chloro-2'5'-dihydroxychalcone). The parent compound for this study.

Initially a preliminary three concentration screen was carried out at 100 μ M 10 μ M and 1 μ M. Compounds at 100 μ M displayed potent activity with little variations in effects between the compounds suggesting the 100 μ M was too concentrated. At 1 μ M anti-proliferative activity was minimal with again very little discrepancies between the compounds, suggesting too dilute of a concentration. But at 10 μ M there was clear differences in activity to conduct Quantitative structure activity relationships (QSARs) and thus it was the chosen concentration to take forward. EC_{50} of these lead candidates were evaluated (Yusof *et al.*, 2014). Three day incubation of the drugs was used for all anti proliferative studies (both preliminary and main experiments) to allow for comparison with the parent compound data, as Nam et al (2003) performed their experiments across 3 days allowing time for cell proliferation to occur.

4.2 Results and discussion:

4.2.1 Anti-proliferative activity:

Following, is a report of the rationales for the groups of compounds synthesised and the data gathered for each of them with structure activity relationship analyses. This is followed by a table representing the percentage reduction in HUVEC viability \pm SEM at 10 μ M for each particular series.

4.2.1.1 Substituent changes of the B ring 2 position to assess the importance of the chlorine group in AH1 (series 1)

As discussed in Chapter 1.5.2 studies by Nam and colleague antiangiogenic activity of 2-chloro-2'5'-dihydroxychalcone (AH1) was greatly dependent on the positioning of the chlorine group on the benzaldehyde ring (B ring) (Nam *et al.*, 2003). Therefore this group of compounds was developed to better understand the importance of the B ring 2-position by synthesising various 2-positioned substituted 2'5'-dihydroxychalcones. For instance, a methyl group was used to assess if bulking the 2 position would cause significant activity. Bromine substitution was put in to see if an increase in size of the atom with similar electronegativity could cause an increase in activity. Stronger EWGs such as a nitro group were employed to see if further reducing the electrophilicity of the β carbon would contribute to more potent activity. In comparison, ERGs like methoxy and ethoxy were used to assess what affect they would have at the ortho position specifically compared to the parent compound and other EWG analogues.

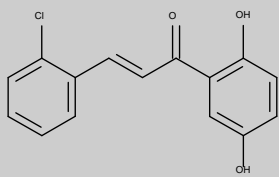
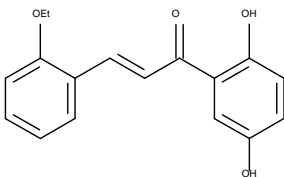
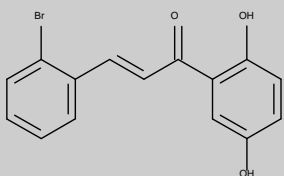
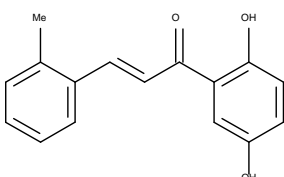
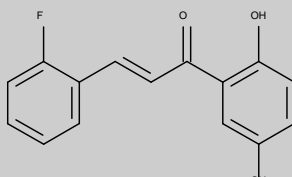
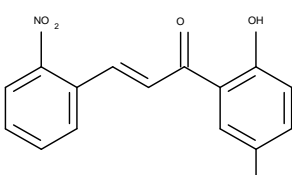
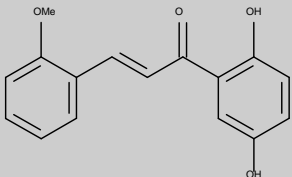
Within this series of dihydroxychalcones, anti-proliferative activity was greatly influenced by the functional group at the B ring 2 position, as hypothesised. The parent compound **AH1** exhibited $95\% \pm 1.64$ reduction in HUVEC viability at $10 \mu\text{M}$, **AH9** also exhibited potent activity ($79.62\% \pm 4.45$). This indicated that the bromine group was showing similar effects to the chlorine group in exhibiting the anti-endothelial activity observed at that position. **AH11**, bearing the fluorine group, showed weaker activity ($67.96\% \pm 2.47$) compared to **AH1** and **AH9** but still higher than the unsubstituted 2-position 2'5'-dihydroxychalcone (**AHXRS3**, see series 3). This is line with the studies conducted by Nam et al (Nam *et al.*, 2003). Fluorine is the most electronegative halogen, but occupies the same size in space as hydrogen. Given that chlorine and bromine are less

electronegative but larger in size, points towards the size of the substituent being an important factor in the activity observed at the 2-position. This links back to Cheng et al 2010 hydroxyaurone study, as they concluded that the size and shape of the substitute group was more important than the electronegativity at least in terms of anti-proliferative activity against HUVECs (Cheng *et al.*, 2010).

When assessing the importance of electronegativity, both alkoxy ortho (**AH8** and **AH13**) derivatives displayed lesser activity ($56.86\% \pm 6.90$, $49.29\% \pm 7.47$) upon affecting HUVEC viability compared to **AH1**. Both –OMe and –OEt are ERG in the 2 position compared to –Cl (**AH1**) and –Br (**AH9**) which are weakly EWG (also in the 2 position).

The results of the changes in electronegativity were in accordance to Nam et al 2003 findings of EWG groups on the B ring being more favourable to cause cytotoxicity to HUVECs. **AH10**, an alkyl derivative, used as a substituent to increase lipophilic interactions and as a bulking agent showed reduced activity by 44% ($50.09\% \pm 3.82$) when compared with **AH1**. **AH12** bearing a strong EWG of –NO₂ at the 2 position showed strong anti-proliferative activity at 10 μM ($87.33\% \pm 2.77$), similar to **AH1** and **AH9**. This strongly reinforced, the view that Nam and colleagues had, that increasing the electrophilicity of the β carbon via EWG on the B ring (Nam et al 2003) would increase anti-proliferative activity, especially when compared to the ERGs on **AH8** and **AH13**.

Table 10 Summary of structure and biological activity for Series 1

<i>Compound</i>	<i>Structure</i>	<i>Reduction in HUVEC viability</i> ^{a,b} \pm SEM
AH1		94.94 \pm 1.64
AH8		56.86 \pm 6.90
AH9		79.62 \pm 4.45
AH10		50.09 \pm 3.82
AH11		67.96 \pm 2.47
AH12		87.33 \pm 2.77
AH13		49.29 \pm 7.47

a = Values are means \pm SEM of four independent experiments. Data expressed as a % vs untreated control.

b = Compound administered at 10 μ M concentrations. DMSO 0.1% was used as a normalisation control.

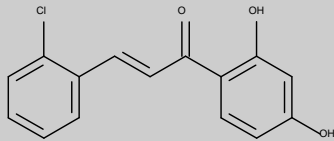
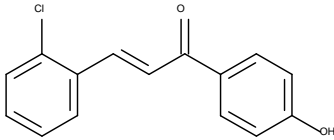
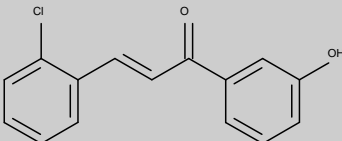
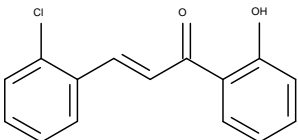
4.2.1.2 Position changes of the A ring hydroxyl groups to assess the importance of 2'5'-dihydroxy moiety of AH1 (series 2)

From the study by Nam et al (2003), it was evident that the ortho positioned chlorine group on B ring was important for the activity observed. But no real investigation was carried out to assess the importance of the 2'5'-dihydroxy A ring moiety. Thus this series was designed to assess the importance of this, by varying the substitution patterns.

Repositioning the hydroxyl groups to a 2'4'-dihydroxy A ring was looked at to form **AH15**. Mono equivalents in ortho and para positions were synthesised to investigate 2-chloro-monohydroxy activities compared to the parent compound.

From the anti-proliferative data, we found that moving the hydroxyl group from 5'-position to the 4'-position (*i.e.* **AH1** to **AH15**) reduced the activity by 30%. A similar result was obtained when the 5'-hydroxy group was removed as in **AH17a** ($56.67\% \pm 2.70$). This was first suggesting that there is importance of the 2'5'-dihydroxy moiety specifically that orientation over the 2'4'-dihydroxy. Secondly, the fact that **AH17a** bearing the 2' positioned-hydroxyl group only showed weak activity in relation to **AH1**, suggests that the ortho-hydroxyl group alone was not sufficient to cause activity. To add **AH16** bearing only a single hydroxyl groups in the 4'-positions exhibited 55% but moving the hydroxyl group to the 3' position, **AH17**, reduced the activity to 15%. This was suggesting that the 3'-positioned hydroxyl group was unfavourable for exhibiting anti-proliferative activity. This further supports the importance of the 2'5'-dihydroxy moiety on the A ring specifically in relation to the anti-proliferative activity of **AH1** towards HUVECs.

Table 11 Summary of structure and biological activity for Series 2

<i>Compound</i>	<i>Structure</i>	<i>Reduction in HUVEC viability</i> ^{a,b} \pm SEM
AH15		61.00 \pm 1.78
AH16		54.79 \pm 1.92
AH17		15.35 \pm 4.39
AH17a		56.67 \pm 2.70

a = Values are means \pm SEM of four independent experiments. Data expressed as a % vs untreated control.

b = Compound administered at 10 μ M concentrations. DMSO 0.1% was used as a normalisation control.

4.2.1.3 Assessing part derivatives of AH1 to see what substituents are key to the activity observed (series 3)

Another approach was used here to focus on the parent compound itself by identifying active components of the 2-chloro-2'5'-dihydroxychalcone molecule (**AH1**). This was done by synthesising part derivatives of the parent compound as seen in Table 8 to see the importance of the second phenyl ring but keeping the alpha beta unsaturated ketone moiety and chlorophenyl in place. This would help determine at what point does the observed activity drop off and therefore help in determining the components responsible for the antiangiogenic activity observed. The following **XRS** suffix refers to the compounds that were designed as part derivatives of **AH1** in this particular series.

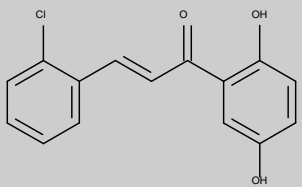
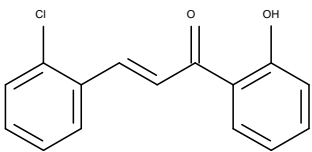
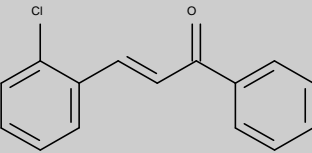
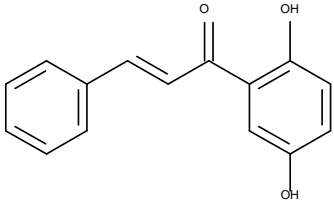
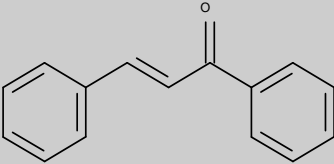
It was interesting to see for **AHXRS1** that removing the 2'-hydroxyl from **AH17a** does not reduce activity *i.e.* both exhibiting similar inhibitory activities (56% and 57%). **AHXRS1** showed no improved anti-proliferative effect towards HUVECs compared to **AH17a**. To add **AHXRS3** showed less activity compared to AH1 (82% reduction), this is in line with the findings Nam and colleagues concluded in their study (Nam *et al.*, 2003). This further proves that the 2'5'-dihydroxy moiety alone is not sufficient enough to cause potent anti-proliferative activity against HUVECs. Collectively for this particular series the SARs data showed that yes the ortho chlorine group on the B ring is important, but only in conjunction with a dihydroxy moiety on A ring specifically for maximum anti-endothelial effect on HUVECs.

Between the **AHXRS** compounds it was remarkable to see that between **AHXRS3** and **AHXRS4** there was only a slight difference in activity (13% to 21%). But when comparing **AHXRS1** and **AHXRS4**, **AHXRS1** showed greater reduction in HUVEC

viability than **AHXRS4** (50% to 21%). Collectively, this further supports the concept that the ortho-chlorine group on the B ring contributes more to the overall activity of **AH1** than the 2'5'-dihydroxy moiety.

Looking back on the work of Lee et al 2012 on antiangiogenic diphenylpropenones, they reported similar activity for **AHXRS4** against HUVECs using the same cell viability assay (Lee *et al.*, 2012). What is clear is that modifying the parent compound **AH1** does alter the activity observed. This rejects the null hypothesis first proposed in Chapter 2 which was that changing the decoration pattern of **AH1** would *not* alter the anti-endothelial activity.

Table 12 Summary of structure and biological activity for Series 3

<i>Compound</i>	<i>Structure</i>	<i>Reduction in HUVEC viability^{a,b} ± SEM</i>
<i>AH1</i>		94.94 ± 1.64
<i>AH17a</i>		56.67 ± 2.70
<i>AHXRS1</i>		50.14 ± 10.11
<i>AHXRS3</i>		13.62 ± 8.07
<i>AHXRS4</i>		21.87 ± 8.25

a = Values are means ± SEM of four independent experiments. Data expressed as a % vs untreated control.

b = Compound administered at 10 µM concentrations. DMSO 0.1% was used as a normalisation control.

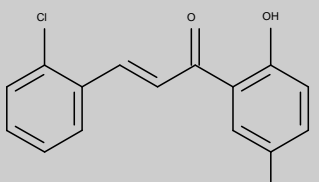
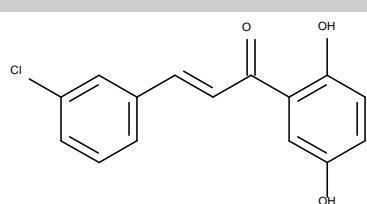
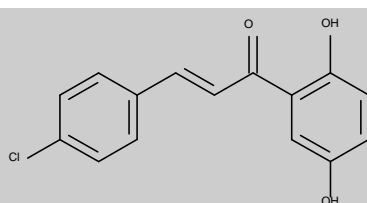
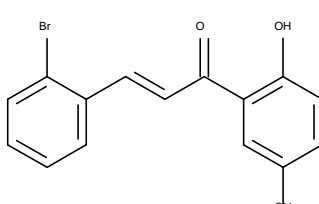
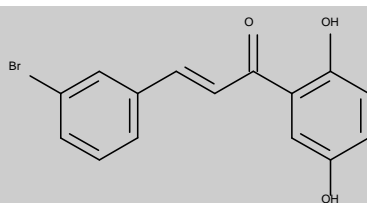
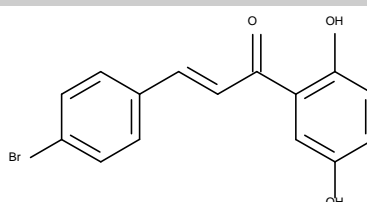
4.2.1.4 Position changes of the halo group on the B ring to further confirm the importance of the halo group at B ring 2 position (series 4)

After establishing the importance of 2-chlorophenyl in the activity of **AH1** over the 2'5'-dihydroxy moiety, the next phase was look 3 and 4 positioned halogenated derivatives. As **AH11** (2-fluoro-2'5'-dihydroxychalcone) did not exhibit significant activity and **AH9** (2-bromo-2'5'-dihydroxychalcone) did, only chlorinated and brominated derivatives were synthesised and not fluorinated. This series was also put together to re confirm the finding of Nam et al and colleagues as they concluded that 3-chloro, 4-chloro and 4-bromo-2'5'-dihydroxychalcone did not show significant activity compared to 2-chloro-2'5'-dihydroxychalcone (**AH1**) as highlighted earlier (Nam *et al.*, 2003).

All 3 and 4 positioned derivatives (**AH3**, **AH4**, **AH4** and **AH5**) showed lesser activity than that of **AH1** and **AH9**. This helps to prove that for **AH1** and **AH9** the positioning of the halophenyl in the 2-position was important to the anti-proliferative activity found.

At the 2 and 4 positions on the B ring both inductive and resonance effects are operating, but at the 3 position only inductive effects occur. To add, at the 2 position steric influences *i.e.* the size of the substituent are also a key factor. Therefore having established that for these particular compounds, the steric effects at the 2 position maybe contributing more to the anti-proliferative activity than the inductive and resonance effects that are also operating.

Table 13 Summary of structure and biological activity for Series 4

<i>Compound</i>	<i>Structure</i>	<i>Reduction in HUVEC viability^{a,b} ± SEM</i>
AH1		94.94 ± 1.64
AH2		45.23 ± 12.70
AH3		66.23 ± 3.20
AH9		79.62 ± 4.45
AH4		67.11 ± 4.98
AH5		68.40 ± 1.57

a = Values are means ± SEM of four independent experiments. Data expressed as a % vs untreated control.

b = Compound administered at 10 µM concentrations. DMSO 0.1% was used as a normalisation control.

4.2.1.5 Replacement of hydroxyl groups with a methoxy group to assess the importance of hydrogen donation on the A ring (series 5)

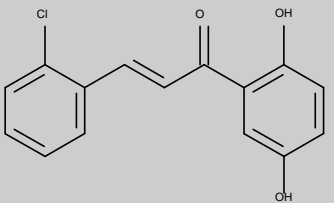
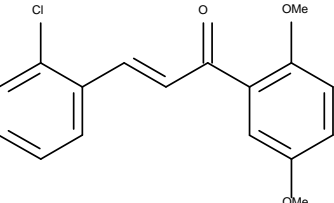
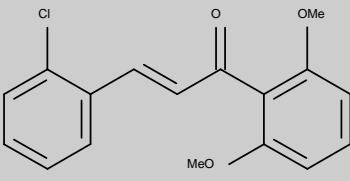
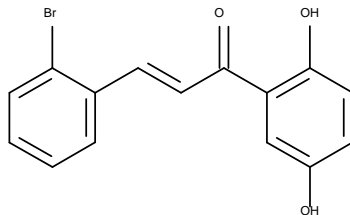
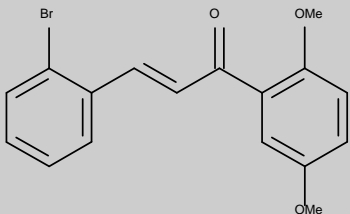
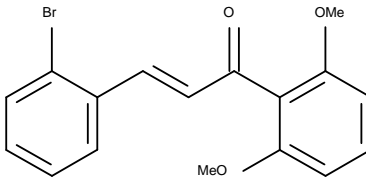
Collectively so far SARs studies have shown the important of the 2'5'-dihydroxy moiety for **AH1** and **AH9**. To assess whether the activity observed is due to hydroxyl groups acting as hydrogen acceptors or donors the following methoxy equivalents of **AH1** and **AH9** were evaluated.

Hydrogen groups can function as both hydrogen bond donors and acceptors. Methoxy groups can only act as hydrogen acceptors because they lack a hydrogen. Masking the hydroxyl groups as the methyl ether helps us to identify if they are functioning as hydrogen bond donors. Methoxy groups are larger than hydroxyl groups and less electron releasing via resonance (in the ortho and para positions). The inductive effect is the same as a hydroxyl group also.

Interestingly the methoxy analogues showed potent anti-endothelial activity in relation to their hydroxyl counterparts at 10 μ M. This could suggest that the hydrogen donating capabilities of the hydroxyl groups are not imperative to exhibit the activity seen. This means that the methoxy groups with their hydrogen accepting ability were able to cause significant reduction in HUVEC viability. Having the methoxy groups on the chalcone increases lipophilicity which would increase permeability across the cell membrane. Therefore the potent activity could be due to the increased lipophilicity allowing the compound to enter the cell better, to invoke an anti-proliferative effect. Whether the activity seen, was due to a combination of the hydrogen donating ability and increased lipophilicity requires further research.

Regarding methoxychalcones, as discussed in Chapter 1, Bert et al (2004) reported nanomolar IC_{50} value concentrations of 3-bromo-2'4'-dimethoxychalcone against HMECs. Although upon a microvascular endothelial cell line (using a different cytotoxic assay), it was interesting to see related structures in this piece of work possess high anti-proliferative activity against an endothelial cell also.

Table 14 Summary of structure and biological activity for Series 4

<i>Compound</i>	<i>Structure</i>	<i>Reduction in HUVEC viability^{a,b} ± SEM</i>
AH1		94.94 ± 1.64
AH21		86.03 ± 3.26
AH21a		85.32 ± 2.27
AH9		79.62 ± 4.45
AH21b		84.72 ± 4.56
AH21c		62.79 ± 9.47

a = Values are means ± SEM of four independent experiments. Data expressed as a % vs untreated control.

b = Compound administered at 10 µM concentrations. DMSO 0.1% was used as a normalisation control.

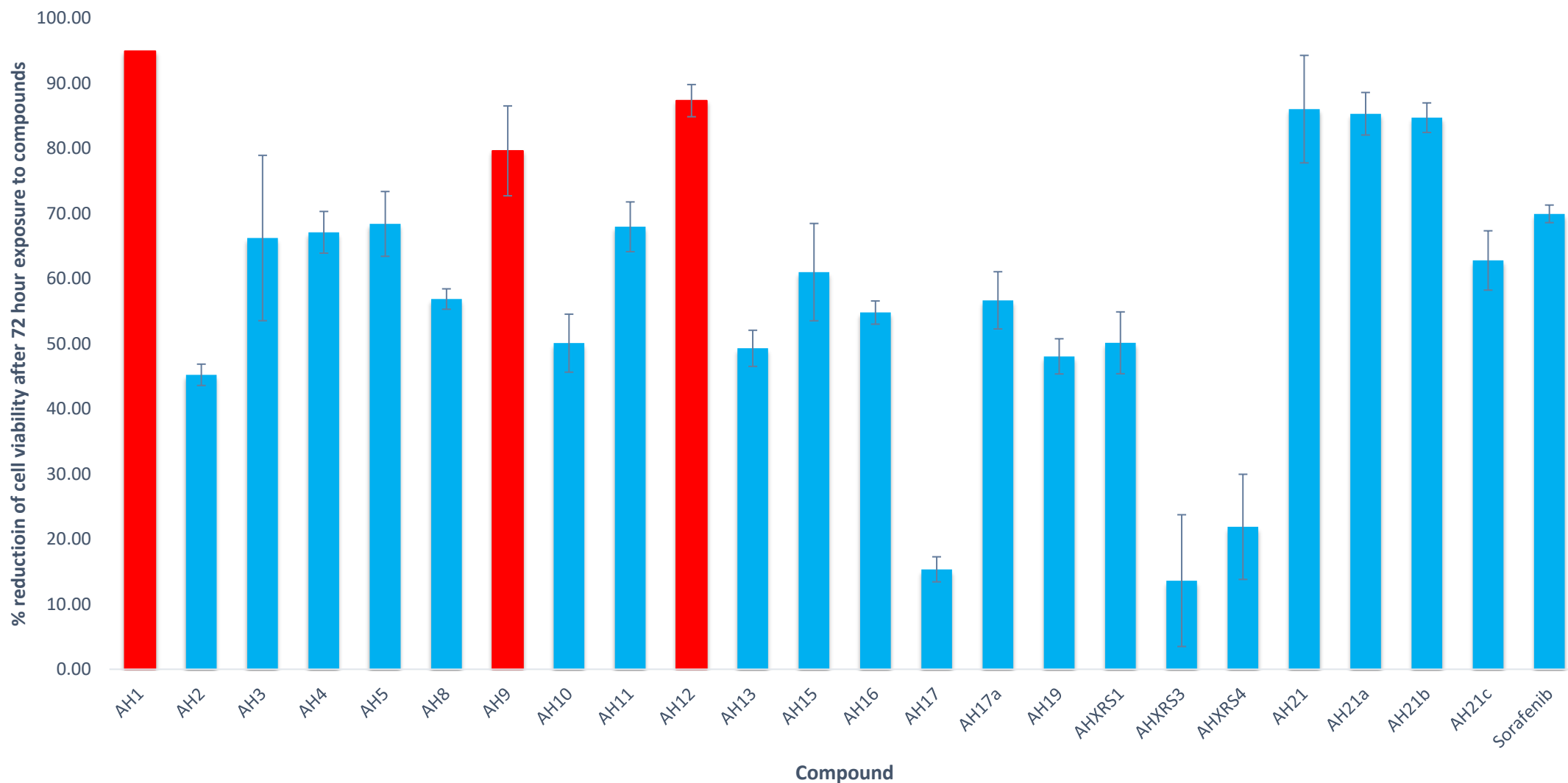


Figure 27 the effects of all the chalcone derivatives on HUVEC viability.

HUVECs were grown in 96 well plates at 5000 cell per well and left overnight. The media was changed and relevant concentrations of each compound was added, the cells were allowed to incubate for 72 hours. Following this 2mg/ml of MTT reagent was added and incubated for 4 hours. All media contents were removed and 100 μ l of DMSO was added. Plates were rocked and then the absorbance was recorded at 560nm.

Dihydroxychalcone derivatives AH9 and AH12 were able to display similar effects to the parent compound AH1. Three and four positioned halogenated dihydroxychalcones (AH2, AH3, AH4 and AH5) did not exhibit as potent activity against HUVEC proliferation than AH1 and AH9 (the two 2-positioned dihydroxychalcone derivatives). Any repositioning or changes to the A ring did not improve the activity of the parent compound (AH15, AH16, AH17 and AH17a). The part derivative compounds (AHXRS1, AHXRS3 and AHXRS4) helped to confirm that the 2'5'-dihydroxy moiety is important to the compounds potent activity but only in conjunction with the 2-chlorine B ring. Also the part derivatives demonstrated how the 2 positioned B ring was more important to the overall activity than the 2'5'-dihydroxy A ring. Methoxylatedchalcone derivatives were able to exhibit potent activity at 10 μ M suggesting that the hydrogen donating ability of the hydroxyl groups were not integral to the activity observed. Values are means \pm SEM of 4 independent experiments. Data expressed as a % vs untreated control. Compound administered at 10 μ M concentrations. DMSO 0.1% was used as a normalisation control.

4.3 Further investigation of AH21 and AH21b (Series 6)

Initial studies identified that hydroxyl groups acting as hydrogen donors on the A ring were not essential to the activity observed. To further explore, a mini SAR study was carried out on **AH21b** and **AH21c**. This was to see if re positioning certain substituent groups could alter the activity

Firstly changing the positioning of the methoxy groups on the A ring from 2'5' to 2'4' (see Figure 28) were looked at to form **AH22** and **AH22a**.

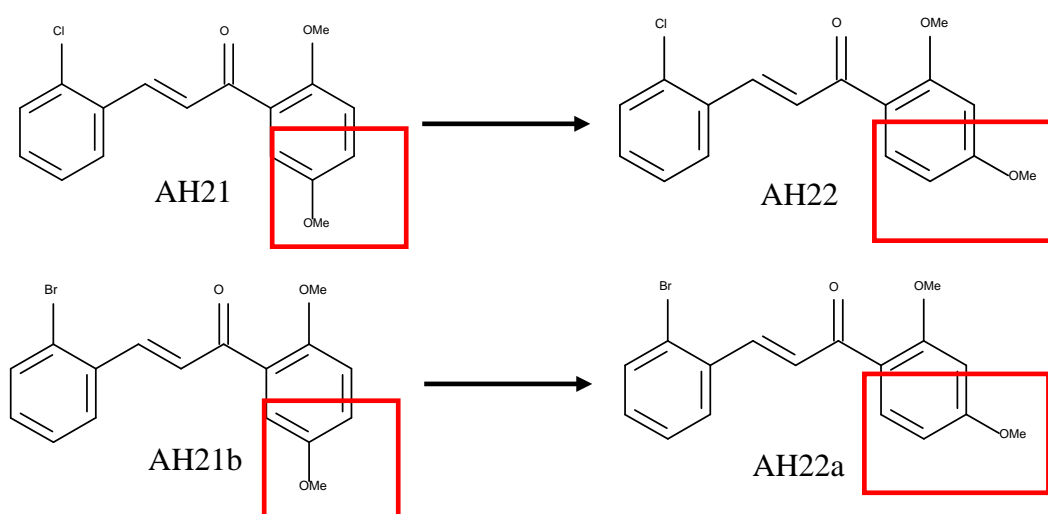


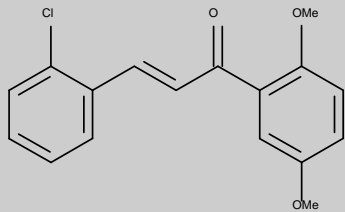
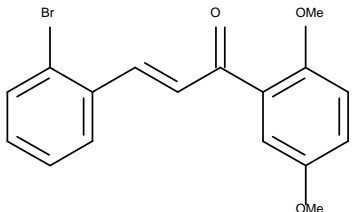
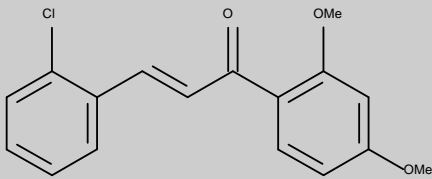
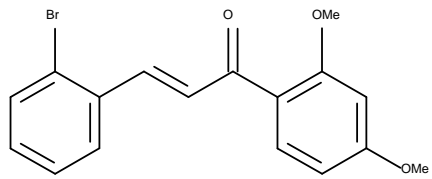
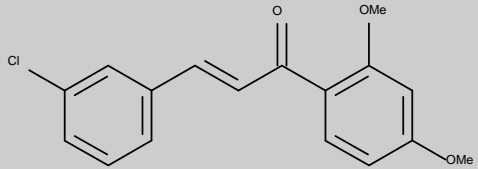
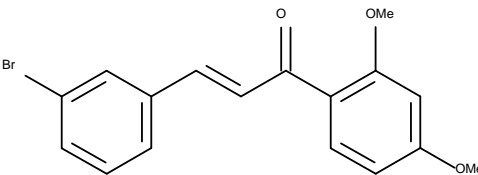
Figure 28 Synthesis of analogues of AH21 and AH21b to form 2'4'-dimethoxy derivatives AH22 and AH22a.

This was carried out by using 2'4'-dimethoxyacetophenone for the starting material instead of 2'5'-dimethoxyacetophenone.

Bertl et al (2004) study, as mentioned earlier, looked at a similar analogue – 3-bromo-2'4'-dimethoxy derivative and exhibited anti endothelial activity and sub micromolar concentrations (Bertl *et al.*, 2004). Therefore 3-bromo-2'4'-dimethoxychalcone (termed **AH22s2** for this study) and 3-chloro-2', 4'-dimethoxychalcone (**AH22a**) were synthesised and tested. **AH22s2** refers to the second compound found in Bertl et al (2004) study that is related **AH22** and its structure, hence s2 for 2nd standard compound.

What we found was that specific orientations were key to the activity observed. The substituents on one ring were important only in conjunction with specific orientation on the other ring. Having the 2-2', 5' orientation showed strong activity, but moving the methoxy group from 5' to the -4' position reduced the activity for both chloro and bromo derivatives (**AH22** and **AH22a**). However keeping the A ring with the 2'4'-dimethoxy positioning but moving the halogen on the B ring from 2 to 3 position showed an increase in activity similar to the 2-2',5' orientation. This was interesting as it appeared to show that stereochemistry between the compounds was pivotal in exhibiting anti-endothelial activity at 10 μ M.

Table 15 Summary of structure and biological activity for Series 6

<i>Compound</i>	<i>Structure</i>	<i>Reduction in HUVEC viability^{a,b} ± SEM</i>
AH21		86.03 ± 3.26
AH21b		84.72 ± 4.56
AH22		38.89 ± 8.49
AH22a		66.45 ± 9.81
AH22b		89.08 ± 1.84
AH22s2		88.01 ± 1.93

a = Values are means ± SEM of four independent experiments. Data expressed as a % vs untreated control.

b = Compound administered at 10 μM concentrations. DMSO 0.1% was used as a normalisation control.

To further investigate potency, EC_{50} determinations of the chosen lead candidates (AH1 and AH9) along with Sorafenib were gathered using HillSlope's nonlinear regression (table 16 and figure 29). It was interesting to see that for anti-proliferative activity against HUVECs across 72 hours, AH1 and AH9 exhibited superior activity than that of Sorafenib.

Table 16 LD_{50} values of AH1 AH9 and Sorafenib, determined using HillSlope's nonlinear regression.

<i>Compound</i>	<i>LD₅₀ (μM)</i>
<i>AH1</i>	4.14
<i>AH9</i>	3.98
<i>Sorafenib</i>	7.93

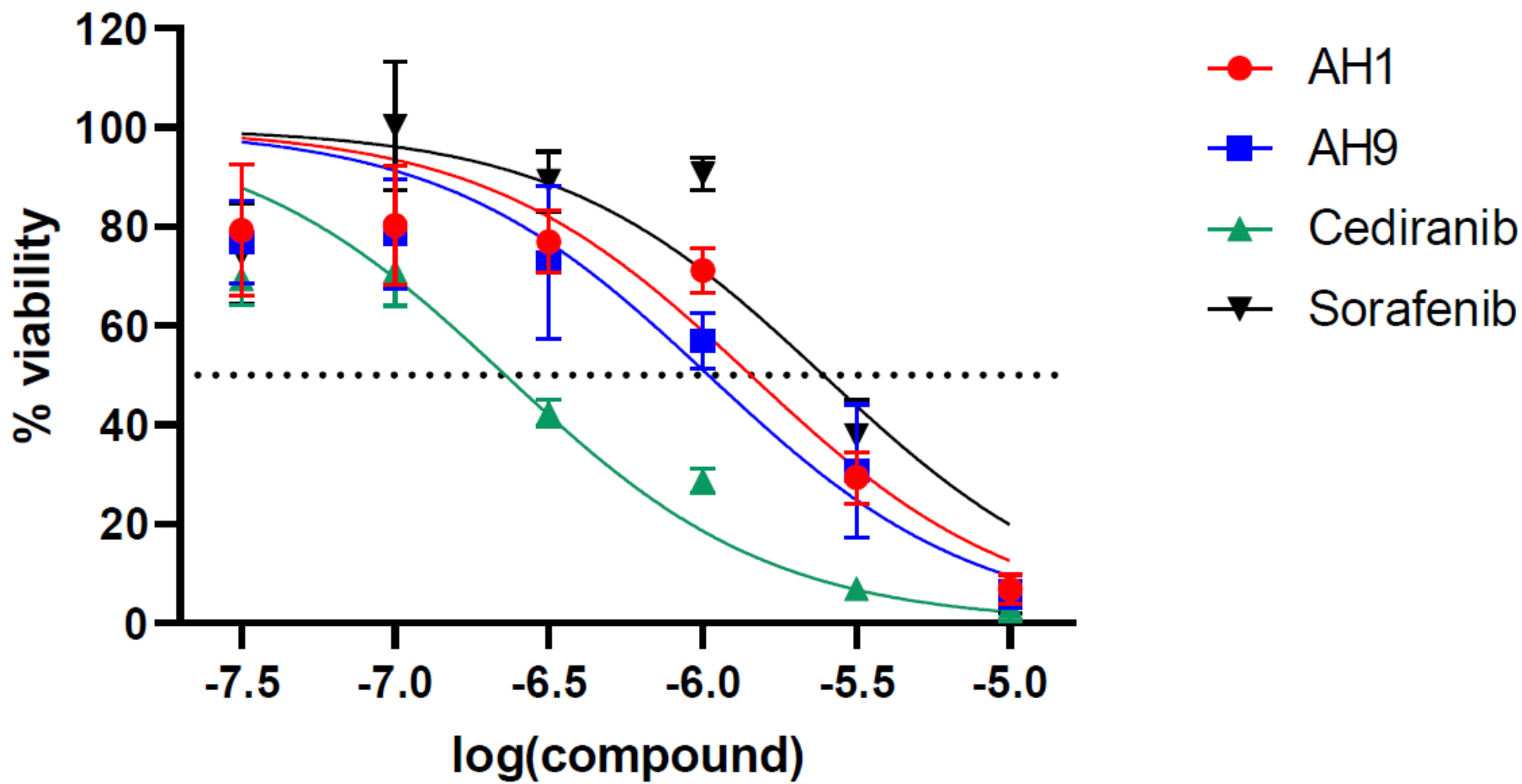


Figure 29 LD₅₀ plots of AH1 AH9 and Sorafenib showing their anti-proliferative activity against HUVECs after 72 hour exposure.

Values represented the averages of three independent experiments. Non-linear regression analyses were performed to obtain the LD₅₀ values.

4.4 Conclusion:

The structure activity relationships between all the compounds showed that a combination of electronegativity, stereochemistry and specific functional groups were vital to the potency of the activity observed. From series 1 it was evident that only specific substituent (EWGs) were favourable over ERG based substituent in that 2 position for exhibiting anti-proliferative activity. For series 2 it was clear that 2'5'-dihydroxy moiety specifically was key to the activity of **AH1**. Looking at series 3 it was interesting to find that the 2-chlorophenyl on the B ring contributed more to the overall activity of **AH1** than the 2'5'-dihydroxy moiety on the A ring. Testing the 3 and 4 positioned chloro and bromo derivatives in series 4, helped to show that the position of the halogen at the 2 ring was integral to the anti-proliferative activity.

Finally assessing the methoxy derivatives in series 5 suggested that the hydrogen donating ability of the hydroxyl groups were not essential in exhibiting anti-endothelial activity and that methoxy group substituents, which only possess hydrogen accepting capabilities, exhibited potent reduction in HUVEC viability at 10 μ M. The parent compound **AH1** displayed the strongest anti-endothelial activity amongst all the tested compounds.

Looking at all the series as a whole, the data suggested that the particular positioning of the chloro and hydroxyl groups on **AH1** were pivotal and any manipulation whether substitution or re positioning (conducted in this study) did not cause *any increase* in activity. Out of the novel synthesised hydroxyl analogues, **AH9** and **AH12** displayed the best anti-proliferative activity towards HUVECs.

Series 5 brought about a few interesting methoxy analogues (**AH21**, **AH21b**, **AH22b**, **AH22s2**) showing promising activity. But to remain within the initial aims, the hydroxyl

analogues were focused on. This was because the Series 2, 3 and 4 were focused on the hydroxyl element of AH1 and Series 5 was designed to just assess the hydrogen accepting ability of the A ring and not yield new methoxy compounds. Although these compounds could be investigated further.

AH12 contains a nitro group that can be metabolically reduced to an aromatic amine which can lead to systemic toxicity (Benigni and Passerini, 2002; Skipper *et al.*, 2010). Therefore, due to **AH9**'s better drug likeness over **AH12**, **AH9** along with **AH1** were put forward as the lead chalcone candidates on which to further test from to better understand their effects on endothelial cells.

Chapter 5: Anti-migratory analysis of
lead candidates AH1 and AH9
against HUVECs

5.1 Introduction:

Reducing tumour induced angiogenesis as a means to regress tumour growth brought about the concept of producing synthetic antiangiogenic compounds (Kerbel and Folkman, 2002; Cook and Figg, 2010). The antiangiogenic activity of synthetic analogues has been assessed using both *in vitro* and *in vivo* models (Nam *et al.*, 2003; Mojzis *et al.*, 2008; Lee *et al.*, 2012). Although *in vivo* assays may offer more clinically relevant information, they are expensive and time consuming. Additionally, they are difficult to maintain due to specialist training and equipment, as opposed to *in vitro* assays (Auerbach *et al.*, 2003). To add, these *in vitro* methods are well established as angiogenic functional assays with the majority of studies using HUVECs as the cell line of choice (Donovan *et al.*, 2001; Nam *et al.*, 2003; Goodwin, 2007; Varinska *et al.*, 2012; Zhong *et al.*, 2012). As the *in vitro* experiments are modelled on the vasculature, primary endothelial cells are suitable to use and can mimic *in vivo* angiogenic processes under the right conditions. To grow tubule networks *in vitro*, support matrices are needed to allow the endothelial cells to sprout. The most common extracellular matrix now used is Matrigel, derived from murine tumours (Kleinman and Martin, 2005). Therein, *in vitro* angiogenesis assays work on the basis that endothelial cells can grow and form tubule-like structures when supported by a culture matrix, mimicking the processes observed *in vivo* (Donovan *et al.*, 2001).

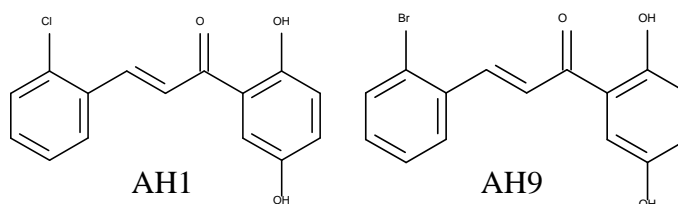


Figure 30 Chemical structures of lead chalcones AH1 and AH9.

Endothelial proliferation, migration and differentiation are three distinct areas studied in antiangiogenic models (as discussed in Chapter 1). Each stage is related to a specific phase in the angiogenesis process and studying these in isolated assays can provide insight as to the where the lead compounds exert their activity. As proliferation studies were conducted via the MTT assay in chapter 4, this chapter centres around the effects of the lead candidates on endothelial migration.

Cell motility is a key target for designing anti-cancer therapies, as cell migration is essential for both tumour invasion and tumour induced angiogenesis (Palmer *et al.*, 2011; Wells *et al.*, 2013). As a result, multiple assays have been utilised *in vitro* to analyse the anti-migratory effects of an agent such as the wound healing, transwell and under-agarose assays (Dredge *et al.*, 2005; Goodwin, 2007). The transwell and under-agarose assays require specific well plates and complex chambers to form the migratory model, which can create difficulty in acquiring consistent reliable results, due to the specialised apparatuses and methodology needed (Staton *et al.*, 2004).

The wound healing (also known as scratch) assay offers simplistic methodology, robust results and is widely used to mimic *in vivo* models (Liang, Park and Guan, 2007). The wound healing assay works by creating a synthetic wound across a endothelial cell monolayer. The width or area of the wound is measured thereafter (this equals time zero), then subsequent migration is characterised over a period of time.

A study by Dredge and colleagues (2002) used the scratch assay to identify anti-migratory activity of immunomodulatory thalidomide analogues. Njardarson and colleagues (2004) identified a potent tumour cell migration inhibitor, an analogue of a natural product migrastatin, as a result of using the scratch assay (Dredge *et al.*, 2002; Njardarson *et al.*,

2004). As a result, it was chosen as the most suitable assay to determine the migratory response of endothelial cells to the lead candidates AH1 and AH9 (Auerbach *et al.*, 2003).

5.2 Results and discussion:

5.2.1 Endothelial cell migration – wound healing assay

The wound healing assay was used to determine the migratory response of endothelial cells to the lead candidates. Cells were cultured in multiwell plates and then scratched down the middle by a pipette tip (see figure 31). The migration that occurred was measured by assessing the width of the wound between monolayers over time. In this case preliminary experiments indicated that wound closure (HUVECs in 6 well plates with EM200 media (supplemented with LSGS)) occurred around 8 hours. Therefore we elected to use 8 hours as the end point with one interval in between for comparison (4hr). Images were taken at these regular time points (0hr, 4hr and 8hr) to observe the development of any migration seen. The average distance between the wound was calculated over the time points as a measure of migration. Images were taken of 3 randomly selected fields at 100x magnification.

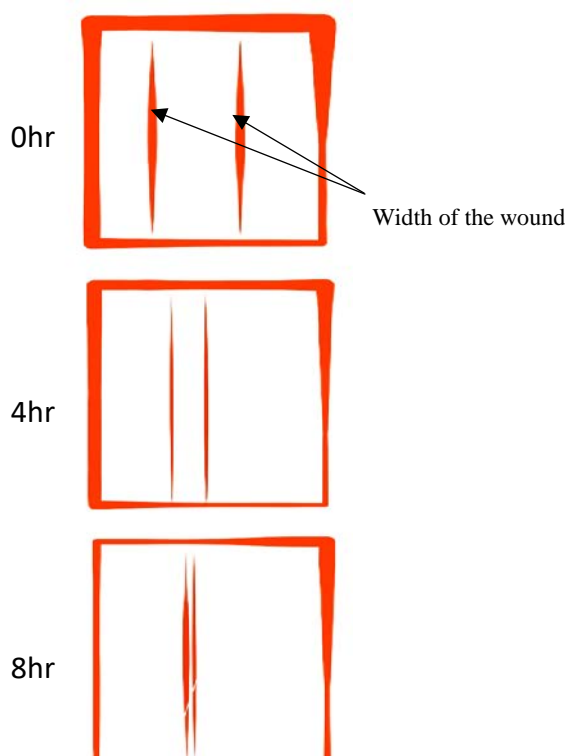


Figure 31 A abstract diagrammatic representation of wound closure in a wound healing assay over 8 hours.

The diagram illustrates the width of the wound closing over time, therefore this assay can be used to measure endothelial cell migration in the presence or absence of stimulating factors or synthesised compounds.

5.2.2 Preliminary study to identify optimal concentration for the wound healing assay

Preliminary experiments were conducted at 10 μ M, 3 μ M and 1 μ M for both AH1 and AH9. At 10 μ M cell death was seen by 8 hours, this was indicating the concentration was too toxic for the cells. Figure 32 illustrates the comparison in the change of morphology in HUVECs across the time points with different concentrations, with 10 μ M concentration showing aforementioned cell death by 8 hours. From these images it is clear that the viability of the cells were healthier in the 3 μ M and 1 μ M concentrations experiments.

Having identified that 10 μ M concentration was too high for this particular assay, the two lower non-toxic concentrations (3 μ M and 1 μ M) were taken forward. Sorafenib (3 μ M) was also used as a positive control.

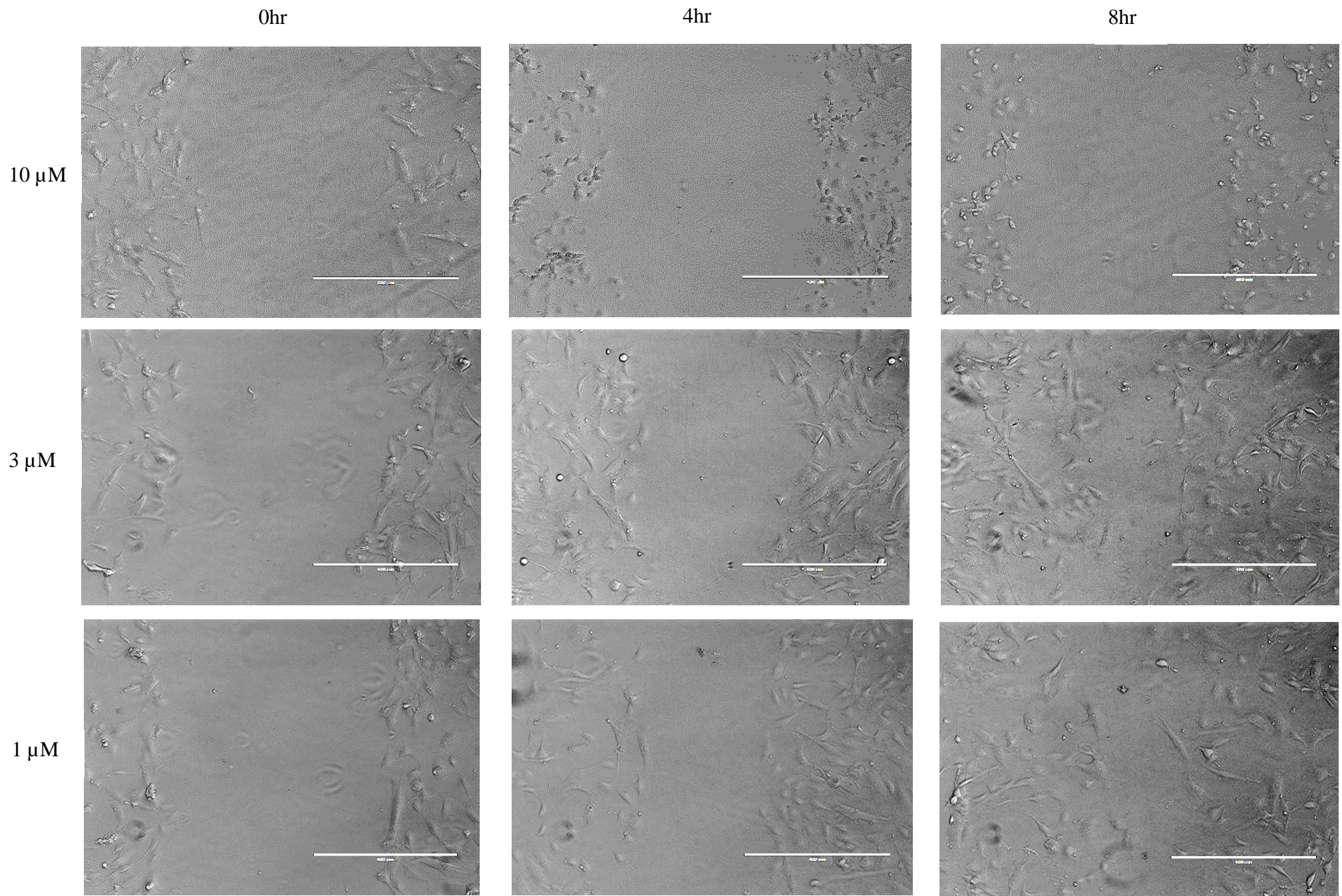


Figure 32 The effects of AH1 on HUVEC migration:

The images iterate how at 10 μM AH1 showed apoptotic cell death by 8 hours. This suggested the concentration was too high as a dose to use in this scratch assay. To further support this the images taken at 3 μM and 1 μM showed healthy HUVECs by 8 hours. Therefore, 3 μM and 1 μM were taken forward as the concentrations to use in this assay.

5.2.3 AH1

Results for AH1 showed that at 3 μ M, the parent compound displayed similar anti-migratory activity to that of Sorafenib when compared to time 0hr control (at 4 hours, AH1 vs Sorafenib = (28.8%) vs (34.5%), respectively, $p = 1.0$). Table 17 demonstrates the width of wounds gathered for each experiment and shows a clear difference in width between the untreated control, AH1 3 μ M and Sorafenib 3 μ M. At 8 hours also, no significant difference was seen in migration between AH1 and Sorafenib at 3 μ M (AH1 vs Sorafenib = (47%) vs (52.7%), respectively, $p = 1.0$). Figure 33 illustrates the images taken during the scratch assay experiment.

When compared to the untreated control at both 4 and 8 hours, AH1 and Sorafenib (at 3 μ M) did not show any significant difference in terms of % migration (see Table 18); (at 4 hours, AH1 vs Untreated control = (28.8%) vs (44.9%), respectively, $p = 0.77$); (at 4 hours, Sorafenib vs Untreated control = (34.52%) vs (44.9%), respectively, $p = 1.0$); (at 8 hours, AH1 vs Untreated control = (47.2%) vs (75.2%), respectively, $p = 0.19$); (at 8 hours, Sorafenib vs Untreated control = (52.68%) vs (75.2%), respectively, $p = 0.41$). Figure 34 illustrates the change in migration observed for the AH1 experiment.

Untreated control

AH1 3 μ M

Sorafenib 3 μ M

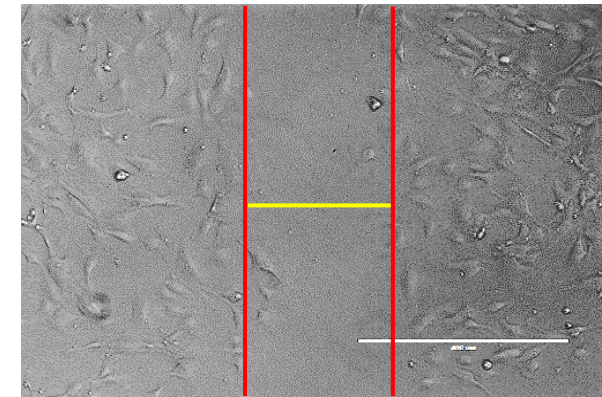
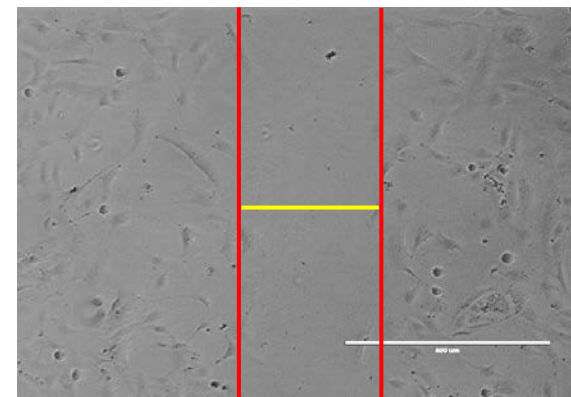
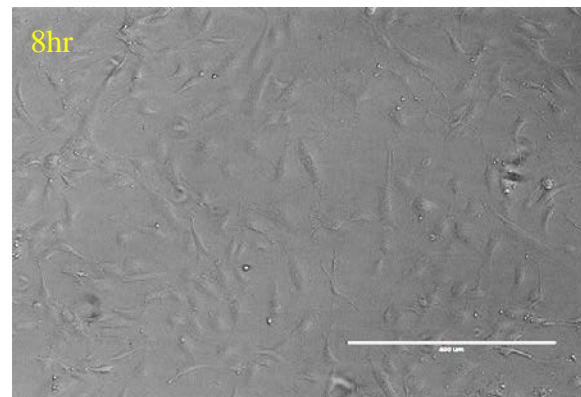
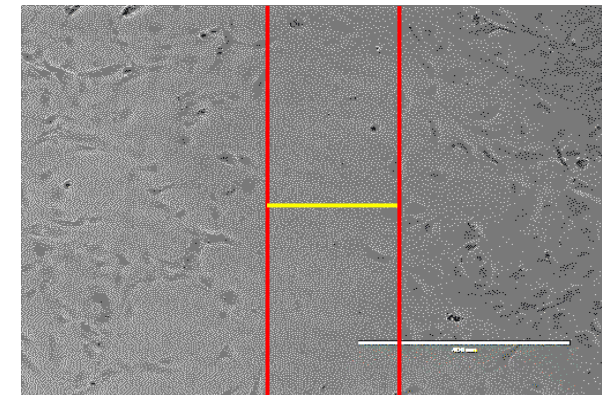
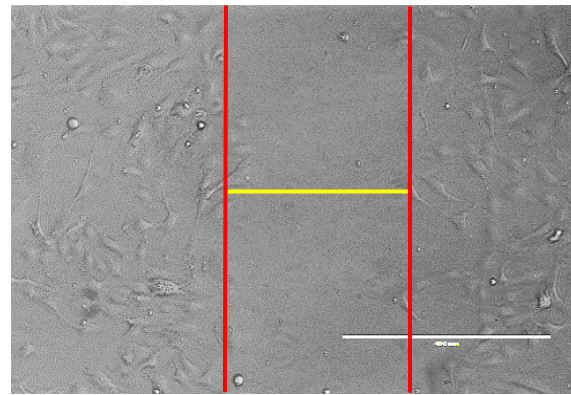
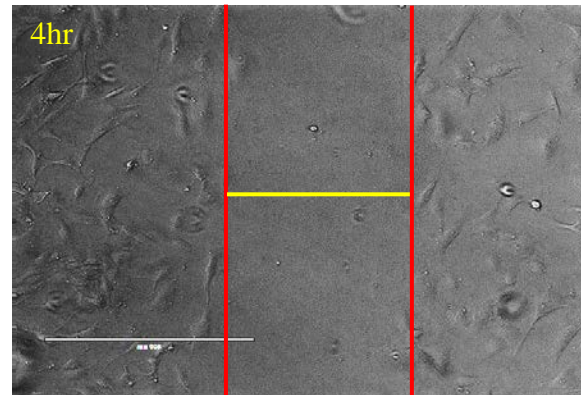
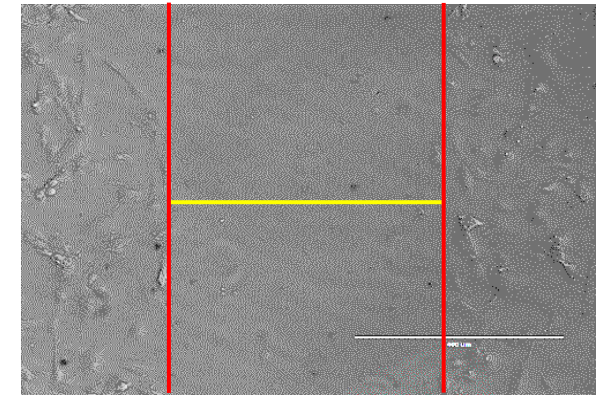
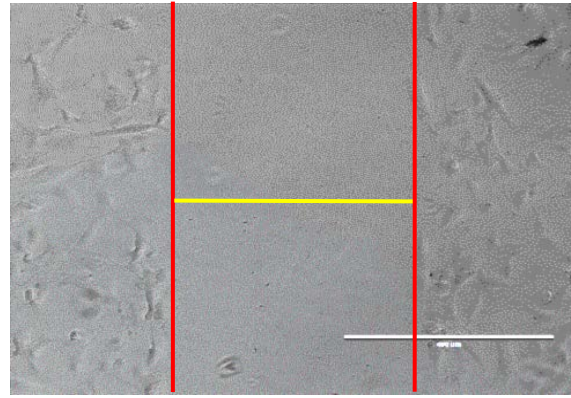
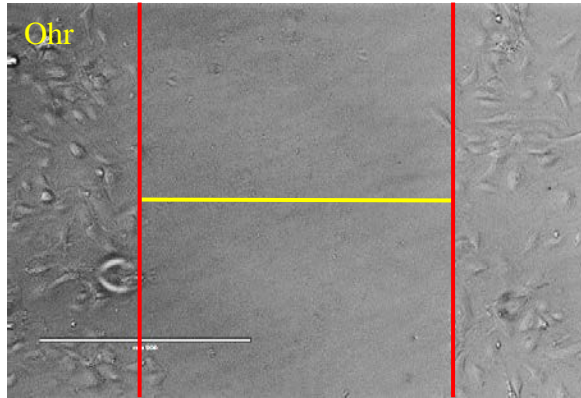


Figure 33 Select photos of from the unstimulated scratch assay.

From the wells of untreated control, AH1 3 μ M and Sorafenib 3 μ M. The images show the wound closure as expected in the untreated control. Anti-migratory effects were seen with AH1 and Sorafenib at 3 μ M.

Table 17 Showing the average width of wounds (μm) for each gathered from three independent experiments (untreated control, AH1 $3\mu\text{M}$, $1\mu\text{M}$ and Sorafenib $3\mu\text{M}$) with time points \pm SEM. * = $p < 0.05$ vs time matched untreated control (statistical analysis carried out by one way –ANOVA followed by Tukey-Kramer post hoc t test for multiple comparisons).

<i>Time</i>	<i>Untreated control</i>	<i>AH1 $1\mu\text{M}$</i>	<i>AH1 $3\mu\text{M}$</i>	<i>Sorafenib $3\mu\text{M}$</i>
<i>0hr</i>	523.93 \pm 30.01	575.47 \pm 30.25	511.57 \pm 28.24	611.64 \pm 39.55
<i>4hr</i>	286.28 \pm 25.22	343.53 \pm 28.63	363.21 \pm 13.01	410.27 \pm 16.75
<i>8hr</i>	157.55 \pm 25.99	116.52 \pm 58.83	269.75 \pm 37.24	266.86 \pm 18.73

Table 18 showing the % migration of the untreated control, AH1 ($3\mu\text{M}$) and Sorafenib ($3\mu\text{M}$) after 8hrs of incubation.

Values are % migrations compared to time 0 hr.

<i>% migration across 8 hours</i>	
<i>Untreated control</i>	69.81
<i>AH1</i>	47.23
<i>Sorafenib</i>	55.77

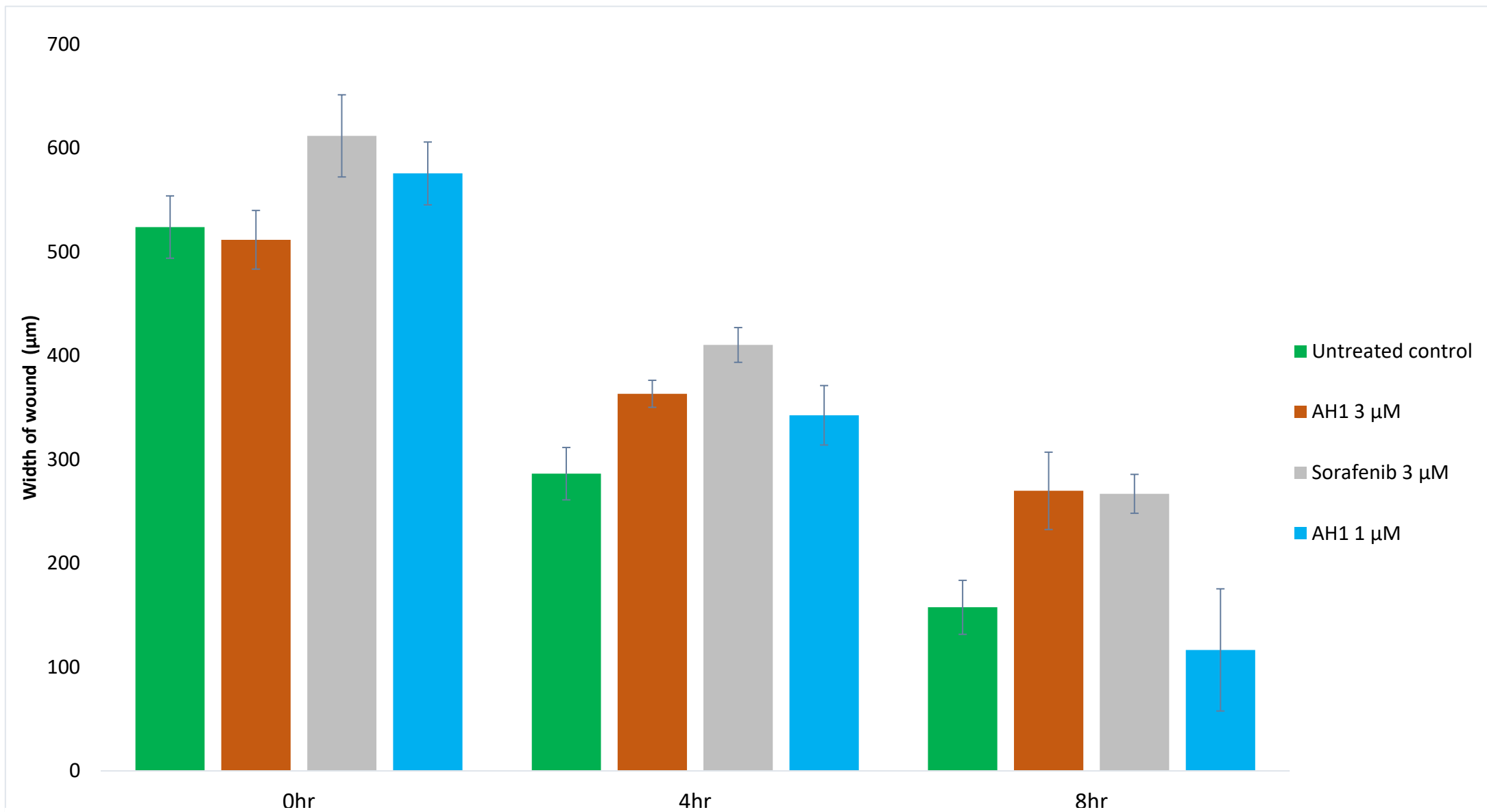


Figure 34 Effects of AH1 on HUVEC migration across 8 hours.

HUVECs (grown in 6 well plates) were scratched down the middle by a p1000 tip and briefly washed with cold PBS. Media was added with the relevant compound and control concentrations. Images were taken at periodic intervals. The data present are mean values gathered from three independent experiments \pm SEM. Responses were compared using one way-ANOVA with Tukey-Kramer multiple comparisons post hoc t test. The inhibitory effects caused by AH1 (3 μ M) were not statistically significantly different to that caused by Sorafenib (3 μ M). * = $P < 0.05$ vs. untreated control.

5.2.4 AH9

Interestingly, results for AH9 at 3 μ M demonstrated a significant increase in anti-migratory activity at both 4 and 8 hours when compared to Sorafenib, with AH9 appearing to show regression in HUVEC migration (when both were compared to their time 0hr controls); (at 4 hours, AH9 vs Sorafenib = (-4.9%) vs (34.5%), respectively, $p < 0.03$); (at 8 hours, AH9 vs Sorafenib = (16.2%) vs (52.7%), respectively, $p < 0.05$). Table 19 and figure 35, demonstrates the width of wounds for each experiment clearing presenting a difference between wounds size for AH9 3 μ M and Sorafenib 3 μ M compared to the untreated control.

Unlike AH1, AH9 did showed significant anti-migratory activity when compared to the Untreated control at both 4 and 8 hours (see Table 20); (at 4 hours, AH9 vs Untreated control = (-4.9%) vs (44.9%), respectively, $p < 0.004$); (at 8 hours, AH9 vs Untreated control = (16.2%) vs (75.2%), respectively, $p < 0.0007$).

AH9 at 3 μ M also exhibited a marked increase in the inhibition of HUVEC migration compared to AH1 at both 4 and 8 hours (see Figure 37).

Table 19 showing the average width of wounds (μm) for each gathered from three independent experiments (untreated control, AH9 3 μM , 1 μM and Sorafenib 3 μM) with time points \pm SEM; * = $p < 0.05$ vs time matched untreated control (statistical analysis carried out by one way –ANOVA followed by Tukey-Kramer post hoc t test for multiple comparisons).

<i>Time</i>	<i>Untreated control</i>	<i>AH9 1 μM</i>	<i>AH9 3 μM</i>	<i>Sorafenib 3 μM</i>
<i>0hr</i>	537.16 \pm 20.25	576.25 \pm 16.64	505.13 \pm 21.77	569.35 \pm 43.91
<i>4hr</i>	297.47 \pm 30.17	369.50 \pm 50.63	526.74 \pm 17.86*	356.47 \pm 3.68
<i>8hr</i>	107.21 \pm 61.59	114.02 \pm 59.64	417.16 \pm 53.02*	287.36 \pm 29.13

Table 20 showing the % migration of the untreated control, AH9 (3 μM) and Sorafenib (3 μM) after 8hrs of incubation.

Values are % migrations compared to time 0 hr.

<i>% migration across 8 hours</i>	
<i>Untreated control</i>	80.04
<i>AH9</i>	17.41
<i>Sorafenib</i>	49.53

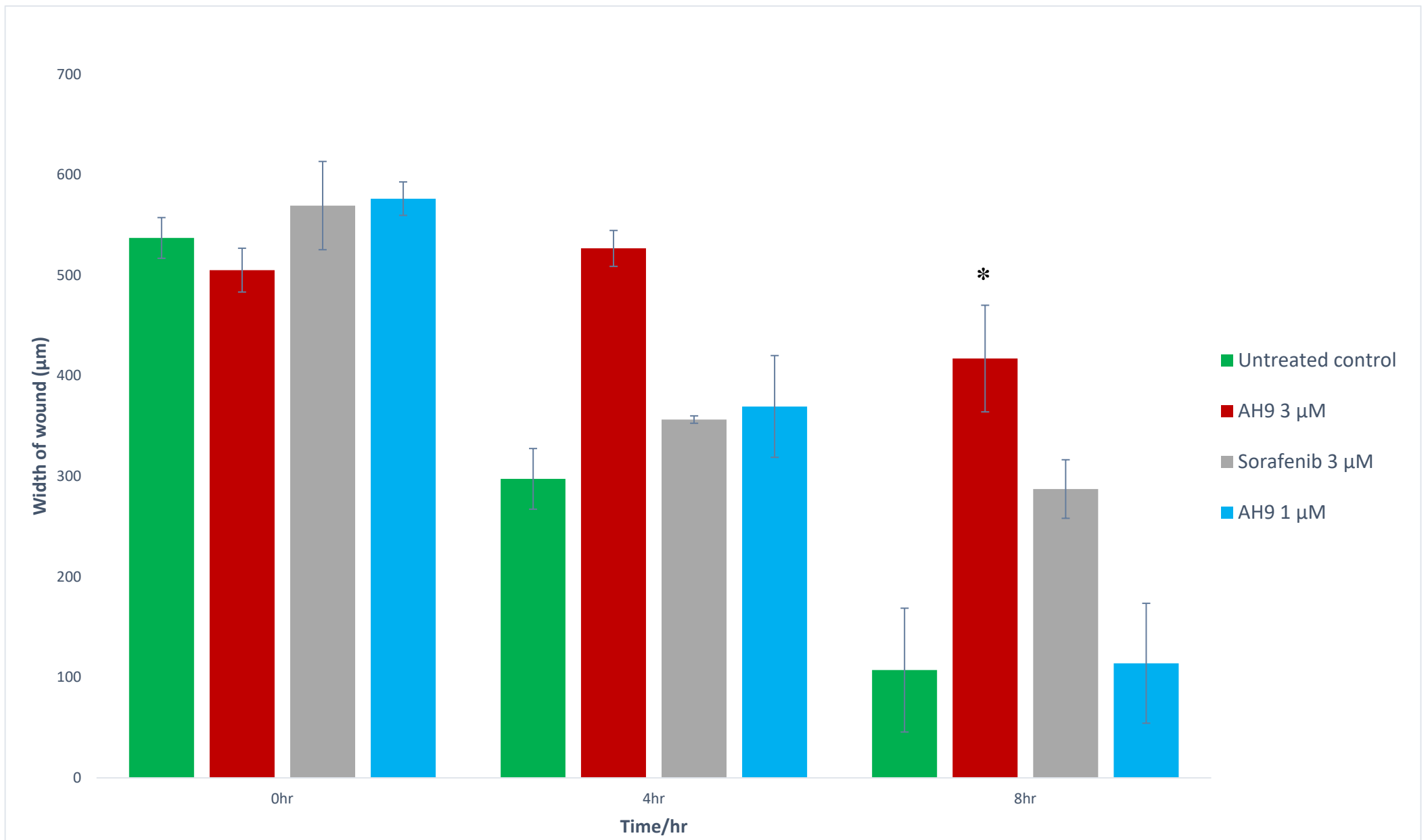


Figure 35 Effects of AH9 on HUVEC migration across 8hrs.

HUVECs (grown in 6 well plates) were scratched down the middle by a p1000 tip and briefly washed with cold PBS. Media was added with the relevant compound and control concentrations. Images were taken at periodic intervals. The data present are mean values gathered from three independent experiments \pm SEM. Responses were compared using one way-ANOVA with Tukey-Kramer multiple comparisons post hoc t test. The anti-migratory effects caused by AH9 were statistically significantly different to that of the untreated control. * = $P < 0.05$ vs. time matched (8 hours) untreated control.

5.3 Conclusion

Overall, AH9 across 8hrs was able to limit HUVEC migration to 16% ($p < 0.0007$) compared to the untreated control of 80% (See table 18 and 19). Sorafenib at 3 μM was able to limit migration to 52.7% ($p > 0.4$).

Figure 37 illustrates the difference in activity between AH1 and AH9. AH1 was able to limit migration to 47% whereas AH9 could limit it to 16% at the 8 hour time period.

As both compounds are analogues of each other differing only at the ortho position on the B ring (figure 36), it raises the question as to why the bromine derivative (AH9) demonstrated significantly more potent anti-migratory activity compared to its chlorine counterpart (AH1).

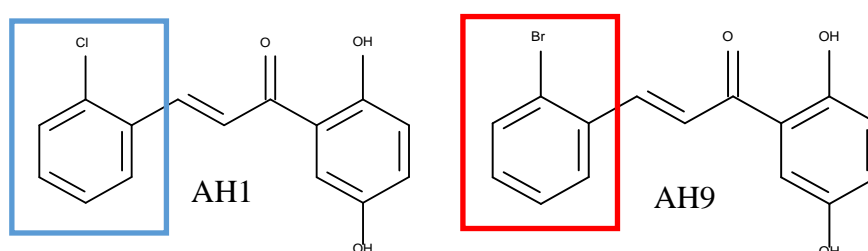


Figure 36 Chemical structures of AH1 and AH9.

Colour boxes highlight the different halophenyl rings and how the change from chlorine to bromine at the ortho position causes a significant increase in the anti-migratory activity observed against HUVECs after 8 hour exposure at 3 μM .

Taken together with the anti-proliferative data in chapter 4, these observations suggest that AH9 inhibits HUVEC proliferation and significantly limits HUVEC migration, two hallmark characteristics of an agent capable of being developed as an angiogenesis inhibitor (Staton *et al.*, 2004).

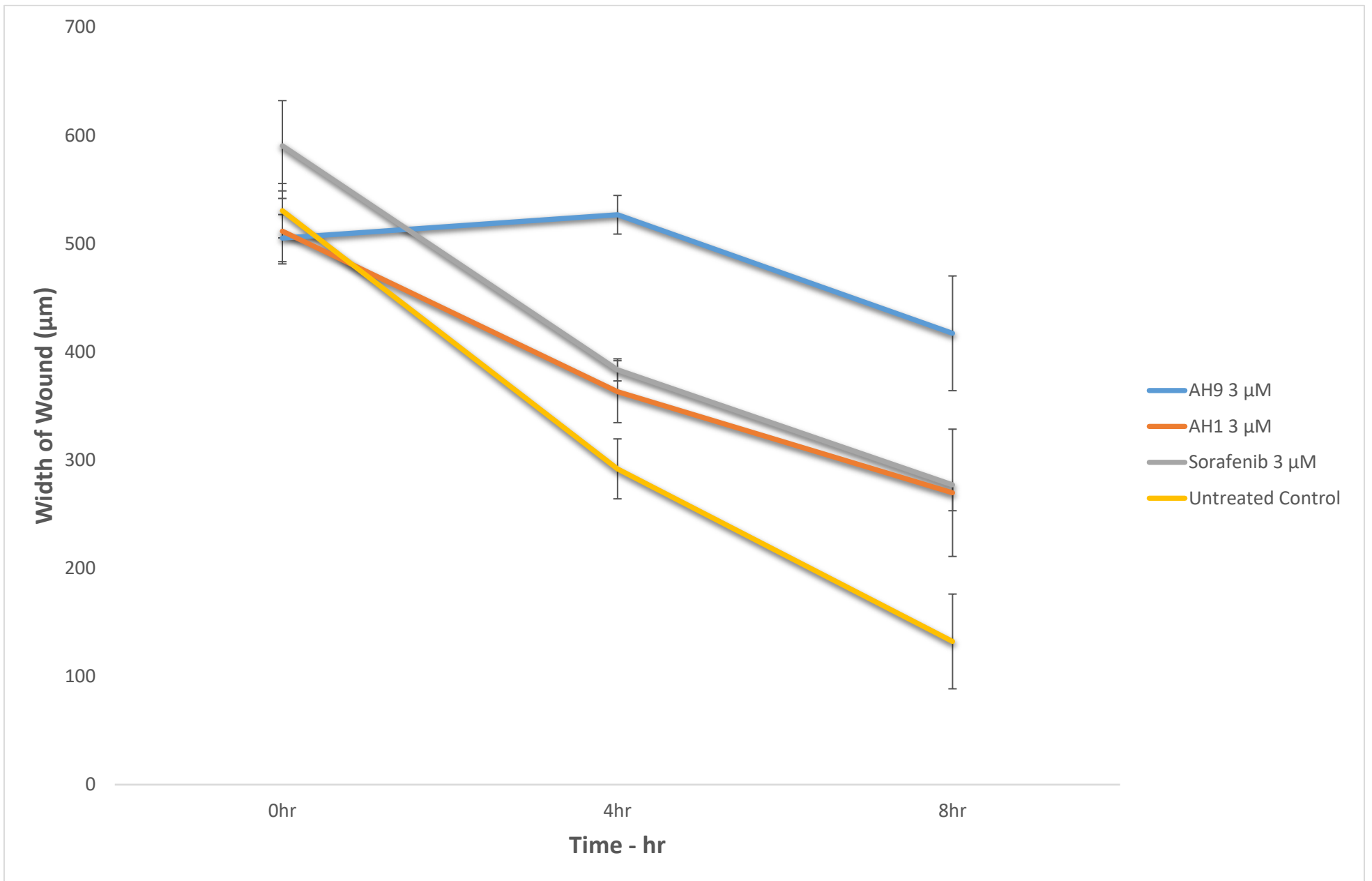


Figure 37 Effects of AH1, AH9 and Sorafenib (3 μM) on HUVEC migration, over 8 hours.

The data present are mean values gathered from three independent experiments ± SEM

Chapter 6: Pharmacological evaluation of AH9

6.1 Introduction:

After establishing that AH9 displayed promising *in vitro* antiangiogenic activity, the next phase of the work was to understand AH9's mechanism of action for the observed anti-migratory activity. Molecular mechanism of actions (MMOA) of lead compounds are an essential criteria in drug development (Schenone *et al.*, 2013). By knowing the MMOA, derivatives can be formulated to build upon the existing efficacy of original drugs (Swinney and Anthony, 2011). In clinical drug detection, MMOA can help to identify drug metabolism and excretion in response to certain proteins the drug targets. Finally having information like MMOA can enable researchers to explore other possible applications and uses for that particular drug (Tari *et al.*, 2012).

Pharmacological profiling is central for lead candidate's progression to pre-clinical stages. Understanding how a drug is causing its desired effect can be analysed in numerous ways. Effects on protein/receptor expression is one the most widely used tool for mechanistic evaluation (Forstner, Leder and Mayr, 2007). Assessing the up-regulation or inhibition of a protein and subsequently their signalling pathways involves techniques such as gel electrophoresis, western blot analysis and immunohistochemistry. Within this, computer modulation and digital molecular docking software's have been employed to predict and visualise drug-protein interactions (Gschwend, Good and Kuntz, 1996; Kitchen *et al.*, 2004; Vilar, Cozza and Moro, 2008).

ERK (extracellular signal-regulated kinase) is a key signalling mediator for cell migration in endothelial cells (Huang, Jacobson and Schaller, 2004; Chen *et al.*, 2009; Srinivasan *et al.*, 2009). As discussed in chapter 1, VEGF mediates its angiogenic property by activating its receptor and initiating downstream signalling pathway including ERK 1/2. Thereon, AH9's effect on VEGF-induced ERK 1/2 activation were initially assessed to see if the anti-migratory activity identified in Chapter 5 is linked to the inhibition of ERK 1/2 expression and/or downregulation of ERK 1/2 phosphorylation. Expression of VEGFR-2 in HUVECs in the presence of AH9 were also preliminarily investigated afterwards.

Several studies use multiple concentrations when assessing the effects of an agent on protein expression or phosphorylation (Lee *et al.*, 2012; Varinska *et al.*, 2012; Xu *et al.*, 2017). Lee and colleagues used 10 μ M, 5 μ M and 1 μ M for their work on assessing inhibitory effects of diphenylpropanones on VEGFR-2 phosphorylation when stimulated with VEGF (Lee *et al.*, 2012). A study conducted by Varinska and colleagues (2012) used 100 μ M and 10 μ M when evaluating the effects of Q797 (4-hydroxychalcone) on ERK and Akt phosphorylation stimulated by bFGF and VEGF separately (Varinska *et al.*, 2012). Xu and colleagues (2007) used a three concentration screen of 10 μ M 5 μ M and 1 μ M when measuring the effects of Cryptotanshinone on ERK phosphorylation (Xu *et al.*, 2017). When considering all of these studies the following concentrations were used for this study, 100 μ M, 30 μ M and 10 μ M. These were selected to match up to previous studies carried out.

6.2 Results and Discussion:

6.2.1 Experimental design for analysis of protein expression

HUVECs were seeded in serum free media and pre-treated with AH9 at indicated concentrations for 1 hour. Cells were stimulated with or without 30 ng/ml of VEGF 15 minutes prior to cell lysate collection. Specific antibodies were used to detect for phosphorylated-ERK, total-ERK, VEGFR-2 and β -actin.

6.2.2 AH9's effects on Erk 1/2 expression and phosphorylation

These studies identified that AH9 significantly inhibited VEGF-induced phosphorylation of ERK 1/2 (figure 39), ($p < 0.0001$). Therefore this could be the reason behind the compound's potent anti-migratory activity towards HUVECs (see chapter 5). Sorafenib, as expected significantly reduced ERK phosphorylation to the point where densitometry analysis could not pick up a signal (see figure 38) when compared to the rest of the bands on the membrane (Murphy *et al.*, 2006). Out of the two ERK isoforms (p44 and p42) identified in Figure 38, VEGF was shown to stimulate p42 ERK phosphorylation.

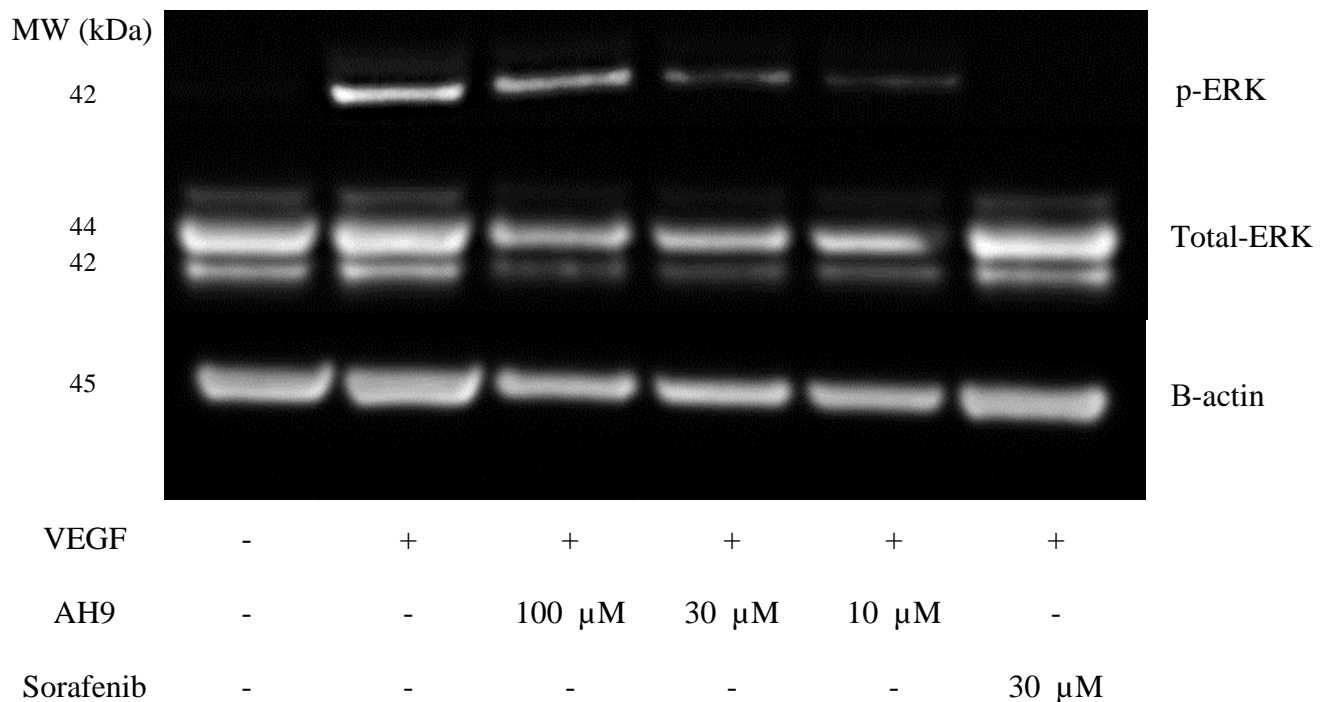


Figure 38 membrane captures of AH9's effect on ERK phosphorylation.

HUVECs were stimulated with or without VEGF, the images presented are the exposures as a result. ECL, made *in situ* was used for chemiluminescence with HRP conjugated secondary antibodies.

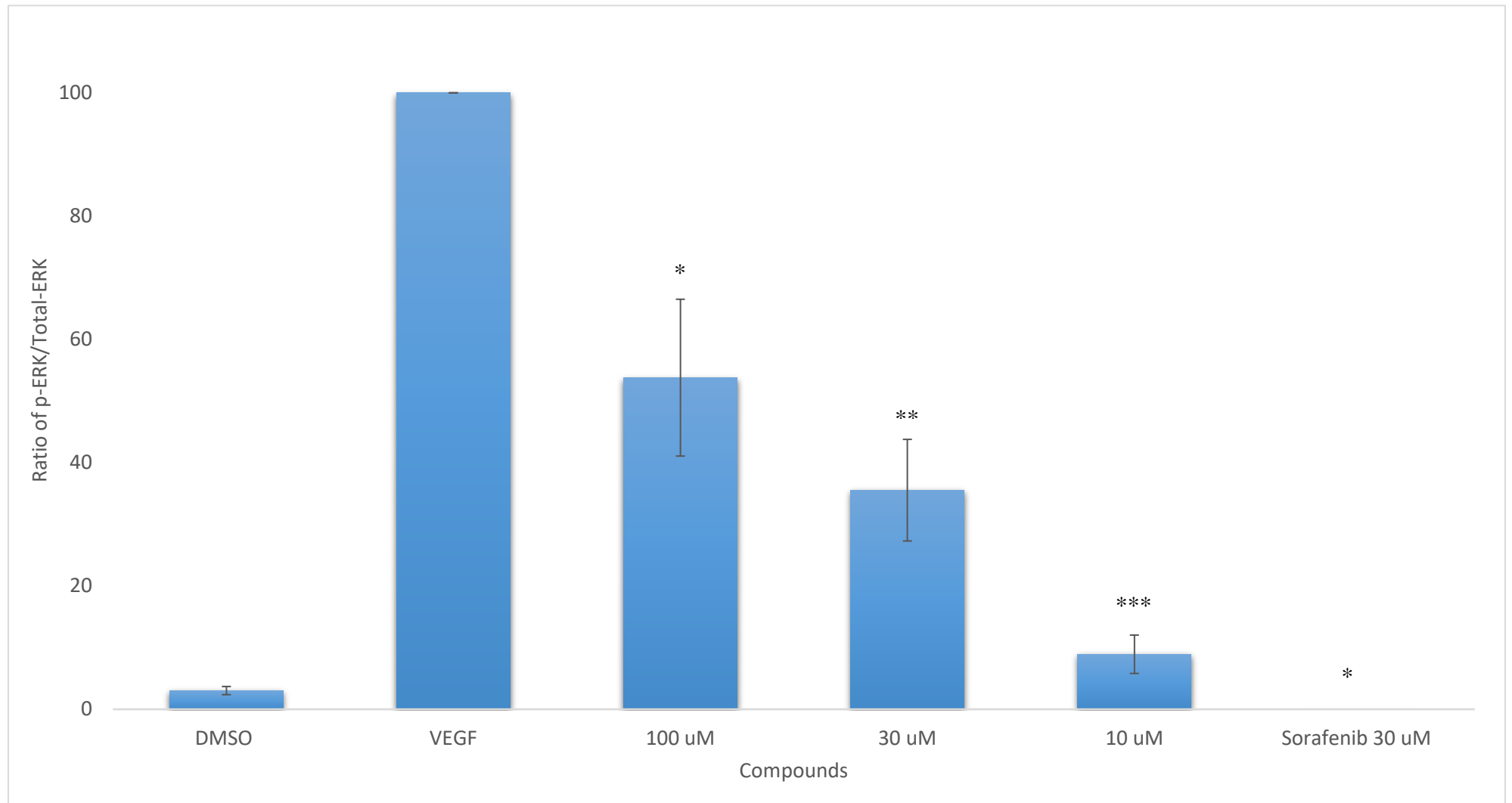


Figure 39 effects of AH9 on ERK phosphorylation.

HUVECs were stimulated with or without VEGF with relevant concentrations of AH9. Cell lysates were gathered and heatblocked. Cell lysates were ran on a SDS-gel page electrophoresis followed by western blot onto a nitrocellulose membrane. Selected primary antibodies were used to probe for desired proteins. HRP-conjugated secondary antibodies and ECL were used to visualise the protein bands via chemiluminescence.

AH9 was able to significantly inhibit at all three concentrations 100 μM (* = $p < 0.003$), 30 μM (** = $p < 0.0002$) and 10 μM (***) = $p < 0.0001$) compared to the VEGF control. Sorafenib at 30 μM showed complete inhibition of ERK $\frac{1}{2}$ phosphorylation (* = $p < 0.0001$) with no observable signal when compared to the rest of the bands on the nitrocellulose membrane. Unexpectedly less inhibition was seen at the higher concentrations (100 μM and 30 μM) when compared to 10 μM results. This could have been due to poor solubility seen when AH9 was administered to serum free media. Precipitation was seen especially at 100 μM . Also these concentration may have been toxic towards the cells as inhibitory studies on protein expression are usually found at lower concentrations for example 10 μM . Membrane captures were quantified using densitometry, levels of proteins were quantified and normalised using B actin as an internal control. Ratio of phosphorylated ERK vs total ERK were expressed as means of three independent experiments \pm SEM. Responses were compared using one way-ANOVA with Tukey-Kramer multiple comparisons post hoc t test.

6.2.3 AH9's effects on VEGFR-2 expression stimulated with VEGF

Assessing the interaction with VEGFR-2. AH9 was able to inhibit the expression of VEGFR-2 in a dose dependent manner (100 μ M, 30 μ M). See figure 40 below and figure 41.

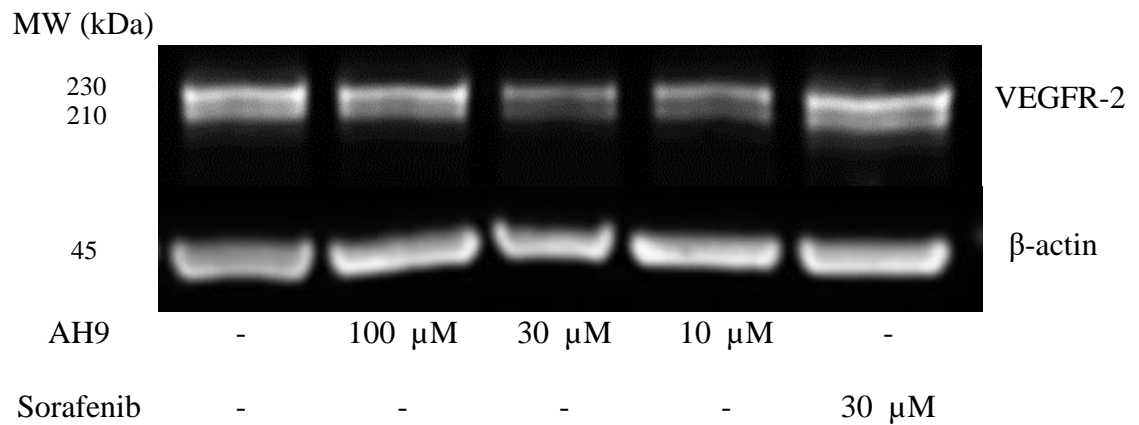


Figure 40 membrane captures of AH9's effect on VEGFR-2 expression.

HUVECs were stimulated with or without VEGF, the images presented are the exposures as a result. ECL, made *in situ* was used for chemiluminescence with HRP conjugated secondary antibodies

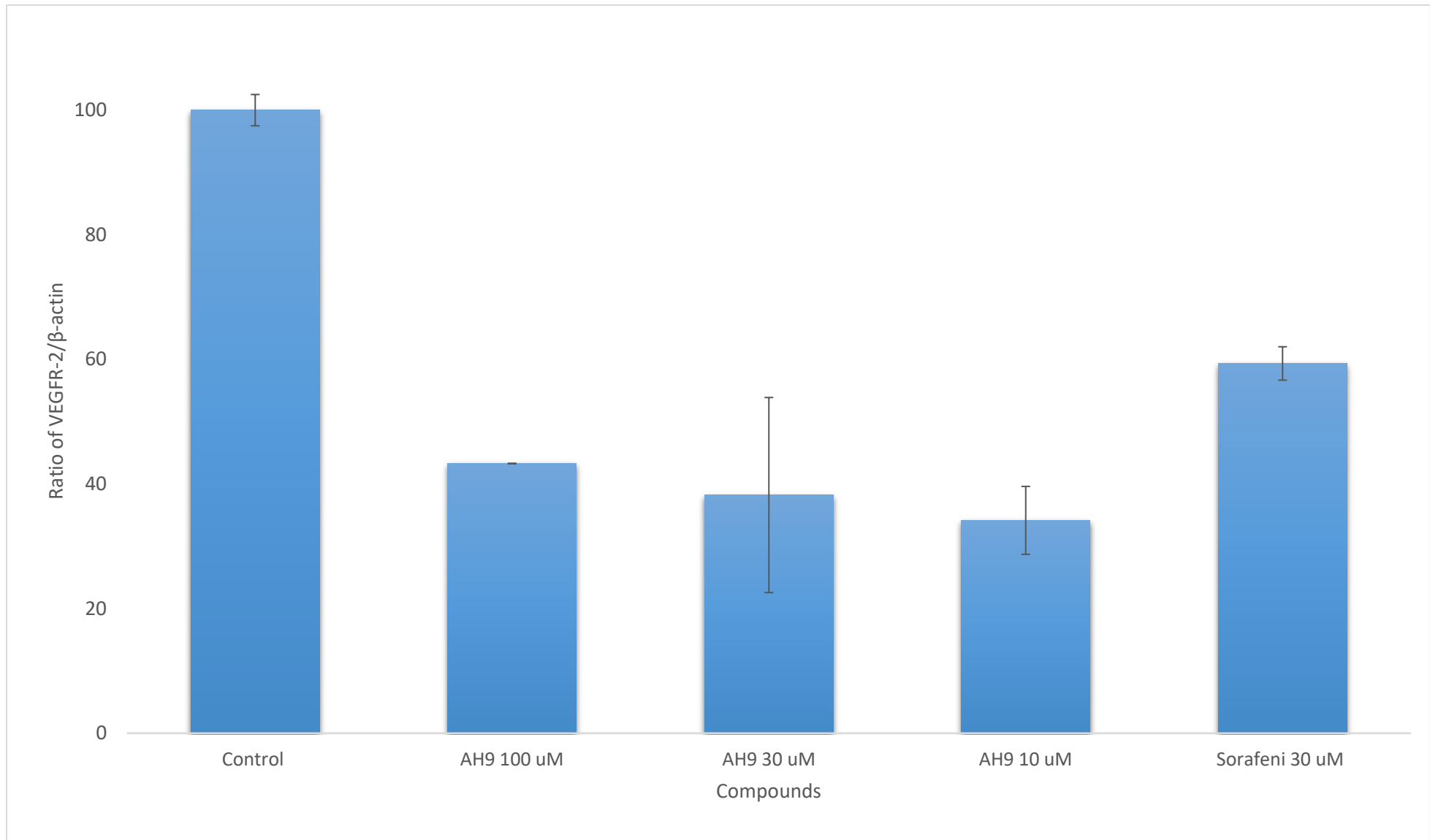


Figure 41 effects of AH9 on VEGFR-2 expression.

HUVECs were stimulated with or without VEGF with relevant concentrations of AH9. Cell lysates were gathered and heatblocked. Cell lysates were run on a SDS-gel page electrophoresis followed by western blot onto a nitrocellulose membrane. Selected primary antibodies were used to probe for desired proteins. HRP-conjugated secondary antibodies and ECL were used to visualise the protein bands via chemiluminescence. AH9 was able to reduce the expression of VEGFR-2 at all three chosen concentrations. Sorafenib also showed reduced in VEGFR-2 expression. Membrane captures were quantified using densitometry, levels of proteins were quantified and normalised using β -actin as an internal control. Ratio of VEGFR-2 vs β -actin were expressed as means of two independent experiments \pm SEM.

6.2.4 Overall discussion on mechanistic studies

These results link back to Varinska et al and their work on Q797 (4-hydroxychalcone) (Varinska *et al.*, 2012). They concluded that at 100 μ M Q797 was able to inhibit VEGF-induced ERK-phosphorylation. Here we report a 10-fold lower and much safer concentration (10 μ M) to inhibit ERK phosphorylation ($p < 0.0001$). Further studies will assess the lowest concentration achievable to inhibit ERK phosphorylation.

To note, at the higher concentrations (100 μ M and 30 μ M) inhibition of ERK phosphorylation was significantly less 10 μ M. Looking back at the experimental design, AH9 at the concentrated doses showed poor solubility in serum free media. In 5% serum media used for the anti-proliferative work in Chapter 4 AH9 was well tolerated up to concentrations of 30 μ M. With 10 μ M being further diluted before being administered into the well, we believe its solubility was more favoured and as a result it was able to exhibit the inhibitory activity seen in Figure 39. Intracellular over saturation of AH9 could also be the reason behind the reduced ERK inhibition when compared to a more commonly seen dose (10 μ M) in ligand binding studies of lead compounds. Also the preliminary studies on the effect of AH9 on VEGFR-2 expression showed a decreased in receptor expression. This would correlate to a reduction in receptor activation and as a result reduce the phosphorylation of the interactive downstream signalling mediators. Therefore the reduction in ERK phosphorylation by AH9 could be the result of reduced VEGFR expression. Whether this is linked to a reduction in VEGFR phosphorylation requires further investigation. However as this stage we cannot identify with kinase (MAP3K, MAP2K and MAPK) AH9 is affecting in particular and would need further probing. To add, we cannot rule out that AH9 could be increasing the activity of phosphatases that could cleave off phosphate groups causing the decrease

phosphorylation seen. This would also need investigating via phosphatase colorimetric assays for example.

To summarise, these results provide an introductory understanding about the molecular mechanism of action for AH9; in relation to its anti-migratory effect against HUVECs. ERK function as highlighted in Chapter 1.2.3. is a fundamental signalling molecule for endothelial proliferation and migration. These results show AH9 as a potent ERK phosphorylation inhibitor. The findings also relate to the significant inhibition of ERK phosphorylation by Sorafenib conducted in this study ($p < 0.0001$). As highlighted in Chapter 1.3 these outcomes support the literature studies on Sorafenib's effects on ERK expression. But they also further demonstrates how AH9, a simple molecular compound, exhibited similar activities to that of a licensed FDA approved drug for antiangiogenic therapy, on reducing ERK phosphorylation *in vitro*.

Further work is needed to investigate the VEGFR-2 phosphorylation, in response to exposure to AH9 to gauge a better understanding of the molecular mechanism of action. Especially if AH9 is affecting other signalling pathways that stimulate ERK *e.g.* FGFR pathway or exhibiting deregulation effects on ERK phosphorylation directly. As mentioned in Chapter 1.2.4, FGFR and ANGPT-2 pathways are important in the angiogenesis cascade especially after the onset of resistance to VEGFR targeted therapies. Therefore AH9's effects on these pathways should be further explored. Figure 42, illustrates a preliminary mechanism of action for AH9.

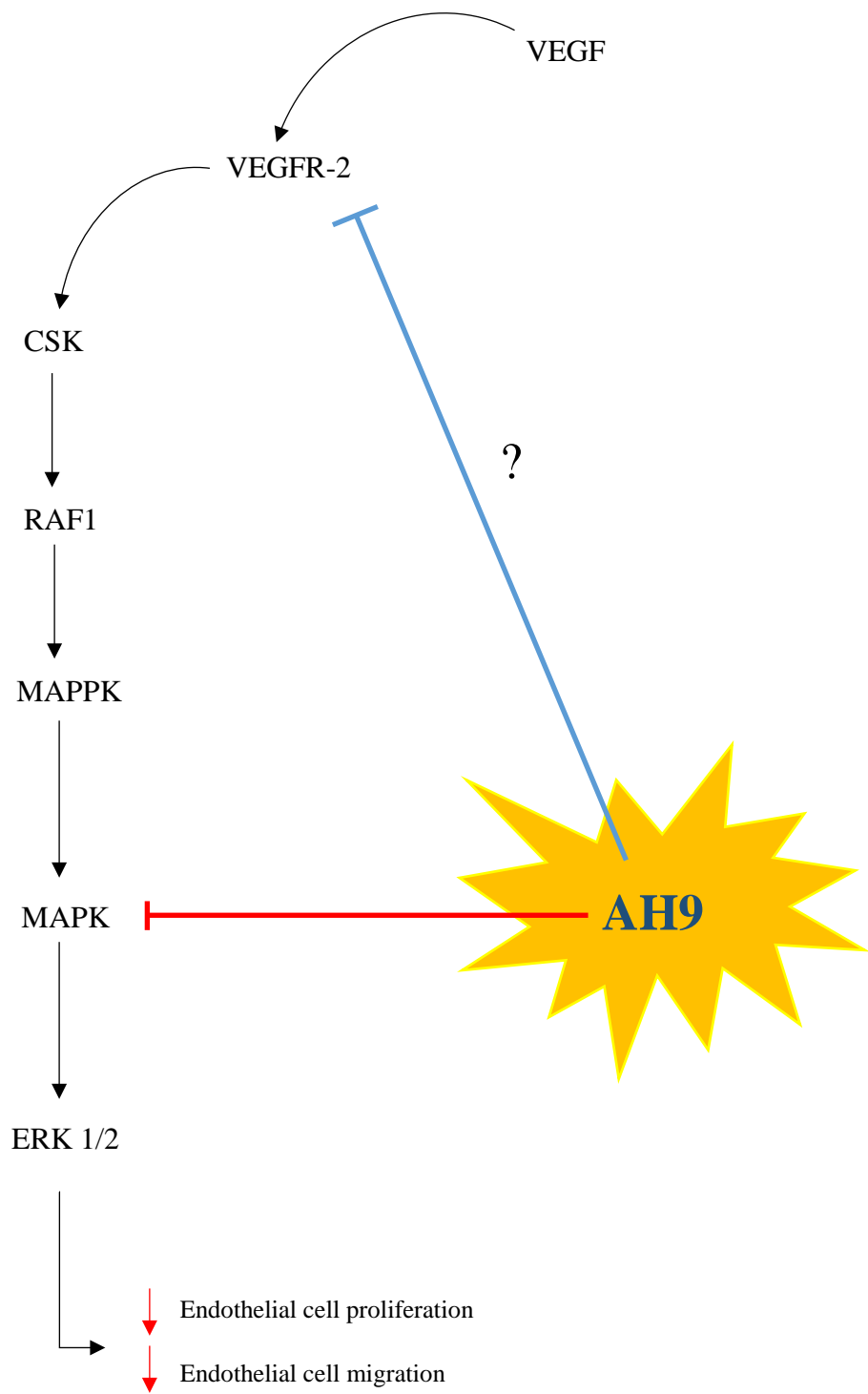


Figure 42 preliminary mechanism of action of AH9.

Studies have confirmed the significant inhibition of ERK phosphorylation that could be the cause of the anti-migratory activity seen. The question mark relates to further testing needed to support if AH9 is inhibiting VEGFR-2 phosphorylation.

Chapter 7: Conclusion and Future

Directions

7.1 Conclusion:

The main aim of this project was to identify derivatives with superior anti-angiogenic properties to AH1 and to evaluate a preliminary mechanism of action. In order to achieve this, five series of chalcones were designed and synthesised, all addressing a key part of the parent compound AH1. Lead compounds were identified first through anti-proliferative screening. Thereafter, anti-migratory analysis of the lead candidate AH9 (2-bromo-2'5'-dihydroxychalcone) and parent compound AH1 (2-chloro-2'5'-dihydroxychalcone) compounds were evaluated. In addition, the preliminary molecular mechanism of action of AH9 has also been investigated.

Our data suggests that both AH1 and AH9 exhibit similar anti-proliferative activity at micromolar concentrations against HUVECs. But more importantly, AH9 exhibited significantly more potent anti-migratory effects against HUVECs than AH1 and Sorafenib. Our studies have shown that AH9 has strong inhibitory effects on endothelial cell proliferation and significant potent effects on endothelial migration. These are two hallmark characteristics of an agent capable of being developed as an angiogenesis inhibitor. Mechanistic evaluation identified that AH9 could be exhibiting its anti-proliferative and anti-migratory activity via inhibiting VEGF-induced phosphorylation of ERK. Therefore, the study has successfully identified an agent superior to AH1 and demonstrated a preliminary mechanism of action, meeting the original aims of the project. This work also demonstrates how chalcones are suitable parent compounds on which to identify lead compounds of interest like AH9 and presents a strong case for further lead optimisation cycles.

As an inhibitor of endothelial cell migration, AH9 stands as a promising agent for anti-angiogenic therapy and warrants further investigation.

7.2 Study limitations

For the organic synthesis, there were limitations that restricted the range of compounds that could have been made. The availability of the NMR was a significant issue which limited the progression of the syntheses. Intermediates or co running spots on the TLCs for the hydroxychalcones, caused difficulty in separation via column chromatography. This resulted in the lower yields seen for some compounds.

The biggest limitations for this study was the amount of time taking to optimise experimental conditions for the syntheses and to gain access to core materials (thionyl chloride and the HUVECs). It took an extra 8 months than scheduled to synthesise all the designed compounds and, in this time, the HUVECs were still not obtained. As a result, the window to screen all the compounds was significantly reduced and limited the scale of assays that could have been conducted.

In regard to the wound healing assay, automated or commercial computer software like the Wimasis Image Analysis or Ibidi Wound Healing ACAS Image Analysis are available to analyse the images. Analysis is done far quicker than the manual method that was used in this study (1-2 days compared to 1-2 weeks per experiment). This would have allowed time to take more photos for a better, more representative analysis of the wound migration over time. However, the manually-obtained images were sufficient to demonstrate the effects of synthesised compounds on endothelial migration.

To add, *in vivo* migratory models would have strengthened the defence for the anti-migratory activity identified. However as highlighted earlier the shortened window to screen all the compounds also meant there was a reduced time to assess the functional

capabilities of lead candidates. This was also the reason why other *in vitro* assays assessing endothelial differentiation were not able to be completed in this study.

7.3 Future directions

AH9 was generated and analysed using hit-to-lead optimisations, *in vitro* and mechanistic studies. However further lead optimisations and mechanistic studies are still needed. AH9 exhibited potent activity in *in vitro* cell assays, but the enone moiety of AH9 may be subjected to significant metabolic breakdown by the liver. On top, AH9 is quite lipophilic (c log p) and thus possesses poor water solubility, therefore lead optimisation cycles for improving pharmacokinetic parameters would be useful to improve the overall drug likeness of AH9. Examples such as converting the chalcone structure into heterocyclic compounds like pyridine and pyrimidines could be carried out. These compounds can be formed as water soluble salts in an attempt to improve water solubility.

The angiogenic process encompasses several key receptors and signalling mediators. Two of out the three hallmarks (proliferation and migration) have been investigated preliminarily in this study. The effects of AH9 on endothelial cell differentiation (third hallmark) via *in vitro* assays like the tube formation assay would help to solidify or better understand how AH9 exerts in anti-angiogenic effects.

Assessing the effects of AH9 on VEGFR-2 phosphorylation, as discussed in Chapter 6.2.4, is important to gauge a more complete view on the mechanism of action for AH9.

Stimulated studies using VEGF and other angiogenic ligands *e.g.* ANG-1 in more advance *in vitro* cell models is quite a key development from this study. Models like 3D cell culture and co culture would generate deeper insights into the anti angiogenic effects

of AH9 in more specific and representative conditions *i.e.* selecting specific tumours cells to grow with HUVECs to assess AH9's interactions in a dual approach study.

Synergistic or combinatorial studies (as mention in Chapter 1.3.3) are becoming a focal point in modern day pharmacology. As complex diseases progress the efficacy of monotherapy is reducing and the need for polypharmacology increasing. Therefore, studies assessing AH9 with current licensed antiangiogenic drugs could be a strong progression, stemming from this study as a foundation.

Synergistic interactions and improving the drug likeness of AH9 will be the main goals in future studies.

Chapter 8: Experimental

8.1 Experimental:

8.2 General chemical procedures (Materials & Methods)

8.2.1 Reagents

Starting materials and reagents were used as received from Sigma-Aldrich Chemical Company (Dorset UK). General laboratory solvents were purchased from Fisher Scientific, Loughborough, UK.

8.2.2 Equipment:

Nuclear magnetic resonance spectroscopy (NMR) was used as the primary structure confirmation tool. ^1H and ^{13}C NMR spectra were recorded on a Bruker Avance superconducting AV400 NMR spectrometer at 30°C. Chemical shifts are reported in units relative to the TMS signal standard and coupling constants (J) are expressed as Hertz (Hz). ^1H NMR peak information is provided in the following format: number of protons, multiplicity, coupling constant (where appropriate) and peak signal. Multiplicities are reported as: singlet (s), doublet (d), triplet (t), doublet of doublets (dd), doublet of doublet of doublets (ddd), doublet of triplets (dt), triplet of doublets (td), multiplet (m).

High resolution mass spectrometry (HRMS) was carried out using a Thermo Scientific LTQ Orbitrap XL mass spectrometer at EPSRC UK National Mass Spectrometry Facility, Swansea University. Infra-red (IR) spectra were recorded on a Bruker Alpha ATR module (101873) spectrophotometer with bond absorptions reported as cm^{-1} .

Melting points (M.P) were carried using a Gallenkamp melting point apparatus in open glass capillary tubes and are uncorrected. Thin layer chromatography (TLC) was performed using Merck Aluminium Sheet – Silic Gel 60f254 coated plates. TLC plates were visualised using a Multiband UVGL-58 UV 254/366nm lamp. Staining of TLC

plates to visualise compounds were done using 2,4-diphenylhydrazine (DNP), phosphomolybdic acid (PMA) or iodine absorbed on sand. Silica gel (Fluka Silica 60; standard 25-70u or fine grade 2-45u) were used to perform flash column chromatography.

Ultraviolet (UV) spectra were recorded on a Thermo Scientific Helios Gamma 110-240 Volts UV-VIS spectrophotometer. HPLC was carried out on a Perkin Elmer 200 series chromatography system using a Perkin Elmer C18 (250 x 4.6mm) column using the following isocratic elution methods:

Method 1: 70 % acetonitrile/ water (Flow rate = 1.5 mL/ min, $\lambda = \lambda_{\text{max}}$ of compound)

Method 2: 90 % acetonitrile/ water (Flow rate = 1.5 mL/ min, $\lambda = \lambda_{\text{max}}$ of compound)

All samples had purity of 95% or greater.

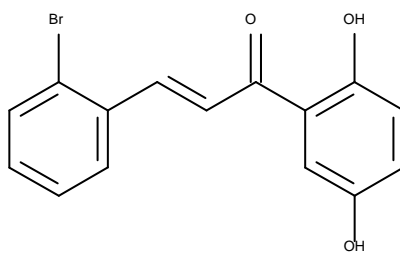
8.2.3.1 Experimental protocols:

8.2.3.2 Chalcone synthesis method 1 (Nam et al, 2003)

2',5'-Dihydroxyacetophenone (1.00g 6.57mmol) and pyridinium *p*-toulene sulphonate (0.04g 0.159mmol) were dissolved in anhydrous dichloromethane and stirred for 30 mintues at room temperature. A solution of 3,4-dihydro-2H-pyran (3.4 mL 37mmol) in dichloromethane (20 mL) was added and stirring continued for 4h. The solution was washed with water (2x30 mL) and the organic layer dried over anhydrous magnesium sulphate. Removal of the solvent under vacuo yielded crude 2'5'-bis(tetrahydropyran-2-yloxy)acetophenone as a straw coloured oil.

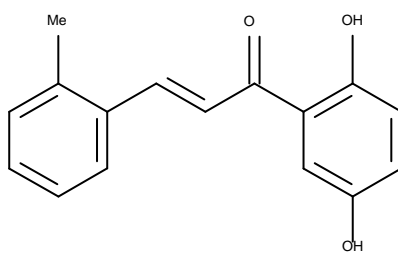
Barium hydroxide octahydrate (2.15g 6.57mmol) was added to a stirred solution of the appropriate benzaldehyde (6.57mmol) and crude 2'5'-bis(tetrahydro-pyran-2-yloxy)acetophenone at room temperature. After 18h the reaction mixture was washed with water (2x30 mL) and the organic layer dried over anhydrous magnesium sulphate. Removal of the solvent *in vacuo* yielded crude (E)-1-[2,5-(bis(tetrahydropyran-2-yloxy)-phenyl)]-3-phenyl-2-propene-1-one as an orange solid.

A solution of *p*-toulenesulphonic acid (0.44g 2.34mmol) and crude (E)-1-[2'5'-(bis(tetrahydropyran-2-yloxy)-phenyl)]-3-phenyl-2-propene-1-one in methanol (30 mL) was stirred at room temperature for 30mins. The reaction mixture was quenched with water (30 mL) and extracted with ethyl acetate (2x30 mL). The oragnic extracts were dried over anhydrous magnesium sulphate and the solvent removed under vacuum. The residue was purified by either flash column chromatography (hexane/ethyl acetate 8:2) or recrystalisation from ethanol.



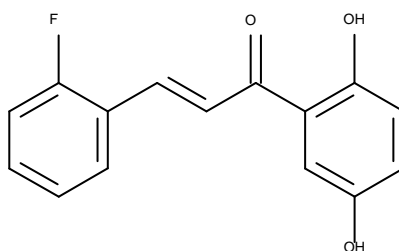
(E)-3-(2-Bromophenyl)-1-(2,5-dihydroxyphenyl)-2-propene-1-one (AH9)

Recrystallisation from ethanol. Red/orange crystals (35%). mp 177-179°C; TLC: $R_f = 0.13$ (hexane/ethyl acetate 8:2); IR: (ATR)/ cm^{-1} 3354 (OH), 1641 (C=O); ^1H NMR (ppm, DMSO- d_6): 6.85 (1H, d, $J = 9.4\text{Hz}$, Ar), 7.04 (1H, dd, $J = 9.4, 3.1\text{Hz}$, Ar), 7.39 (1H, ddd, $J = 7.8, 1.9\text{Hz}$ Ar), 7.48 (2H, m, Ar), 7.75 (1H, dd, $J = 9.4, 1.4\text{Hz}$, Ar), 7.91 (1H, $J = 15.6\text{Hz}$, C=CH), 8.02 (1H, $J = 15.6\text{Hz}$, C=CH), 8.14 (1H, dd, $J = 9.4, 1.4\text{Hz}$ Ar), 9.20 (1H, s, OH), 11.50 (1H, s, OH); ^{13}C NMR (DMSO- d_6) 115.1, 118.3, 121.3, 124.5, 125.4, 125.5, 128.8, 132.3, 133.3, 133.8, 141.1, 149.6, 154.2, 192.6; HMRS found $[\text{M}+1]^+$ 318.9969, $\text{C}_{15}\text{H}_{11}\text{O}_3\text{Br}$ $[\text{M}+1]^+$ 318.9964; Purity > 99% HPLC method 1 (Retention time 4.114 min).



(E)-1-(2,5-dihydroxyphenyl)-3-(2-methylphenyl)-2-propene-1-one. (AH10)

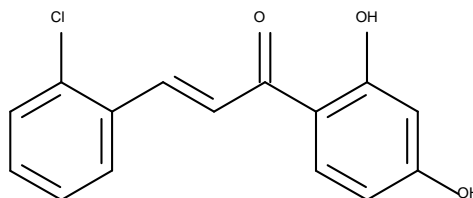
Recrystallisation from ethanol. Bright red crystals (20%); mp 174-176°C; TLC: $R_f = 0.54$ (hexane/ethyl acetate 7:3); IR: (ATR)/ cm^{-1} 3291 (OH), 1635 (C=O); ^1H NMR (ppm, DMSO- d_6): 2.44 (3H, s, CH_3), 6.86 (1H, d, $J = 9.1\text{Hz}$, Ar), 7.03 (1H, dd, $J = 9.1, 3.6\text{Hz}$, Ar), 7.20-7.38 (2H, m, Ar), 7.36 (1H, td, $J = 5.5, 1.8\text{Hz}$, Ar), 7.48 (1H, d, $J = 3.8\text{Hz}$, Ar), 7.81 (1H, d, Ar) (1H, $J = 14.5\text{ Hz}$, C=CH), 7.94 (1H, d, $J = 9.1\text{Hz}$, Ar), 8.02 (1H, d, Ar) (1H, $J = 14.5\text{ Hz}$, C=CH), 9.20 (1H, s, OH), 11.65 (1H, s, OH); ^{13}C NMR (DMSO- d_6) 115.0, 118.3, 121.1, 123.2, 124.3, 126.4, 127.0, 130.6, 130.9, 133.1, 138.2, 141.2, 149.5, 154.4, 193.0; HMRS found $[\text{M}+1]^+$ 255.1018, $\text{C}_{16}\text{H}_{14}\text{O}_3$ $[\text{M}+1]^+$ 255.1016; Purity > 98% HPLC method 1 (Retention time 3.57 min).



(E)-1-(2,5-dihydroxyphenyl)-3-(2-fluorophenyl)-2-propene-1-one. (AH11)

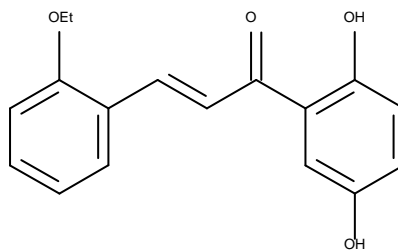
Recrystallisation from ethanol. Dark brown crystals (26%); mp 192-194°C; TLC: $R_f = 0.45$ (hexane/ethyl acetate 7:3); IR: (ATR)/ cm^{-1} 3346 (OH), 1643 (C=O); ^1H NMR (ppm,

DMSO-d₆): 6.85 (1H, d, $J = 8.6$ Hz, Ar), 7.03 (1H, dd, $J = 8.6, 2.9$ Hz, Ar), 7.27-7.35 (2H, m, Ar), 7.40 (1H, d, $J = 2.9$ Hz, Ar), 7.49-7.56 (1H, m, Ar), 7.83 (1H, $J = 16$ Hz, C=CH), 7.93 (1H, $J = 16$ Hz, C=CH), 8.04 (1H, ddd, $J = 8.6, 1.4$ Hz, Ar), 9.30 (1H, s, OH), 11.50 (1H, s, OH); ¹³C NMR (DMSO-d₆) 114.9, 116.0, 116.2, 118.4, 121.3, 122.1, 122.2, 124.4, 124.9, 124.9, 125.0, 129.6, 132.8, 132.9, 135.4, 135.4, 149.6, 154.2, 192.7; HMRS found [M+1]⁺ 259.0768, C₁₅H₁₁O₃F [M+1]⁺ 259.0765; Purity > 98% HPLC method 1 (Retention time 3.223 min).



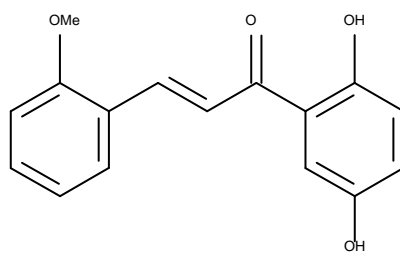
(E)-1-(2,4-dihydroxyphenyl)-3-(2-chlorophenyl)-2-propene-1-one. (AH15)

Recrystallisation from dichloromethane. Dark yellow crystals (%); mp 127-130 °C; TLC: R_f 0.34 (hexane/ethyl acetate 7:3); IR: (ATR)/cm⁻¹ 3234 (OH), 1637 (C=O); ¹H NMR (δ ppm, DMSO-d₆): 6.32 (1H, d, $J = 1.2$ Hz, Ar), 6.45 (1H, dd, $J = 8.6, 1.2$ Hz, Ar), 7.44-7.57 (2H, m, Ar), 7.58 (1H, dd, $J = 8.6, 1.2$ Hz, Ar), 8.02 (1H, $J = 17.2$ Hz, C=CH), 8.06 (1H, $J = 17.2$ Hz, C=CH), 8.23 (2H, m, Ar), 10.85 (1H, s, OH), 13.22 (1H, s, OH); ¹³C NMR (DMSO-d₆) 102.6, 108.5, 113.0, 124.2, 127.7, 128.0, 130.0, 132.0, 132.2, 133.3, 134.4, 138.0, 165.6, 165.8, 190.9; HMRS found [M+1]⁺ 275.0471, C₁₅H₁₂O₃Cl [M+1]⁺ 275.0475; Purity > 98% HPLC method 1 (Retention time 2.960 min).



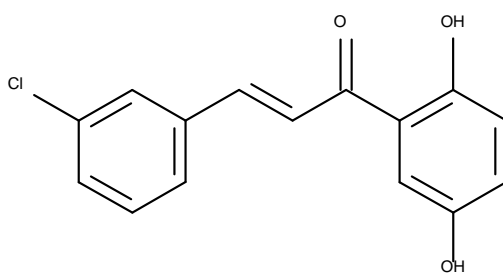
(E)-1-(2,5-dihydroxyphenyl)-3-(2-ethoxyphenyl)-2-propene-1-one. (AH8)

Column chromatography. Red/orange powder (60%); mp 89-91°C; TLC: $R_f = 0.28$ (hexane/ethyl acetate 7:3); IR: (ATR)/ cm^{-1} 3324 (OH), 1639 (C=O); ^1H NMR (ppm, DMSO- d_6): 1.44 (3H, t, $J = 4.2\text{Hz}$, CH_3), 4.16 (2H, q, $J = 4.2, 4.2\text{Hz}$, CH_2), 6.85 (1H, d, $J = 8.3\text{Hz}$, Ar), 7.04 (2H, dd, $J = 8.3, 2.3\text{Hz}$, Ar), 7.13 (1H, d, $J = 8.3\text{Hz}$, Ar), 7.46 (2H, ddd, $J = 8.3, 1.2\text{Hz}$, Ar), 7.94 (1H, ddd, $J = 8.3, 1.2\text{Hz}$, Ar), 7.95 (1H, J = 15.5 Hz, C=CH), 8.09 (1H, J = 15.5 Hz, C=CH), 9.20 (1H, s, OH), 11.80 (1H, s, OH); ^{13}C NMR (DMSO- d_6) 14.6, 63.8, 112.7, 114.8, 118.4, 120.7, 121.0, 122.0, 122.8, 124.3, 129.4, 132.5, 139.3, 149.5, 154.6, 157.8, 159.8, 193.2; HMRS found $[\text{M}+1]^+$ 285.1124, $\text{C}_{17}\text{H}_{16}\text{O}_4$ $[\text{M}+1]^+$ 285.1121; Purity > 98% HPLC method 1 (Retention time 3.744 min).



(E)-1-(2,5-dihydroxyphenyl)-3-(2-methoxyphenyl)-2-propene-1-one. (AH13)

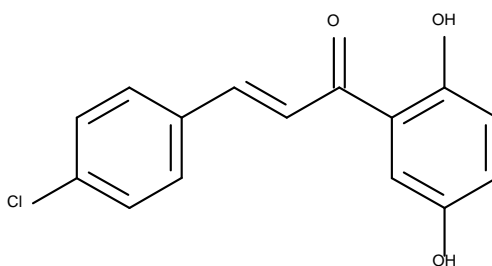
Column chromatography. Dark red powder (14%); mp 146-149°C; TLC: R_f 0.28 (hexane/ethyl acetate 7:3) IR: (ATR)/ cm^{-1} 3353 (OH), 1638 (C=O); ^1H NMR (ppm, DMSO- d_6): 3.92 (3H, s, OCH₃), 6.85 (1H, d, $J = 9.5\text{Hz}$, Ar), 7.00-7.08 (2H, m, Ar), 7.15 (1H, d, $J = 9.5\text{Hz}$, Ar), 7.44-7.53 (2H, ddd, $J = 9.5, 3.2\text{Hz}$, Ar), 7.89 (1H, $J = 16\text{ Hz}$, C=CH), 7.95 (1H, dd, $J = 9.5, 3.2\text{Hz}$, Ar), 8.09 (1H, $J = 16\text{ Hz}$, C=CH), 9.19 (1H, s, OH), 11.79 (1H, s, OH); ^{13}C NMR (DMSO- d_6) 55.8, 111.7, 114.8, 118.3, 120.8, 120.9, 121.9, 122.7, 124.3, 129.0, 132.6, 139.0, 149.46, 154.6, 158.4, 193.22; HMRS found $[\text{M}+1]^+$ 271.0967, C₁₆H₁₄O₄ $[\text{M}+1]^+$ 271.0965; Purity > 98% HPLC method 1 (Retention time 3.083 min).



(E)-1-(2,5-dihydroxyphenyl)-3-(3-chlorophenyl)-2-propene-1-one. (AH2)

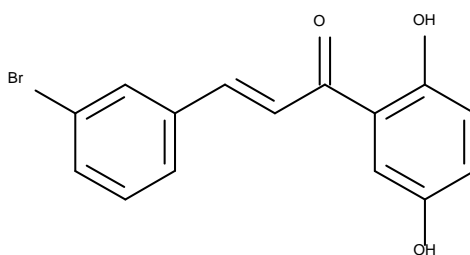
Column chromatography. Bright red solid (52%); mp 168-170°C; TLC: R_f 0.2 (hexane/ethyl acetate 7:3); IR: (ATR)/ cm^{-1} 3370 (OH), 1644 (C=O); ^1H NMR (δ ppm,

DMSO-d₆): 6.86 (1H, d, $J = 8.6$ Hz, Ar), 7.06 (1H, dd, $J = 8.6, 2.9$ Hz, Ar), 7.45-7.57 (2H, m, Ar), 7.57 (1H, d, $J = 2.9$ Hz, Ar), 7.77 (1H, $J = 16$ Hz, C=CH), 8.01 (1H, $J = 16$ Hz, C=CH), 7.83 (1H, ddd, $J = 7.2, 1.4$ Hz, Ar), 8.08 (1H, s, Ar), 9.20 (1H, s, OH), 11.70, (1H, s, OH); ¹³C NMR (DMSO-d₆) 115.3, 118.3, 121.0, 123.9, 124.6, 128.0, 130.3, 130.4, 130.7, 133.8, 136.8 142.5, 149.5, 154.6, 193.1; HMRS found [M+1]⁺ 273.0323, C₁₅H₁₁O₃Cl [M+1]⁺ 273.0324; Purity > 97% HPLC method 1 (Retention time 3.929 min).



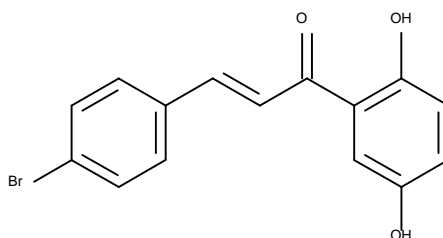
(E)-1-(2,5-dihydroxyphenyl)-3-(4-chlorophenyl)-2-propene-1-one. (AH3)

Column chromatography. Bright red powder (22%); mp 187-188°C; TLC: R_f 0.56 (hexane/ethyl acetate 7:3); IR: (ATR)/cm⁻¹ 3383 (OH), 1642 (C=O); ¹H NMR (δ ppm, DMSO-d₆): 6.90 (1H, d, $J = 8.8$ Hz, Ar), 7.10 (1H, dd, $J = 8.8, 2.2$ Hz, Ar), 7.45-7.53 (3H, m, Ar), 7.83 (1H, $J = 16.0$ Hz, C=CH), 7.85-7.95 (2H, m, Ar) 8.02 (1H, $J = 16.0$ Hz, C=CH), 9.20 (1H, s, OH), 11.70, (1H, s, OH); ¹³C NMR (DMSO-d₆) 79.3, 80.2, 83.0, 88.5, 123.5, 126.3, 128.4, 129.7, 134.3, 136.0, 138.8, 140.6, 154.8, 159.8, 180.6, 190.7; HMRS found [M+1]⁺ 273.0323, C₁₅H₁₁O₃Cl [M+1]⁺ 273.0324; Purity > 97% HPLC method 1 (Retention time 2.892 min).



(E)-1-(2,5-dihydroxyphenyl)-3-(3-bromophenyl)-2-propene-1-one. (AH4)

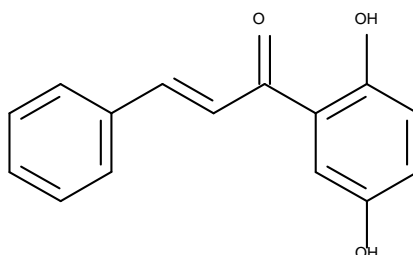
Column chromatography. Bright red powder (42%); mp 152-154°C; TLC: R_f 0.33 (hexane/ethyl acetate 7:3); IR: (ATR)/ cm^{-1} 3386 (OH), 1635 (C=O); ^1H NMR (δ ppm, DMSO- d_6): 6.82 (1H, d, $J = 8.2\text{Hz}$, Ar), 7.10 (1H, dd, $J = 8.2, 2.7\text{Hz}$, Ar), 7.40 (1H, dd, $J = 16.4, 8.2\text{ Hz}$, Ar), 7.55 (1H, d, $J = 2.7\text{Hz}$, Ar), 7.60-7.62 (1H, m, Ar), 7.72 (1H, d, $J = 16.4\text{ Hz}$, C=CH), 7.82 (1H, d, $J = 8.2\text{Hz}$, Ar), 8.00 (1H, d, $J = 16.4\text{ Hz}$, C=CH), 8.2 (1H, s, Ar), 9.20 (1H, s, OH), 11.70, (1H, s, OH); ^{13}C NMR (DMSO- d_6); 118.0, 121.0, 123.6, 125.1, 126.5, 127.3, 131.1, 133.7, 133.7, 135.4, 135.9, 139.7, 145.2, 152.2, 157.4; Purity > 96% HPLC method 1 (Retention time 3.786 min).



(E)-1-(2,5-dihydroxyphenyl)-3-(4-bromophenyl)-2-propene-1-one. (AH5)

Column chromatography. Bright red powder (17%); mp 188-189°C; TLC: R_f 0.35 (hexane/ethyl acetate 8:2); IR: (ATR)/ cm^{-1} 3390 (OH), 1639 (C=O); ^1H NMR (δ ppm, DMSO- d_6): 6.85 (1H, d, $J = 8.5\text{Hz}$ Ar), 7.05 (1H, dd, $J = 8.8, 3.4\text{Hz}$ Ar), 7.51 (1H, d, J

= 3.4Hz Ar), 7.68 (2H, d, $J = 6.8\text{Hz Ar}$), 7.76 (1H, d, $J = 13.5\text{Hz, C=CH}$), 7.86 (2H, d, $J = 6.8\text{Hz Ar}$), 7.96 (1H, d, $J = 13.5\text{Hz, C=CH}$), 9.2 (1H, s, OH), 11.7 (1H, s, OH); ^{13}C NMR (DMSO- d_6) 115.4, 118.3, 121.0, 123.5, 124.5, 130.9, 131.9, 134.1, 142.8, 149.4, 154.7, 193.0; HMRS found $[\text{M}+1]^+$ 316.9817, $\text{C}_{15}\text{H}_{11}\text{O}_3\text{Br}$ $[\text{M}+1]^+$ 316.9819; Purity > 97% HPLC method 1 (Retention time 2.929 min).

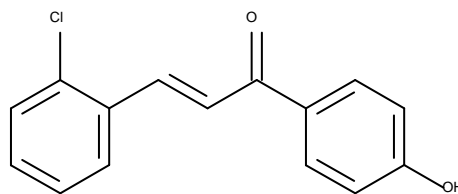


(E)-1-(2,5'-dihydroxyphenyl)-3-(phenyl)-2-propene-1-one. (AHXRS3)

Column chromatography. Bright red powder (25%); mp 164-167°C TLC: R_f 0.45 (hexane/ethyl acetate 7:3); IR: (ATR)/ cm^{-1} 3390 (OH), 1639 (C=O); ^1H NMR (δ ppm, DMSO- d_6): 6.86 (1H, d, $J = 8.4\text{Hz Ar}$), 7.04 (1H, dd, $J = 8.4, 2.1\text{Hz, Ar}$), 7.45-7.5 (3H, m, Ar), 7.52 (1H, d, $J = 2.1\text{Hz Ar}$), 7.79 (1H, $J = 16.8\text{Hz, C=CH}$), 7.87-7.92 (2H, m, Ar), 7.93 (1H, d, $J = 16.8\text{Hz, C=CH}$), 9.2 (1H, s, OH), 11.7 (1H, s, OH); ^{13}C NMR (DMSO- d_6) 68.7, 78.7, 87.1, 115.1, 119.0, 121.0, 122.3, 124.8, 126.5, 128.5, 130.8, 134.5, 151.6, 193.15; HMRS found $[\text{M}+1]^+$ 239.0704, $\text{C}_{15}\text{H}_{12}\text{O}_3$ $[\text{M}+1]^+$ 239.0703; Purity > 95% HPLC method 1 (Retention time 3.044 min).

8.2.3.3 Chalcone synthesis method 2 (acid catalysis SOCl₂) modification of (Petrov, Ivanova and Gerova, 2008):

4-hydroxyacetophenone (0.68g 5.55mmol) and 2-chlorobenzaldehyde (0.56mL 5.55mmol) were dissolved in absolute ethanol (2.5mL). Thionyl chloride (0.25mL mmol) was then added dropwise. The reaction mixture was allowed to stir at room temperature for 2 hours and then left to stand overnight. The resultant mixture was quenched with water (10ml) to induce a precipitate. The resultant precipitate was recrystallised from ethanol.

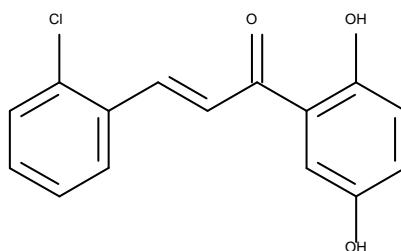


(E)-1-(4'-hydroxyphenyl)-3-(2-chlorophenyl)-2-propene-1-one. (AH16)

Recrystalliation from ethanol. Purple crystals (33%); mp 167-169°C; TLC: R_f = 0.4 (hexane/ethyl acetate 7:3); IR: (ATR)/cm⁻¹ 3218 (OH), 1649 (C=O) ; ¹H NMR (ppm, DMSO-d₆): 6.91 (2H, dt, J = 9.3, 1.6Hz, Ar), 7.42-7.50 (2H, m, Ar), 7.54-7.59 (1H, m, Ar), 7.96 (1H, J = 18.2 Hz, C=CH), 8.01 (1H, J = 18.2 Hz, C=CH), 8.10 (2H, dt, J = 9.3, 1.6Hz, Ar), 8.18-8.23 (1H, m, Ar), 10.50 (1H, s, OH); ¹³C NMR (DMSO-d₆) 115.4, 124.9, 127.6, 128.5, 128.8, 130.0, 131.3, 131.7, 132.5, 134.2, 137.3, 162.4, 186.9; HMRS found [M+1]⁺ 259.0523, C₁₅H₁₁O₂Cl [M+1]⁺ 259.0520; Purity > 99% HPLC method 1 (Retention time 3.110 min).

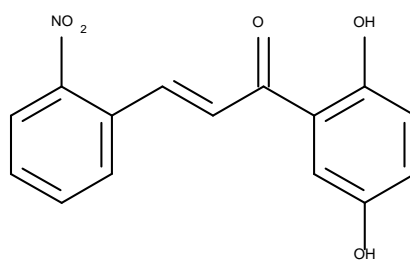
8.2.3.4 Chalcone synthesis method 3 (acid catalysis H₂SO₄) modification of (Konieczny *et al.*, 2007).

Concentrated sulphuric acid (0.3 mL 5.6 mmol) was added dropwise to a stirred solution of the acetophenone (1.64 mmol) and a benzaldehyde (1.81 mmol) in acetic acid (2 mL). The reaction mixture was heated for 1hr at 80°C and allowed to cool to room temperature and stirred for 24h resulting in the formation of a red precipitate. The reaction was quenched with water (30 mL) and extracted with ethyl acetate (2x30 mL). The combined organic extracts were washed with water (2x30 mL) and dried over anhydrous magnesium sulphate. After the removal of the solvent under vacuum the crude product was recrystallised from ethanol.



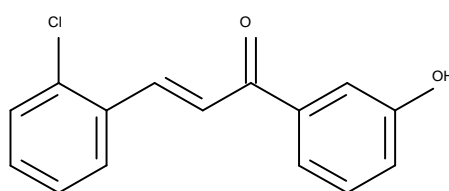
(E)-1-(2,5'-dihydroxyphenyl)-3-(2-chlorophenyl)-2-propene-1-one. (AH1)

Column chromatography. Bright red solid (29%); mp 187-189°C; TLC: R_f 0.55 (hexane/ethyl acetate 7:3); IR: (ATR)/cm⁻¹ 3354 (OH), 1639 (C=O); ¹H NMR (δ ppm, DMSO-d₆): 6.87 (1H, d, *J* = 8.2Hz, Ar), 7.06 (1H, dd, *J* = 8.2, 2.7Hz, Ar), 7.49 (3H, m, Ar), 7.59 (1H, dd, *J* = 8.2, 1.4Hz, Ar), 7.96 (1H, *J* = 16.4 Hz, C=CH), 8.08 (1H, *J* = 16.4 Hz, C=CH), 8.18 (1H, dd, *J* = 8.2, 1.4Hz, Ar), 9.20 (1H, s, OH), 11.48, (1H, s, OH); ¹³C NMR (DMSO-d₆) 115.1, 118.3, 121.3, 124.5, 125.4, 127.7, 128.7, 130.1, 132.1, 132.1, 134.4, 138.4, 149.6, 154.3, 192.6; HMRS found [M+1]⁺ 275.0471, C₁₅H₁₁O₃Cl [M+1]⁺ 275.0469; Purity > 99% HPLC method 1 (Retention time 3.921 min).



(E)-1-(2,5'-dihydroxyphenyl)-3-(2-nitrophenyl)-2-propene-1-one. (AH12)

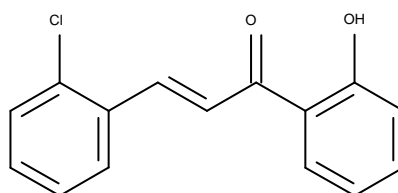
Column chromatography. Bright red solid (27%); mp 190-192°C; TLC: $R_f = 0.20$ (hexane/ethyl acetate 6:4); IR: (ATR)/ cm^{-1} 3396 (OH), 1647 (C=O), 1518 (NO₂), 1345 (NO₂); ¹H NMR (δ ppm, DMSO-d₆): 6.88 (1H, d, $J = 9.5\text{Hz}$, Ar), 7.06 (1H, dd, $J = 9.5, 3.2\text{Hz}$, Ar), 7.45 (1H, d, $J = 3.2\text{Hz}$, Ar), 7.73 (1H, ddd, $J = 9.5, 1.2\text{Hz}$, Ar), 7.84 (1H, d, $J = 9.5\text{Hz}$, Ar), 7.88 (1H, $J = 15.8\text{ Hz}$, C=CH), 8.02 (1H, $J = 15.8\text{ Hz}$, C=CH), 8.14 (2H, m, $J = 9.5, 1.2\text{Hz}$, Ar), 9.20 (1H, s, OH), 11.34 (1H, s, OH); ¹³C NMR (DMSO-d₆) 115.1, 118.4, 121.4, 124.5, 124.7, 127.2, 129.5, 129.6, 131.1, 133.8, 138.1, 148.8, 149.6, 154.1, 192.3; HMRS found $[\text{M}+1]^+$ 286.0712, C₁₅H₁₁O₅N $[\text{M}+1]^+$ 286.0710; Purity > 97% HPLC method 1 (Retention time 2.573 min).



(E)-1-(3'-hydroxyphenyl)-3-(2-chlorophenyl)-2-propene-1-one. (AH17)

Column chromatography. Light green solid (20%) mp 112-115 °C TLC: $R_f = 0.35$ (hexane/ethyl acetate 8:2); IR: (ATR)/ cm^{-1} 2945 (OH), 1678 (C=O); ¹H NMR (δ ppm,

DMSO-d₆): 7.09 (1H, dd, $J = 9.2, 3.1\text{Hz}$, Ar), 7.40 (1H, dd, $J = 15.3, 9.2\text{Hz}$, Ar), 7.43-7.52 (3H, m, Ar), 7.59 (1H, dd, $J = 9.2, 3.1\text{Hz}$, Ar), 7.66 (1H, ddd, $J = 9.2\text{Hz}$, Ar), 7.93 (1H, $J = 15.3\text{ Hz}$, C=CH), 8.03 (1H, $J = 15.3\text{ Hz}$, C=CH), 8.23 (1H, dd, $J = 9.2, 3.1\text{Hz}$, Ar), 9.90 (1H, s, OH); ¹³C NMR (DMSO-d₆) 117.4, 122.5, 123.3, 127.6, 130.4, 131.3, 132.6, 132.7, 134.7, 134.9, 137.0, 141.0, 141.3, 160.5, 191.6; HMRS found [M-1] 257.0377, C₁₅H₁₁O₂Cl [M-1] 257.0375 Purity > 95% HPLC method 1 (Retention time 3.786 min).

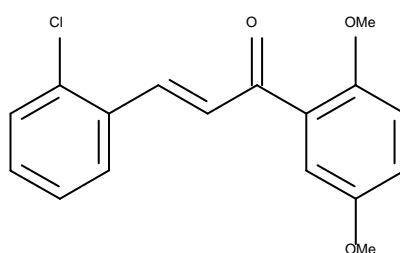


(E)-1-(2'-hydroxyphenyl)-3-(2-chlorophenyl)-2-propene-1-one. (AH17a)

Recrystallisation from ethanol. Light brown crystals (18%) mp 77-81°C TLC: R_f = 0.52 (hexane/ethyl acetate 9:1); IR: (ATR)/cm⁻¹ 2932 (OH), 1639 (C=O); ¹H NMR (δ ppm, DMSO-d₆): 7.02 (1H, m, Ar), 7.44-7.55 (2H, m, Ar), 7.56-7.62 (2H, m, Ar), 8.06 (1H, $J = 17.8\text{ Hz}$, C=CH), 8.13 (1H, $J = 17.8\text{ Hz}$, C=CH), 8.22 (2H, dd, 7.4, 1.5Hz, Ar), 12.22 (1H, s, OH); HMRS found [M+1]⁺ 259.0523, C₁₅H₁₁O₂Cl [M+1]⁺ 259.0520; Purity > 97% HPLC method 1 (Retention time 8.386 min).

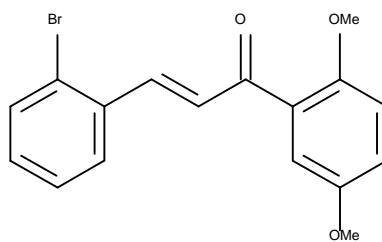
8.2.3.5 Chalcone synthesis method 4 (Detsi *et al.*, 2009)

The acetophenone (3.23mmol) and benzaldehyde (3.23mmol) were dissolved in absolute ethanol (9 mL). Potassium hydroxide (3ml of 20% aqueous solution) was added dropwise. The reaction mixture was allowed to stir at room temperature and monitored by TLC. After 1 hour the reaction mixture was quenched with cold water (10ml) to induce a precipitate. The crude was purified by recrystallisation from ethanol and dried *in vacuo*.



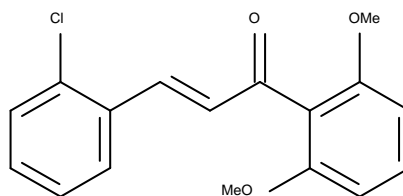
***(E)*-1-(2,5'-dimethoxyphenyl)-3-(2-chlorophenyl)-2-propene-1-one. (AH21)**

Recrystallisation from ethanol. Bright yellow crystals (55%); mp 88-92°C TLC: $R_f = 0.63$ (hexane/ethyl acetate 8:2); IR: (ATR)/ cm^{-1} 1652 (C=O), 1287 (C-O); ^1H NMR (ppm, DMSO- d_6): 3.74 (3H, s, OCH₃), 3.82 (3H, s, OCH₃), 7.07 (1H, dd, $J = 1.7\text{Hz}$, Ar), 7.12-7.16 (2H, m, Ar), 7.39-7.5 (3H, m, Ar), 7.55 (1H, dd, $J = 6.9, 0.1\text{Hz}$, Ar), 7.8 (1H, $J = 13.8\text{ Hz}$, C=CH), 7.95 (1H, dd, $J = 6.9, 0.1\text{Hz}$, Ar); ^{13}C NMR (DMSO- d_6): 55.6, 56.4, 113.9, 114.0, 119.1, 127.9, 128.2, 128.8, 129.4, 130.0, 131.8, 132.3, 134.1, 137.3, 152.1, 153.1, 191.4; HMRS found $[\text{M}+1]^+$ 303.0783, C₁₇H₁₅O₃Cl $[\text{M}+1]^+$ 303.0782; Purity > 95% HPLC method 2 (Retention time 2.774 min).



(E)-1-(2'5'-dimethoxyphenyl)-3-(2-bromophenyl)-2-propene-1-one. (AH21b)

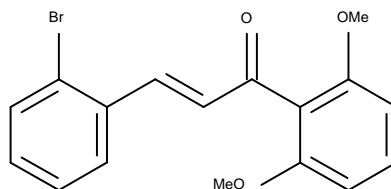
Recrystallisation from ethanol. Bright yellow crystals (88%); mp 100-102°C TLC: R_f 0.29 (hexane/ethyl acetate 8:2); IR: (ATR)/ cm^{-1} 1665 (C=O), 1015 (C-O); ^1H NMR (ppm, DMSO- d_6): 3.76 (3H, s, OCH₃), 3.83 (3H, s, OCH₃), 7.08 (1H, dd, Ar), 7.16 (2H, m, Ar), 7.38 (1H, td, Ar), 7.45 (2H, dd, Ar), 7.73 (1H, dd, Ar), 7.79 (1H, d, Ar), 7.94 (1H, dd, Ar); ^{13}C NMR (DMSO- d_6): 58.3, 59.1, 116.6, 116.6, 121.8, 127.8, 131.1, 131.1, 131.5, 132.1, 134.8, 136.0, 136.6, 142.7, 154.8, 155.7, 194.2; HMRS found $[\text{M}+1]^+$ 347.0279, C₁₇H₁₅O₃Br $[\text{M}+1]^+$ 347.0277; Purity > 99% HPLC method 2 (Retention time 2.945 min).



(E)-1-(2'6'-dimethoxyphenyl)-3-(2-chlorophenyl)-2-propene-1-one. (AH21a)

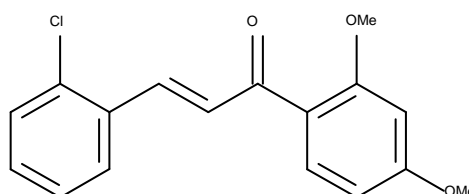
Recrystallisation from ethanol. Bright yellow crystals (56%); mp 132-139°C TLC: R_f 0.3 (Hexane/Ethyl Acetate 8:2); IR: (ATR)/ cm^{-1} 1652 (C=O), 1251 1102 (C-O); ^1H NMR (δ ppm, DMSO- d_6): 3.72 (6H, s, (OCH₃)₂), 6.76 (2H, d, $J = 8.7\text{Hz}$ Ar) 7.01 (1H, d, $J = 17.4\text{Hz}$, C=CH), 7.37-7.42 (3H, m, Ar) 7.53 (2H, m, Ar), 7.96 (1H, dd, $J = 8.7, 2.2\text{Hz}$ Ar); ^{13}C NMR (DMSO- d_6): 55.8, 104.4, 117.4, 127.8, 130.0, 130.8, 131.2, 131.8, 132.1,

133.8, 139.4, 156.9, 193.9; HMRS found $[M+1]^+$ 303.0784, $C_{17}H_{15}O_3Cl$ $[M+1]^+$ 303.0782; Purity > 99% HPLC method 2 (Retention time 2.269 min).



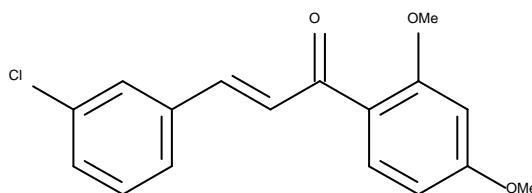
(E)-1-(2'6'-dimethoxyphenyl)-3-(2-bromophenyl)-2-propene-1-one. (AH21c)

Recrystallisation from ethanol. Bright yellow crystals (61%); mp 159-160°C TLC: R_f 0.2 (hexane/ethyl acetate 8:2); IR: (ATR)/ cm^{-1} 1667 (C=O), 1252 (C-O); 1H NMR (ppm, DMSO- d_6): 3.74 (6H, s, OCH₃), 6.78 (2H, d, $J = 9.1Hz$, Ar), 6.98 (1H, d, $J = 15.2Hz$, C=CH), 7.36 (1H, ddd, $J = 12.1, 3.0, 1.5Hz$, Ar), 7.43 (2H, m, Ar), 7.51 (1H, d, $J = 15.2Hz$, C=CH, Ar), 7.69 (1H, dd, $J = 9.1, 1.5Hz$, Ar), 7.95 (1H, dd, $J = 9.1, 1.5Hz$, Ar), ^{13}C NMR (DMSO- d_6): 55.8, 104.4, 117.4, 124.9, 128.4, 128.5, 130.9, 131.2, 132.2, 133.2, 133.5, 142.3, 156.9, 193.9; HMRS found $[M+1]^+$ 347.0279, $C_{17}H_{15}O_3Br$ $[M+1]^+$ 347.0277; Purity > 99% HPLC method 2 (Retention time 2.483 min).



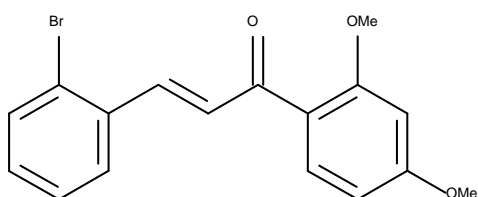
(E)-1-(2'4'-dimethoxyphenyl)-3-(2-chlorophenyl)-2-propene-1-one. (AH22)

Recrystallisation from ethanol. Bright yellow crystals (67%); mp 112-115°C TLC: R_f 0.23 (Hexane/Ethyl Acetate 8:2); IR: V_{max} cm⁻¹ 1645 (C=O); ¹H NMR (δ ppm, DMSO-d₆): 3.85 (3H, s, OCH₃), 3.90 (3H, s, OCH₃), 6.67 (2H, m, Ar), 7.43-7.50 (2H, m, Ar), 7.53-7.66 (3H, m, Ar), 7.83 (1H, d, *J* = 16.9Hz, C=CH), 7.91-7.96 (1H, m, Ar); ¹³C NMR (DMSO-d₆) 55.6, 56.0, 98.6, 106.2, 121.0, 127.8, 128.1, 129.8, 130.0, 131.5, 132.2, 132.6, 134.0, 135.9, 160.5, 164.3, 189.0; HMRS found [M+1]⁺ 303.0781, C₁₇H₁₅O₃Cl [M+1]⁺ 303.0782; Purity > 95% HPLC method 2 (Retention time 2.578 min).



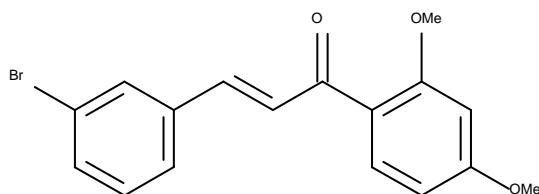
(E)-1-(2,4'-dimethoxyphenyl)-3-(3-chlorophenyl)-2-propene-1-one. (AH22b)

Recrystallisation from ethanol. Bright yellow crystals (81%); mp 123-125°C TLC: R_f 0.3 (Hexane/Ethyl Acetate 7:3); IR: V_{max} cm⁻¹ 1648 (C=O); ¹H NMR (δ ppm, DMSO-d₆): 3.86 (3H, s, OCH₃), 3.90 (3H, s, OCH₃), 6.65 (1H, dd, *J* = 12.4, 2.55Hz, Ar), 6.70 (1H, d, *J* = 2.55Hz, Ar), 7.47 (2H, m, Ar), 7.52 (1H, d, *J* = 17.1 Hz, C=CH), 7.59 (1H, d, *J* = 17.1 Hz, C=CH), 7.63 (1H, d, *J* = 7.65Hz, Ar), 7.68-7.75 (1H, m, Ar), 7.81 (1H, s, Ar); ¹³C NMR (DMSO-d₆) 55.6, 56.0, 98.6, 106.0, 121.2, 126.7, 128.0, 128.6, 129.7, 130.7, 132.1, 133.7, 137.2, 139.4, 160.4, 164.1, 189.2; HMRS found [M+1]⁺ 303.0780, C₁₇H₁₅O₃Cl [M+1]⁺ 303.0782; Purity > 97% HPLC method 2 (Retention time 2.614 min).



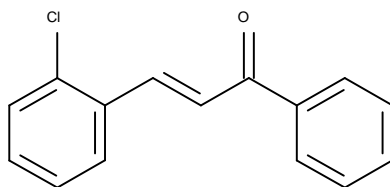
(E)-1-(2,4'-dimethoxyphenyl)-3-(2-bromophenyl)-2-propene-1-one. (AH22a)

Recrystallisation from ethanol. Bright yellow crystals (81%); mp 123-125°C TLC: R_f 0.3 (Hexane/Ethyl Acetate 7:3); IR: V_{max} cm⁻¹ 1648 (C=O); ¹H NMR (δ ppm, DMSO-d₆): 3.87 (3H, s, OCH₃), 3.92 (3H, s, OCH₃), 6.66 (1H, ddd, *J* = 12.2, 3.05Hz, Ar), 6.71 (1H, d, *J* = 3.05Hz, Ar), 7.36 (1H, ddd, *J* = 15.3, 6.1, 3.05Hz, Ar), 7.47 (1H, dd, *J* = 15.3, 6.1Hz, Ar), 7.56 (1H, d, *J* = 15.3Hz, C=CH), 7.65 (1H, d, *J* = 9.2Hz, Ar), 7.73 (1H, dd, *J* = 9.2, 1.5Hz, Ar), 7.81 (1H, d, *J* = 15.3Hz, C=CH), 7.92 (1H, dd, *J* = 9.2, 1.5Hz, Ar); ¹³C NMR (DMSO-d₆) 55.6, 56.0, 98.6, 106.2, 121.0, 124.9, 128.2, 128.4, 129.8, 131.7, 132.2, 133.3, 134.3, 138.6, 160.4, 164.3, 188.9; HMRS found [M+1]⁺ 347.0279, C₁₇H₁₅O₃Br [M+1]⁺ 347.0277; Purity > 98% HPLC method 2 (Retention time 2.635 min).



(E)-1-(2,4'-dimethoxyphenyl)-3-(3-bromophenyl)-2-propene-1-one. (AH22s2)

Recrystallisation from ethanol. Bright yellow crystals (80%); mp 89-90°C TLC: R_f 0.4 (Hexane/Ethyl Acetate 7:3); IR: V_{\max} cm^{-1} 1648 (C=O); ^1H NMR (δ ppm, DMSO- d_6): 3.86 (3H, s, OCH₃), 3.90 (3H, s, OCH₃) 6.65 (1H, dd, $J = 10.0, 2.5\text{Hz}$, Ar), 6.69 (1H, d, $J = 1.5\text{Hz}$, Ar), 7.40 (1H, dd, $J = 15, 7.5\text{Hz}$, Ar), 7.51 (1H, d, $J = 15\text{ Hz}$, C=CH), 7.58 (1H, d, $J = 15\text{ Hz}$, C=CH), 7.62 (2H, d, $J = 7.5\text{Hz}$, Ar), 7.75 (1H, d, $J = 7.5\text{Hz}$ Ar), 7.94 (1H, s, Ar); ^{13}C NMR, (DMSO- d_6) 55.6, 56.0, 98.6, 106.0, 121.2, 122.3, 127.0, 128.6, 130.9, 131.0, 132.1, 132.6, 137.5, 139.3, 160.4, 154.1, 189.2; HMRS found $[\text{M}+1]^+$ 347.0280, C₁₇H₁₅O₃Br $[\text{M}+1]^+$ 347.0283; Purity > 98% HPLC method 2 (Retention time 2.717 min).



(E)-1-(phenyl)-3-(2-chlorophenyl)-2-propene-1-one. (AHXRS1)

Recrystallisation from ethanol. Bright red crystals (91%) mp 52-54°C TLC: $R_f = 0.58$ (hexane/ethyl acetate 8:2); IR: (ATR)/ cm^{-1} 1661 (C=O); ^1H NMR (δ ppm, DMSO- d_6) 7.48 (2H, m, Ar), 7.60 (3H, m, Ar), 7.70 (1H, tt, Ar), 8.02 (1H, $J = 16\text{ Hz}$, C=CH), 8.07 (1H, $J = 16\text{ Hz}$, C=CH), 8.18 (2H, dd, Ar), 8.24 (1H, dd, Ar); HMRS found $[\text{M}+1]^+$ 243.0576, C₁₅H₁₁OCl $[\text{M}+1]^+$ 243.0577; Purity > 99% HPLC method 2 (Retention time 2.969 min).

8.3. General biology procedures

8.3.1 Materials

8.3.1.1 Cell culture

HUVEC (pooled, P1) Gibco Invitrogen (cat: C-015-10C); EM-200 media Gibco Invitrogen (cat: M200500); LSGS Gibco Invitrogen (cat: S-003-10); PBS 7.4 Gibco Invitrogen (cat: 10010023); Trypsin EDTA 10x (cat: T4174); Foetal calf serum (cat: C8056); VEGF (recombinant human protein; cat: PHC9394).

8.3.1.2 MTT assay

MTT (98%) Sigma-Aldrich (cat: M2128-1G); DMSO (99.6%) (cat: 471267); tissue culture plates, 96 well flat bottom with low evaporation lid, Corning Ltd (cat: 353072)

8.3.2.2 Western blot analysis

Colour burst™ electrophoresis protein ladder: 8,000 – 220,000 Da Sigma (cat: C1992) Bovine serum albumin (BSA) Sigma (cat: A7906); Sodium orthovanadate (powder) Sigma (cat: S6508); DTT Sigma (cat: D0632); Bolt 4-12% Bix-Tris Plus Gels, 10 well, gel packs Gibco Invitrogen (cat: NW04120BOX); iBlot™ 2 Transfer Stacks, nitrocellulose, regular size Gibco Invitrogen (cat: IB23001); 20x Bolt MES SDS Running Buffer 500ml, Gibco Invitrogen (cat: B0002); TBS: Trizma™ Base, Sigma (cat: T1503); NaCl, Sigma (cat: S9888), HCL, Fisher Scientific (cat: 11478333); TBS-Tx100: TBS, Triton 100x bio ultra (cat: T9284); Reblot: Re-Blot Plus-Mild (10x), EMD Milipore, (cat: 2502).

Table 21 Buffers and solutions

TBST 10x (500ml)	Tris (50 mM), NaCl (150 mM), pH adjusted to 7.5 using HCl, 0.5% Tween 20.
TBS Tx-100 (500ml)	450ml dH ₂ O, 50ml TBST 10x, 2.5ml (20%)Triton 100x
Tris 1M pH 6.8	Tris base (1 M), 80ml dH ₂ O, pH adjusted to 6.8 with HCL, made up to 100ml
Tris 1M pH 8.5	Tris base (1 M), 80ml dH ₂ O, pH adjusted to 8.5 with HCL, made up to 100ml
Sample buffer (SB) 3x	3.75ml 1 M Tris pH 6.8, 6.0ml 20% SDS, 6.0ml 100% glycerol, 3.0ml 100 mM EDTA pH 6.8, 1.25ml dH ₂ O, bromophenol blue
Laemmli buffer	600 µl 3x SB, 300 µl dH ₂ O, 0.03g DTT, 80 µl 1 mM Sodium orthovanadate
Blocking solution (10ml)	0.5g milk powder, 10ml TBS TX-100
Stripping buffer (10ml)	1ml, 10x reblot (mild), 9ml dH ₂ O

Table 22 ECL solution

Solution	Volume/concentration	Company	Cat:
Solution A (p-coumaric acid)	22 µl of 90 mM	Sigma	C9008
Solution B (Luminol)	50 µl of 250 mM	Sigma	123072
Hydrogen peroxide	3 µl of 30% w/w in H ₂ O	Sigma	216763
dH ₂ O	9ml	-	-
Tris 1M pH 8.5	1ml	-	-

Table 23 Antibodies

Antibody	Dilution	Storage	Company	Cat:
VEGFR-2	1:1000	-20°C	Cell signalling	#9698S
Erk1/2	1:1000	-20°C	Cell signalling	#9102S
p-Erk1/2	1:1000	-20°C	Cell signalling	#4377S
B-actin	1:1000	-20°C	Cell signalling	#8457S
Anti-rabbit IgG	1:2000	-20°C	Cell signalling	#7074P2

All primary antibodies were made up in 5ml of TBSTx-100 with 5% BSA per blot. Secondary antibodies were made up in 5ml TBSTx-100 with 5% skimmed milk.

8.3.2 Methods:

8.3.2.1 General cell culture:

Primary HUVECs were acquired from Gibco Invitrogen, subcultured and stored in liquid nitrogen. Cells were maintained with EM-200 media supplemented with 10% foetal bovine serum (FBS) and 50x low serum growth supplement (LSGS).

8.3.2.2 Preparation of compound solutions

Compounds were weighed using a Fisherbrand MH-214 series analytical balance scale and dissolved with DMSO to make up 100 mM concentration stock solutions. These were stored at -20°C.

8.3.2.3 MTT cell proliferation assay (72 hr)

The MTT cell proliferation assay was conducted in a 3 stage process.

Stage 1: Cells were seeded at 3.5×10^3 per well in a 96 well plate in a volume of 180 μ L of 5% serum culture medium. One triplicate per plate was left with no cells as a negative control. Plates were then incubated at 37°C with 5% CO₂ overnight.

Stage 2: Test compound, at 100 mM solution, were diluted down to ranges of 100 μ M to 1 μ M in fresh 5% serum culture medium, 20 μ l of each concentration was added to wells in triplicates to form final set of concentrations between 10 μ M to 100 nM in media. Positive and vehicle controls (H₂O₂ and DMSO), respectively, at chosen concentrations were also made up in 5 % serum culture medium and 20 μ l was added to a triplicate of wells. Plates were then allowed to incubate at 37°C with 5% CO₂ for 72 hours.

Stage 3: To each well, 20 μ l of 2 mg/ml MTT reagent dissolved in PBS was added and then allowed to further incubate for 4 hours at 37°C with 5% CO₂. Media was then removed and 100 μ l of DMSO was added to each well to lyse the cells and solubilise the

purple formazan product. The plate was then wrapped in tin foil and then allowed to rock for 15 minutes on a Star Lab rocking shaker. Absorbance of each well was measured/quantified at 560 nM using a Promega GloMax Discovery system, data was exported to Microsoft Excel and analysed to form % control cell viabilities. Each assay was performed 4 times for preliminary screens and 5-6 times for EC/IC₅₀ determinations.

8.3.2.4 Cell stimulation and lysate preparation

HUVECs were grown in 6 well plates until 70-80% confluency. Media was removed and washed with PBS and then 1 ml of serum-free media was added. Compounds of known concentration with or without VEGF (30 ng/ml – added 15 minutes prior to cell lysate collection) were added and incubated for 1 hour. Media was then removed and each well washed with cold PBS. 30 µl of laemelli buffer containing sodium orthovanadate (protein phosphotyrosyl phosphatases (PTP) inhibitor) and dithiothreitol (to break disulphide bridges between proteins) was added to each well and placed on ice. Each well was then scraped using a Jet Biofil disposable cell scraper and the subsequent cell lysates transferred into 0.5 ml eppendorfs. Each cell lysate sample was sonicated using a Qsonica sonicator for 20 seconds at 20% pulse amplication. All samples were then heat blocked for 5 minutes at 95°C using a Star Lab dry bath system. Then each cell lysates was centrifuged for 1 min at room temperature at speed 1,300 rpm using a Heraeus Fresco 21 centrifuge.

8.3.2.5 Gel electrophoresis

Proteins were separated using gel electrophoresis. Pre cast Bolt 4-12% Bix-Tris Plus gel packs were used. Cell lysates prepared as shown in 10.3.2.4 were loaded using Gel Saver 2 natural pipette tips. In well 2, Colour Burst™ electrophoresis protein ladder was added

to monitor the protein separation as well as being a standard to compare protein molecular weights. Proteins were separated at 200v using MES running buffer (ingrediance) until the loading front reached the bottom of the gel. The gel was then removed from the cassette plate.

8.3.2.6 Transfer of proteins and staining western blotting

Protein separated on Bis-Tris Plus Gels were electro-transferred onto nitrocellulose membranes using the iBlot™ 2 dry blotting system. Western blot analysis was conducted using the Invitrogen mini gel tank and Bolt 4-12% Bix-Tris Plus Gels for gel electrophoresis. Gel transfers onto nitrocellulose membranes were carried out using the iBlot™ 2 gel transfer device with iBlot™ 2 Transfer Stacks. Selected antibodies were used to probe for desired proteins.

The membranes were briefly washed with TBS-Tx100 and blocked using 5% dried skimmed milk in TBS-Tx100 for one hour at room temperature on a gentle rock using Star Lab rocking shaker. All antibodies (primary and secondary) were used as shown in Table 3. To remove residual primary antibody membranes were washed 3 times with TBS-Tx100 for 10 minutes with gentle shaking. HRP-conjugated secondary antibody was then added to the membranes for 1 hour followed by 3 TBS-Tx 100 washes for 10 minutes.

8.3.2.7 Detection

All membranes were visualise using the enhanced chemiluminsence (made up in the lab see Table 2). Chemiluminsence images were immediately taken using the GeneGnome – syngene bio imaging with GeneSys V1.4.1.0 software. Membrane captures were then quantified using densitometry via the Image J software. Levels of proteins were

quantified and normalised using β actin as an internal control. Ratio of phosphorylated (activated) protein vs total protein were expressed as means \pm SEM.

8.3.2.8 Scratch assay

HUVECs were initially cultured in T-75 flasks until 80% confluent before being transferred into six well plates (cells of 1 flask split equally into 6 wells). Six well plates were then loaded with 1ml of LSGS media +/- compound at 10 μ M, 3 μ M and 1 μ M concentrations. Cells were cultured to 70-80% confluency before being scratched down the middle by a p1000 pipette tip. Images were taken at regular time points (0hr, 4hr and 8hr) using the EVOS FL Cell Imaging System and the average distance between the wound was calculated over the time points as a measure of migration. Photos were taken of 3 randomly selected fields at 100x magnification at 0hr, 4hrs and 8hrs. Three independent experiments were carried out. Relevant statistical analyses were performed thereafter.

8.3.2.9 Statistical analysis

Experiments were conducted in triplicates and repeated at least three times. Ordinary one way ANOVA analysis was conducted using Microsoft Excel STAT package. For multiple comparative analysis, the Tukey-Kramer multiple comparisons post hoc t-test was used via Graphpad Prism 7.0b software.

Chapter 9: References

- Abdollahi, A. and Folkman, J. (2010) Evading tumor evasion: Current concepts and perspectives of anti-angiogenic cancer therapy, *Drug Resistance Updates*, 13(1–2):16–28
- Abrams T. J., Murray L. J., Pesenti E., Holway V., Colombo T., Lee L., Cherrington J. and Pryer N. (2003) Preclinical evaluation of the tyrosine kinase inhibitor SU11248 as a single agent and in combination with “standard of care” therapeutic agents for the treatment of breast cancer, *Molecular Cancer Therapeutics*, 2:1011–1021
- Abrams T. J., Lee L. B., Murray L., Pryer N. and Cherrington J. (2003) SU11248 inhibits KIT and platelet-derived growth factor receptor beta in preclinical models of human small cell lung cancer, *Molecular cancer therapeutics*, 2(5):471–478
- Adair, T. H. and Montani, J.-P. (2010) Angiogenesis, *Colloquium Series on Integrated Systems Physiology: From Molecule to Function*, 2(1):1-84
- Adams J. M. and Cory S. (2007) The Bcl-2 apoptotic switch in cancer development and therapy, *National Institute of Health*, 26(9):1324–1337
- Adams R. H. and Alitalo K. (2007) Molecular regulation of angiogenesis and lymphangiogenesis, *Nature reviews. Molecular cell biology*, 8(6):464–478
- Adnane L., Trail P., Taylor I., Wilhelm S. (2006) Sorafenib (BAY 43-9006, Nexavar®), a Dual-Action Inhibitor That Targets RAF/MEK/ERK Pathway in Tumor Cells and Tyrosine Kinases VEGFR/PDGFR in Tumor Vasculature, *Methods in enzymology*, 407:597–612
- Al-Abd A. M., Alamoudi A., Abdel-Naim A, Neamatallah T. and Ashour O (2017) Anti-angiogenic agents for the treatment of solid tumors: potential pathways, therapy and current strategies – A review, *Journal of Advanced Research*. 8(6):591-605

- Albini, A., Dell'Eva R., Vené R., Ferrari N., Buhler D., Noonan D. and Fassina G (2006) Mechanisms of the antiangiogenic activity by the hop flavonoid xanthohumol: NF-kappaB and Akt as targets, *The FASEB journal : official publication of the Federation of American Societies for Experimental Biology*, 20(3):527–529
- Albini A., Tosetti F., Li V., Noonan D. and Li W. (2012) Cancer prevention by targeting angiogenesis, *Nature Reviews Clinical Oncology*, 9:498–509
- Allen E., Walters I. B. and Hanahan, D. (2011) Brivanib, a dual FGF/VEGF inhibitor, is active both first and second line against mouse pancreatic neuroendocrine tumors developing adaptive/evasive resistance to VEGF inhibition, *Clinical Cancer Research*, 17(16):5299–5310
- Anand P., Kunnumakara A., Sundaram C., Harikumar., Tharakan S., Lia O., Sung B. and Aggarwal B (2008) Cancer is a preventable disease that requires major lifestyle changes, *Pharmaceutical research*, 25(9):2097–2116
- Anto R. J., Sukumaran K., Kuttan G., Rao M., Subbaraju V and Kuttan R. (1995) Anticancer and antioxidant activity of synthetic chalcones and related compounds, *Cancer Letters*, 97(1):33–37
- Auerbach R., Lewis R., Shinnars B., Kubai L. and Akhtar N. (2003) Angiogenesis assays: A critical overview, *Clinical Chemistry*, 49(1):32–40
- Auguste P., Javerzat S. and Bikfalvi, A. (2003) Regulation of vascular development by fibroblast growth factors, *Cell and Tissue Research*, 314(1):157–166
- Bailey S. M. and Murnane J. P. (2006) Telomeres, chromosome instability and cancer, *Nucleic acids research*, 34(8):2408–2417

- Balunas M. J. and Kinghorn A. D. (2005) Drug discovery from medicinal plants, *Life Sciences*, 78(5):431–441
- Bandgar B. P., Gawande S., Bodade R., Totre J and Khobragade C. (2010) Synthesis and biological evaluation of simple methoxylated chalcones as anticancer, anti-inflammatory and antioxidant agents, *Bioorganic and Medicinal Chemistry*, 18(3):1364–1370
- Batovska D. I. and Todorova I. T. (2010) Trends in utilization of the pharmacological potential of chalcones, *Current clinical pharmacology*, 5:1–29
- Benigni R. and Passerini L. (2002) Carcinogenicity of the aromatic amines: from structure-activity relationships to mechanisms of action and risk assessment, *Mutation Research*, 511(3):191–206
- Bergers G. Brekken R., McMahon G., Vu T., Itoh T., Tamaki K., Tanzawa K., Thorpe P., Itohara S., Werb Z. and Hanahan D. (2000) Matrix metalloproteinase-9 triggers the angiogenic switch during carcinogenesis, *Nature cell biology*, 2(10):737–744
- Bergers G. and Benjamin L. E. (2003) Angiogenesis: Tumorigenesis and the angiogenic switch, *Nature Reviews Cancer*, 3(6):401–410
- Bergers G. and Hanahan D. (2008) Modes of resistance to anti-angiogenic therapy, *Nature reviews. Cancer*, 8(8):592–603
- Bertelli A., Ferrara F., Diana G., Fulgenzi A., Corsi M., Ponti W., Ferrero M. and Bertelli A. (1999) Resveratrol, a natural stilbene in grapes and wine, enhances intraphagocytosis in human promonocytes: a co-factor in antiinflammatory and anticancer chemopreventive activity, *International journal of tissue reactions*, 21(4):93–104

- Bertl E., Becker H., Eicher T., Herhaus C., Kapadia G., Bartsch H. and Gerhäuser C (2004) Inhibition of endothelial cell functions by novel potential cancer chemopreventive agents, *Biochemical and Biophysical Research Communications*, 325(1):287–295
- Berx G. and van Roy F. (2009) Involvement of members of the cadherin superfamily in cancer, *Cold Spring Harbor perspectives in biology*, 6(1): 1-27
- Bhagat S., Sharma R., Sawant D., Sharma L. and Chakraborti A. (2006) LiOH·H₂O as a novel dual activation catalyst for highly efficient and easy synthesis of 1,3-diaryl-2-propenones by Claisen-Schmidt condensation under mild conditions, *Journal of Molecular Catalysis A: Chemical*, 244(1–2):20–24
- Bielenberg D. R. and Zetter B. R. (2015) The Contribution of Angiogenesis to the Process of Metastasis, *Cancer journal*, 21(4):267–73
- Bikfalvi A. (1995) Significance of angiogenesis in tumour progression and metastasis, *European Journal of Cancer*, 31(7):1101–1104
- Bleicher K. H., Böhm H-J., Müller K. and Alanine A I. (2003) Hit and lead generation: beyond high-throughput screening, *Nature Reviews Drug Discovery*, 2(5):369–378
- Blumenkranz M. S., Leung L., Martin D., Rosenfield P. and Zarbin M. (2013) Pharmacotherapy of Age-Related Macular Degeneration, *Retina*, 2:1213–1255
- Bray F., Jemal A., Grey N., Ferlay J. and Forman D. (2012) Global cancer transitions according to the Human Development Index (2008-2030): A population-based study, *The Lancet Oncology*, 13(8):790–801
- Brown D. G., Lister T. and May-Dracka, T. L. (2014) New natural products as new leads for antibacterial drug discovery, *Bioorganic & medicinal chemistry letters*, 24(2):413–8

- Cabrera M., Simoens M. and Falchi G (2007) Synthetic chalcones, flavanones, and flavones as antitumoral agents: Biological evaluation and structure–activity relationships, *Bioorganic & Medicinal Chemistry*, 15(10):3356–3367
- Cao Y. H. and Pettersson, R. F. (1990) Human acidic fibroblast growth factor overexpressed in insect cells is not secreted into the medium, *Growth Factors*, 3(1):1–13
- Carmeliet P. and Jain R. K. (2000) Angiogenesis in cancer and other diseases, *Nature*, 407(6801):249–257
- Carmeliet P. and Jain R. K. (2011) Principles and mechanisms of vessel normalization for cancer and other angiogenic diseases, *Nature reviews. Drug discovery*, 10(6):417–27
- Casanovas O., Hicklin D., Bergers G. and Hanahan D. (2005) Drug resistance by evasion of antiangiogenic targeting of VEGF signaling in late-stage pancreatic islet tumors, *Cancer Cell*, 8(4):299–309
- Cavallaro U. and Christofori G. (2004) Cell adhesion and signalling by cadherins and Ig-CAMs in cancer, *Nature reviews. Cancer*, 4(2):118–132
- Chen H., Zhu G., Li Y., Padia R., Dong Z., Pan Z., Liu K and Huang S. (2009) Extracellular Signal-Regulated Kinase Signaling Pathway Regulates Breast Cancer Cell Migration by Maintaining slug Expression, *Cancer Research*, 69(24):9228–9235
- Cheng H., Zhang L., Liu Y., Chen S., Cheng H., Lu X., Zheng Z and Zhou G (2010) Design, synthesis and discovery of 5-hydroxyaurone derivatives as growth inhibitors against HUVEC and some cancer cell lines, *European Journal of Medicinal Chemistry*, 45(12):5950–5957

Christiansen A. and Detmar M. (2011) Lymphangiogenesis and cancer, *Genes & cancer*, 2(12):1146–1158

Climent M. J., Corma A., Iborra S. and Primo J. (1995) Base Catalysis for Fine Chemicals Production: Claisen-Schmidt Condensation on Zeolites and Hydrotalcites for the Production of Chalcones and Flavanones of Pharmaceutical Interest, *Journal of Catalysis*, 151(1):60–66

Compagni A., Wilgenbus P., Impagnatiello M., Cotton M. and Christofori G. (2000) Fibroblast growth factors are required for efficient tumor angiogenesis, *Cancer Research*, 60(24):7163–7169

Cook K. M. and Figg W. (2010) Angiogenesis Inhibitors- Current Strategies and Future Prospects, *CA: A cancer journal for clinicians*. 60(4):222-243

Cooper, G. M. (2000) *The Development and Causes of Cancer*. Sunderland, Massachusetts: Sinauer Associates.

Counter C., Avilion A., Lefeuvrel C., Stewart N., Greider C., Harley C., Bacchetttil S. (1992) Telomere shortening associated with chromosome instability is arrested in immortal cells which express telomerase activity, *The EMBO Journal*, 1(1):921–1929

Coxon A., Bready J., Min H., Kaufman S., Leal J., Yu D., Lee T., Sun J., Estrada J., Bolon B., McCabe J., Wang L., Rex K., Caenepeel S., Hughes P., Cordover D., Kim H., Han S., Michaels M., Hsu E., Shimamoto G., Cattley R., Hurh E., Nguyen L., Wang S., Ndifor A., Hayward I., Falcone B., McDonald D., Li L., Boone T., Kendall R., Randinsky R and Oliner J (2010) Context-dependent role of angiopoietin-1 inhibition in the suppression of angiogenesis and tumor growth: implications for AMG 386, an angiopoietin-1/2-neutralizing peptibody, *Molecular cancer therapeutics*, 9(10):2641–2651

Denizot F. and Lang, R. (1986) Rapid colorimetric assay for cell growth and survival, *Journal of Immunological Methods*, 89(2):271–277

Deprez-Poulain R. and Deprez B. (2004) Facts, figures and trends in lead generation, *Current topics in medicinal chemistry*, 4(6):569–580

Detsi A., Majdalani M., Kontogiorgis C., Hadjipavlou-Litina D and Kefalas P. (2009) Natural and synthetic 2'-hydroxy-chalcones and aurones: Synthesis, characterization and evaluation of the antioxidant and soybean lipoxygenase inhibitory activity, *Bioorganic and Medicinal Chemistry*, 17(23):8073-8085

DeVita V. T., Hellman S. and Rosenberg S. A. (2005) Cancer, principles & practice of oncology. Sixth Edition. Philadelphia, United States: Lippincott Williams & Wilkins.

Dias T., Duarte C., Lima C., Proença M. and Pereira-Wilson C (2013) Superior anticancer activity of halogenated chalcones and flavonols over the natural flavonol quercetin, *European Journal of Medicinal Chemistry*, 65:500–510

Donovan D., Brown N., Bishop E. and Lewis C. (2001) Comparison of three *in vitro* human “angiogenesis” assays with capillaries formed *in vivo*, *Angiogenesis*, 4(2):113–121

Dredge K., Marriott J., Macdonald C., Man H., Chen R., Muller G., Stirling D. and Dalgleish A. (2002) Novel thalidomide analogues display anti-angiogenic activity independently of immunomodulatory effects, *British Journal of Cancer*, 87(10):1166–1172

Dredge K., Horsfall R., Robinson S., Zhang L., Lu L., Tang Y., Shirely M., Muller G., Schafer P., Stirling D., Dalgleish A. and Bartlett J. (2005) Orally administered

lenalidomide (CC-5013) is anti-angiogenic *in vivo* and inhibits endothelial cell migration and Akt phosphorylation *in vitro*, *Microvascular Research*, 69(1):56–63

Dreys J., Zirrgiebel U., Schmidt-Gersbach C., Mross K., Medinger M., Lee L., Pinheiro J., Wood J., Thomas A., Unger C., Henry A., Steward W., Laurent D., Lebwohl D., Dugan M and Marmé D. (2005) Soluble markers for the assessment of biological activity with PTK787/ZK 222584 (PTK/ZK), a vascular endothelial growth factor receptor (VEGFR) tyrosine kinase inhibitor in patients with advanced colorectal cancer from two phase I trials, *Annals of Oncology*, 16(4):558–565

Ebos J. M. L. and Kerbel R. S. (2011) Antiangiogenic therapy: impact on invasion, disease progression, and metastasis, *Nature Reviews Clinical Oncology*, 8(4):210–21

Eddarir S., Cotelle N., Bakkour Y and Rolando C. (2003) An efficient synthesis of chalcones based on the Suzuki reaction, *Tetrahedron Letters*, 44(28) 5359-5363

Egeblad M. and Werb Z. (2002) New functions for the matrix metalloproteinases in cancer progression, *Nature Reviews Cancer*, 2(3):161–174

Enseleit F., Michels S. and Ruschitzka, F. (2010) Anti-VEGF therapies and blood pressure: More than meets the eye, *Current Hypertension Reports*, 12(1):33–38

Ethiraj K. R., Aranjani J. M. and Khan, F. R. N. (2013) Synthesis of methoxy-substituted chalcones and *in vitro* evaluation of their anticancer potential, *Chemical Biology and Drug Design*, 82(6):732–742

Evan G. and Littlewood T. (1998) A matter of life and cell death, *Science*, 281(5381):1317–1322

- Falcón B. L., Hashizume H., Koumoutsakos P., Chou J., Bready J., Coxon A., Oliner J. and McDonald D. (2009) Contrasting Actions of Selective Inhibitors of Angiopoietin-1 and Angiopoietin-2 on the Normalization of Tumor Blood Vessels, *The American Journal of Pathology*, 175(5):2159–2170
- Fan T., Yeh J., Leung K., Yue P and Wong R. (2006) Angiogenesis: from plants to blood vessels, *Trends in Pharmacological Sciences*, 27(6):297–309
- Feitelson M., Arzumanyan A., Kulathinal R., Blain S., Holcombe R., Mahajna J., Marino M., Martinez-Chantar M., Nawroth R., Sanchez-Garcia I., Sharma D., Saxena N., Singh N., Vlachostergios P., Guo S., Honoki K., Fujii H., Georgakilas A., Bilsland A., Amedei A., Nicolai E., Amin A., Ashraf S., Boosani C., Guha G., Ciriolo M., Aquilano K., Chen S., Mohammed S., Azmi A., Bhakta D., Galicka D., Keith W and Nowsheen S. (2015) Sustained proliferation in cancer: Mechanisms and novel therapeutic targets, *Seminars in Cancer Biology*, 35:25–54
- Ferlay J., Soejomataram I., Dikshit R., Eser S., Mathers C., Rebelo M., Parkin D., Forman D. and Bray F. (2015) Cancer incidence and mortality worldwide: Sources, methods and major patterns in GLOBOCAN 2012. *International Journal of Cancer*, 136(5):359–386
- Ferrara N. and Kerbel R. S. (2005) Angiogenesis as a therapeutic target, *Nature*, 438(7070):967–974
- Foda H. D. and Zucker S. (2001) Matrix metalloproteinases in cancer invasion, metastasis and angiogenesis, *Drug discovery today*, 6(9):478–482
- Folkman J. (1995) Angiogenesis in cancer, vascular, rheumatoid and other disease, *Nature Medicine*, 1(1):27–30

- Folkman J. (2006) Antiangiogenesis in cancer therapy - Endostatin and its mechanisms of action, *Experimental Cell Research*, 312(5):594-607
- Folkman J. (2007) Angiogenesis: an organizing principle for drug discovery? *Nature reviews. Drug discovery*, 6(4):273-86
- Forstner M., Leder L. and Mayr L. M. (2007) Optimization of protein expression systems for modern drug discovery, *Expert Review of Proteomics*, 4(1):67-78
- Frantz C., Stewart K M. and Weaver V M. (2010) The extracellular matrix at a glance, *Journal of cell science*, 123(Pt 24):4195-200
- Gately S. and Li W. W. (2004) Multiple roles of COX-2 in tumor angiogenesis: A target for antiangiogenic therapy, *Seminars in Oncology*, 31(7):2-11
- Gerebtzoff G., Li-Blatter X., Fischer H., Frentzel A., and Seelig A. (2004). Halogenation of Drugs Enhances Membrane Binding and Permeation, *ChemBioChem*, 5(5): 676-684
- Ghorab M. M., Alsaïd M S., Al-Ansary G H., Abdel-Latif G A. and Abou El Ella D A. (2016) Analogue based drug design, synthesis, molecular docking and anticancer evaluation of novel chromene sulfonamide hybrids as aromatase inhibitors and apoptosis enhancers, *European Journal of Medicinal Chemistry*, 124:946-958
- Goede V., Coutelle O., Neuneier J., Reinacher-Schick A., Schnell R., Koslowsky T C., Weihrauch M R., Cremer B., Kashkar H., Odenthal M., Augustin H G., Schmiegel W., Hallek M. and Hacker U T. (2010) Identification of serum angiopoietin-2 as a biomarker for clinical outcome of colorectal cancer patients treated with bevacizumab-containing therapy, *British Journal of Cancer*, 103(9):1407-1414

- Goodwin A. M. (2007) *In vitro* assays of angiogenesis for assessment of angiogenic and anti-angiogenic agents, *Microvascular Research*, 74(2–3):172–183
- Gotink K. J. and Verheul H. M. W. (2010) Anti-angiogenic tyrosine kinase inhibitors: what is their mechanism of action? *Angiogenesis*, 13(1)1–14
- Gschwend D. A., Good A. C. and Kuntz I. D. (1996) Molecular docking towards drug discovery, *Journal of Molecular Recognition*, 9(2):175–186
- Hainaut P. and Plymoth A. (2013) Targeting the hallmarks of cancer, *Current Opinion in Oncology*, 25(1):50–51
- Hanahan D. and Folkman J. (1996) Patterns and emerging mechanisms of the angiogenic switch during tumorigenesis, *Cell*, 86(3):353–364
- Hanahan D. and Weinberg R. A. (2000) The hallmarks of cancer, *Cell*, 100(1):57–70
- Hanahan D. and Weinberg R. A. (2011) Hallmarks of cancer: The next generation, *Cell*, 144(5):646–674
- Hanrahan V., Currie M J., Gunningham S P., Morrin H R., Scott P A., Robinson B A. and Fox S B. (2003) The angiogenic switch for vascular endothelial growth factor (VEGF)-A, VEGF-B, VEGF-C, and VEGF-D in the adenoma-carcinoma sequence during colorectal cancer progression, *Journal of Pathology*, 200(2):183–194
- Harley C. B. (2008) Telomerase and cancer therapeutics, *Nature reviews. Cancer*, 8(3):167–179
- Vander Heiden M G. and DeBerardinis R J. (2017) Understanding the Intersections between Metabolism and Cancer Biology, *Cell*, 168(4):657–669

- Heldin C.-H. (2004) Development and possible clinical use of antagonists for PDGF and TGF-beta, *Upsala journal of medical sciences*, 109(3):165–78
- Heldin C.-H. (2012) Autocrine PDGF stimulation in malignancies, *Upsala journal of medical sciences*, 117(2):83–91
- Helfrich I., Elder L., Sucker A., Thomas M., Christian S., Schadendorf D. and Augustin H G. (2009) Angiopoietin-2 levels are associated with disease progression in metastatic malignant melanoma, *Clinical cancer research*, 15(4):1384–92
- Hemann M. T., Strong M A., Hao L Y. and Greider C W. (2001) The Shortest Telomere, Not Average Telomere Length, Is Critical for Cell Viability and Chromosome Stability, *Cell*, 107(1):67–77
- Hernandes M. Z., Cavalcanti S M., Moreira D R., de Azevedo Junior W F. and Leite A C. (2010) Halogen atoms in the modern medicinal chemistry: hints for the drug design, *Current drug targets*, 11(3):303–314
- Hicklin D. J. and Ellis L. M. (2005) Role of the vascular endothelial growth factor pathway in tumor growth and angiogenesis, *Journal of Clinical Oncology*, 23(5):1011–1027
- Hillen F. and Griffioen A. W. (2007) Tumour vascularization: sprouting angiogenesis and beyond, *Cancer and Metastasis Reviews*, 26(3–4):489–502
- Hoelder S., Clarke P. A. and Workman P. (2012) Discovery of small molecule cancer drugs: Successes, challenges and opportunities, *Molecular Oncology*, 6(2):155–176
- Hou, H A., Chou W C., Lin L I., Tang J L., Tseng M H., Huang C F., Yao M., Chen C Y., Tsay W. and Tien H F. (2008) Expression of angiopoietins and vascular endothelial

growth factors and their clinical significance in acute myeloid leukemia, *Leukemia research*, 32(6):904–12

Hsieh H K., Tsao L T., Wang J P. and Lin C N. (2000) Synthesis and anti-inflammatory effect of chalcones, *The Journal of pharmacy and pharmacology*, 52(2):163–71

Huang C., Jacobson K. and Schaller M. D. (2004) MAP kinases and cell migration, *Journal of cell science*, 117(Pt 20):4619–28

Huang H. Bhat A., Woodnutt G. and Lappe R. (2010) Targeting the ANGPT-TIE2 pathway in malignancy, *Nature reviews. Cancer*, 10(8):575–585

Huang W.-Y., Cai Y.-Z. and Zhang Y. (2010) Natural phenolic compounds from medicinal herbs and dietary plants: potential use for cancer prevention, *Nutrition and cancer*, 62(1):1–20

Huang Y., Goel S., Duda D G., Fukumura D. and Jain R K. (2013) Vascular normalization as an emerging strategy to enhance cancer immunotherapy, *Cancer research*, 73(10):2943–2948

Hudis, C A. (2007) Trastuzumab — Mechanism of Action and Use in Clinical Practice, *New England Journal of Medicine*, 357(1):39–51

Hughes J. P., Rees S., Kalindjian S B. and Philpott K L. (2011) Principles of early drug discovery, *British journal of pharmacology*, 162(6):1239–1249

Hurwitz H., Fehrenbacher L., Novotny W., Cartwright T., Hainsworth J., Heim W., Berlin J., Baron A., Griffing S., Holmgren E., Ferrara N., Fyfe G., Rogers B., Ross R. and Kabbinavar F. (2004) Bevacizumab plus irinotecan, fluorouracil, and leucovorin for metastatic colorectal cancer, *The New England journal of medicine*, 350(23):2335–2342

- Impola, U., Uitto V J., Hietanen J., Hakkinen L., Zhang L., Larjava H., Isaka K. and Saarialho-Kere U. (2004) Differential expression of matrilysin-I (MMP-7), 92 kD gelatinase (MMP-9), and metalloelastase (MMP-12) in oral verrucous and squamous cell cancer, *Journal of Pathology*, 202(1):14–22
- Itoh T., Tanioka M., Yoshida H., Yoshioka T., Nishimoto H and Itohara S. (1998) Reduced angiogenesis and tumor progression in gelatinase A-deficient mice, *Cancer Research*, 58(5):1048–1051
- Itoh T., Tanioka M., Matsuda H., Nishimoto H., Yoshioka T., Suzuki R and Uehira M. (1999) Experimental metastasis is suppressed in MMP-9-deficient mice, *Clinical and Experimental Metastasis*, 17(2):177–181
- Iurlaro M., Loverro G., Vacca A., Cormio G., Ribatti D., Minischetti M., Ria R., Bruno M., Selvaggi L. (1999) Angiogenesis extent and expression of matrix metalloproteinase-2 and -9 correlate with upgrading and myometrial invasion in endometrial carcinoma, *European Journal of Clinical Investigation*, 29(9):793–801
- Jain R K., Duda D G., Clark J W. and Loeffler J S. (2005) Lessons from phase III clinical trials on anti-VEGF therapy for cancer, *Nature Clinical Practice Oncology*, 3(1):24–40.
- Jain R. K. (2005) Normalization of tumor vasculature: an emerging concept in antiangiogenic therapy, *Science*, 307(5706):58–62
- Jussila L. and Alitalo K. (2002) Vascular growth factors and lymphangiogenesis, *Physiological reviews*, 82(3):673–700

Sahu K., Balbhadra S S., Choudary J. and Kohli D V. (2012) Exploring Pharmacological Significance of Chalcone Scaffold: A Review, *Current Medicinal Chemistry*, 19(2):209–225

Kabbinavar F F., Schulz J., McCleod M., Patel T., Hamm J T., Hecht J R., Mass R., Perrou B., Nelson B. and Novotny W F. (2005) Addition of bevacizumab to bolus fluorouracil and leucovorin in first-line metastatic colorectal cancer: results of a randomized phase II trial, *Journal of Clinical Oncology*, 23(16):3697–3705

Kamba T. and McDonald D. M. (2007) Mechanisms of adverse effects of anti-VEGF therapy for cancer, *British Journal of Cancer*, 96:1788–1795

Karki R., Kang Y., Kim C H., Kwak K., Kim J-A., Lee E-S. (2012) Hydroxychalcones as potential anti-angiogenic agent, *Bulletin of the Korean Chemical Society*, 33(9):2925–2929

Katsuno K., Burrows J N., Duncan K., Huijsduijnen R H., Kaneko T., Kita K., Mowbray C E., Schmatz D., Warner P., Slingsby B T. (2015) Hit and lead criteria in drug discovery for infectious diseases of the developing world, *Nature Reviews Drug Discovery*, 14(11):751–758

Kerbel R. and Folkman J. (2002) Clinical translation of angiogenesis inhibitors, *Nature reviews. Cancer*, 2(10):727–739

Keseru G M. and Makara G M. (2006) Hit discovery and hit-to-lead approaches, *Drug Discovery Today*, 11(15-16):741–748

- Kim K J., Li B., Winer J., Armanini M., Gillett N., Phillips H S. and Ferrara N. (1993) Inhibition of vascular endothelial growth factor-induced angiogenesis suppresses tumour growth *in vivo*, *Nature*, 362(6423):841–844
- Kimura Y., Sumiyoshi M. and Baba K. (2008) Antitumor activities of synthetic and natural stilbenes through antiangiogenic action, *Cancer Science*, 99(10):2083–2096
- Kitchen D B., Decornez H., Furr J R. and Bajorath J. (2004) Docking and scoring in virtual screening for drug discovery: methods and applications, *Nature reviews. Drug discovery*, 3(11):935–49
- Klagsbrun M. and Moses M. A. (1999) Molecular angiogenesis, *Chemistry and Biology*, 6(8):217-224
- Kleinman H K. and Martin G R. (2005) Matrigel: Basement membrane matrix with biological activity, *Seminars in Cancer Biology*, 15(5):378–386
- Knudson A. G. (2001) Two genetic hits (more or less) to cancer, *Nature Reviews Cancer*, 1(2):157–162
- Koehn F E. and Carter G T. (2005) The evolving role of natural products in drug discovery, *Nature Reviews Drug Discovery*, 4(3):206–220
- Koenecke C., Kümpers P., Lukasz A., Dammann E., Verhagen W., Göhring G., Buchholz S., Krauter J., Eder M., Schlegelberger B. and Ganser A. (2010) Shedding of the endothelial receptor tyrosine kinase Tie2 correlates with leukemic blast burden and outcome after allogeneic hematopoietic stem cell transplantation for AML, *Annals of Hematology*, 89(5):459–467

- Konieczny M T., Konieczny W., Sabisz M., Skladanowski A., Wakiec R., Augustnowicz-Kopec E. and Zwolska Z. (2007) Acid-catalyzed synthesis of oxathiolone fused chalcones. Comparison of their activity toward various microorganisms and human cancer cells line, *European Journal of Medicinal Chemistry*, 42(5):729–733
- Korkola J. and Gray J W. (2010) Breast cancer genomes—form and function, *Current Opinion in Genetics & Development*, 20(1):4–14
- Kumar S., Lamba M S. and Makrandi J. K. (2008) ‘An efficient green procedure for the synthesis of chalcones using C-200 as solid support under grinding conditions, *Green Chemistry Letters and Reviews*, 1(2):123–125
- Kuntz I. D. (1992) Structure-Based Strategies for Drug Design and Discover, *Science*, 257(5073):1078–1082
- Kurz H., Burri P H. and Djonov V G. (2003) Angiogenesis and vascular remodeling by intussusception: from form to function, *News in Physiology Sciences*, 18:65–70.
- Laird A D., Christensen J G., Li G., Carver J., Smith K., Xin X., Moss K G., Louie S G., Mendel D B. and Cherrington J M. (2002) SU6668 inhibits Flk-1/KDR and PDGFR β *in vivo*, resulting in rapid apoptosis of tumor vasculature and tumor regression in mice, *The FASEB Journal*, 16(7):681–690
- Laudicella M., Walsh B., Burns E and Smith P. (2016) Cost of care for cancer patients in England: evidence from population-based patient-level data, *British Journal of Cancer*, 114(11):1286–1292

- Leahy K M., Ornberg R L., Wang Y., Zweifel B S., Koki A T. and Masferrer J L. (2002) Cyclooxygenase-2 inhibition by celecoxib reduces proliferation and induces apoptosis in angiogenic endothelial cells *in vivo*, *Cancer Research*, 62(3):625–631
- Lee J S., Kang Y., Kim J T., Thapa D., Lee E-S. and Kim J-A. (2012) The anti-angiogenic and anti-tumor activity of synthetic phenylpropenone derivatives is mediated through the inhibition of receptor tyrosine kinases, *European Journal of Pharmacology*, 677(1–3):22–30
- Lee W J., Lee J-L., Chang S E., Lee M W., Kang Y-K., Choi J H., Moon K C. and Koh J K. (2009) Cutaneous adverse effects in patients treated with the multitargeted kinase inhibitors sorafenib and sunitinib, *British Journal of Dermatology*, 161(5):1045–1051
- Lee Y S., Lim S S., Shin K H., Kim Y S., Ohuchi K. and Jung S H. (2006) Anti-angiogenic and Anti-tumor Activities of 2'-Hydroxy-4'-methoxychalcone, *Biological & Pharmaceutical Bulletin*, 29(5):1028–1032
- Li R., Kenyon G L., Cohen F E., Chen X., Gong B., Dominguez J N., Davidson E., Kurzban G., Miller R E and Nuzum E O. (1995) *In Vitro* Antimalarial Activity of Chalcones and Their Derivatives, *Journal of Medicinal Chemistry*, 38(26):5031–5037
- Li W W., Li V W., Hutnik M. and Chiou A S. (2012) Tumor angiogenesis as a target for dietary cancer prevention, *Journal of Oncology*, 2012(879623)
- Liang C-C. C., Park A. Y. and Guan J-L. L. (2007) *In vitro* scratch assay: a convenient and inexpensive method for analysis of cell migration *in vitro*, *Nature Protocols*, 2(2):329–333

Lieu C., Heymach J., Overman M., Tran H. and Kopetz S. (2011) Beyond VEGF: Inhibition of the fibroblast growth factor pathway and antiangiogenesis, *Clinical Cancer Research*, 17(19):6130–6139

Lindsten T., Ross A J., King A., Zong W X., Rathmell J C., Shiels H A., Ulrich E., Waymire K G., Mahar P., Frauwirth K., Chen Y., Wei M., Eng V M., Adelman D M., Simon M C., Ma A., Golden J A., Evan G., Korsmeyer S J., MacGregor G R. and Thompson C B. (2000) The Combined Functions of Proapoptotic Bcl-2 Family Members Bak and Bax Are Essential for Normal Development of Multiple Tissues, *Molecular Cell*, 6(6):1389–1399

Lipinski C A. (2004) Lead- and drug-like compounds: The rule-of-five revolution, *Drug Discovery Today: Technologies*, 1(4):337–341

Little M H. and Sequeira Lopez M L S. (2016) *Kidney Development, Disease, Repair and Regeneration*. New York, United States: Elsevier

Loges S., Heil G., Bruweleit M., Schoder V., Butzal M., Fischer U., Gehling U M., Schuch G., Hossfeld D K. and Fiedler W. (2005) Analysis of concerted expression of angiogenic growth factors in acute myeloid leukemia: expression of angiopoietin-2 represents an independent prognostic factor for overall survival, *Journal of clinical oncology*, 23(6):1109–1117

Loges S., Schmidt T. and Carmeliet P. (2010) Mechanisms of resistance to anti-angiogenic therapy and development of third-generation anti-angiogenic drug candidates, *Genes & cancer*, 1(1):12–25

- Longo R., Sarmiento R., Fanelli M., Capaccetti B., Gattuso D. and Gasparini G. (2002) Anti-angiogenic therapy: Rationale, challenges and clinical studies, *Angiogenesis*, 5(4):237–256
- Lowe S. W., Cepero E. and Evan G. (2004) Intrinsic tumour suppression, *Nature*, 432(7015):307–315
- Maby-El Hajjami H. and Petrova T V. (2008) Developmental and pathological lymphangiogenesis: from models to human disease, *Histochemistry and Cell Biology*, 130(6):1063–1078
- Mahar P., Hanfi A. and Khan A. (2009) Angiogenesis and Role of Anti-VEGF Therapy, *Pakistan Journal of Ophthalmology*, 25(3):169–173
- Mahapatra D K., Bharti S K. and Asati, V. (2015) Anti-cancer chalcones: Structural and molecular target perspectives, *European journal of medicinal chemistry*, 98:69–114
- Maitland M L., Lou X J., Ramirez J., Desai A A., Berlin D S., McLeod H L., Weichselbaum R R., Ratain M J., Altman R B. and Klein T E. (2010) Vascular endothelial growth factor pathway, *Pharmacogenetics and Genomics*, 20(5):346–349
- Malek A M., Connors S., Robertson R L., Folkman J. and Scott R M. (1997) Elevation of cerebrospinal fluid levels of basic fibroblast growth factor in moyamoya and central nervous system disorders, *Paediatric Neurosurgery*, 27(4):182–189
- Malik A K., Baldwin M E., Peale F., Fuh G., Liang W C., Lowman H., Meng G., Ferrara N. and Gerber H P. (2006) Redundant roles of VEGF-B and PlGF during selective VEGF-A blockade in mice, *Blood*, 107(2):550–557

- Martí-Centelles R., Cejudo-Marin R., Falomir E., Murga J., Carda M. and Marco J A. (2013) Inhibition of VEGF expression in cancer cells and endothelial cell differentiation by synthetic stilbene derivatives, *Bioorganic & Medicinal Chemistry*, 21(11):3010–3015
- Martin D., Maguire M., Ying G., Grunwald J., Fine S. and Jaffe G (2011) Ranibizumab and bevacizumab for neovascular age-related macular degeneration, *The New England journal of medicine*, 364(20):1897–908
- Martin T A., Ye L., Sanders A J., Lane J., Jiang W G. (2013) Cancer Invasion and Metastasis: Molecular and Cellular Perspective, *Metastatic Cancer: Clinical and Biological Perspectives*, Chapter January 2013
- Masferrer J L., Leahy K M., Koki A T., Zweifel B S., Settle S L., Woerner B M., Edwards D A., Flickinger A G., Moore R J. and Seibert K. (2000) Antiangiogenic and antitumor activities of cyclooxygenase-2 inhibitors, *Cancer Research*, 60(5):1306–1311
- Mir O., Ropert S., Alexandre J. and Goldwasser F. (2009) Hypertension as a surrogate marker for the activity of anti-VEGF agents, *Annals of Oncology*, 20(5):967–970
- Mishra B B. and Tiwari V K. (2011) Natural products: an evolving role in future drug discovery, *European journal of medicinal chemistry*, 46(10):4769–807
- Mojzis J., Varinska L., Mojzisova G., Kostova I. and Mirossat L. (2008) Antiangiogenic effects of flavonoids and chalcones, *Pharmacological Research*, 57(4):259–265
- Morales D E., McGowan K A., Grant D S., Maheshwari S., Bhartiya D., Cid M C., Kleinman H K., Schnaper H W. (1995) Estrogen Promotes Angiogenic Activity in Human Umbilical Vein Endothelial Cells *In Vitro* and in a Murine Model, *Circulation*, 91(3):755-63

- Morin M J. (2000) From oncogene to drug: development of small molecule tyrosine kinase inhibitors as anti-tumor and anti-angiogenic agents, *Oncogene*, 19(56):6574–6583
- Mosmann T. (1983) Rapid colorimetric assay for cellular growth and survival: Application to proliferation and cytotoxicity assays, *Journal of Immunological Methods*, 65(1–2):55–63
- Motzer R J., Michaelson M D., Redman B G., Hudes G R., Wilding G., Figlin R A., Ginsberg M S., Kim S T., Baum C M., DePrimo S E., Li J Z., Bello C L., Theuer C P., George D J. and Rini B I. (2006) Activity of SU11248, a multitargeted inhibitor of vascular endothelial growth factor receptor and platelet-derived growth factor receptor, in patients with metastatic renal cell carcinoma, *Journal of Clinical Oncology*, 24(1):16–24
- Muenst S., Läubli H., Soysal S D., Zippelius A., Tzankov. And Hoeller S. (2016) The immune system and cancer evasion strategies: therapeutic concepts, *Journal of Internal Medicine*, 279(6):541–562
- Murphy D., Makonnen S., Lassoued W., Feldman M and Carter C (2006) Inhibition of tumor endothelial ERK activation, angiogenesis, and tumor growth by sorafenib (BAY43-9006), *The American journal of pathology*, 169(5):1875–1885
- Naasani I., Seimiya H. and Tsuruo, T. (1998) Telomerase Inhibition, Telomere Shortening, and Senescence of Cancer Cells by Tea Catechins, *Biochemical and Biophysical Research Communications*, 249(2):391–396
- Nagy J A., Chang S H., Dvorak A M., Dvorak H K. (2009) Why are tumour blood vessels abnormal and why is it important to know? *British journal of cancer*, 100(6):865–869

- Nam N H., Kim Y., You Y J., Hong D H., Kim H M. and Ahn B Z. (2003) Cytotoxic 2',5'-dihydroxychalcones with unexpected antiangiogenic activity, *European Journal of Medicinal Chemistry*, 38(2):179–187
- Narender T. and Papi Reddy K. (2007) A simple and highly efficient method for the synthesis of chalcones by using borontrifluoride-etherate, *Tetrahedron Letters*, 48(18):3177–3180
- Neufeld G., Cohen T., Gengrinovitch S. and Poltorak Z. (1999) Vascular endothelial growth factor (VEGF) and its receptors, *The FASEB Journal*, 13(1):9–22
- Ngameni B. (2006) Inhibition of matrix metalloproteinase-2 secretion by chalcones from the twigs of *Dorstenia barteri* Bureau, *Arkivoc*, 2007(ix):91–103
- Nguyen M., Watanabe H., Budson A E., Richie J P., Hayes D F. and Folkman J. (1994) Elevated Levels of an Angiogenic Peptide, Basic Fibroblast Growth Factor, in the Urine of Patients With a Wide Spectrum of Cancers, *Journal of the National Cancer Institute*, 86(5):356–61
- Njardarson J T., Gaul C., Shan D., Huang X Y. Danishefsky S J. (2004) Discovery of Potent Cell Migration Inhibitors through Total Synthesis: Lessons from Structure-activity Studies of (+)-Migrastatin, *Journal of the American Chemical Society*, 126(4):1038–1040
- Olsson A K., Dimberg A., Kreuger J. and Claesson-Welsh L. (2006) VEGF receptor signalling - in control of vascular function, *Nature Reviews Molecular Cell Biology*, 7(5):359–371

Orlikova B., Tasdemir D., Golais F., Dicato M. and Diederich M. (2011) Dietary chalcones with chemopreventive and chemotherapeutic potential, *Genes and Nutrition*, 6(2):125–147

Ostman A. and Heldin C H. (2007) PDGF Receptors as Targets in Tumor Treatment, *Advances in Cancer Research*, 97:247–274

Palmer T D., Ashby W J., Lewis J D. and Zijlstra A. (2011) Targeting tumor cell motility to prevent metastasis, *Advanced drug delivery reviews*, 63(8):568–81

Patrick G L. (2017) *An Introduction to Medicinal Chemistry*. Fifth Edition. Oxford. Oxford University Press.

Pepper M S., Ferrara N., Orci L. and Montesano R. (1992) Potent synergism between vascular endothelial growth factor and basic fibroblast growth factor in the induction of angiogenesis *in vitro*, *Biochemical and Biophysical Research Communications*, 189(2):824–831

Petrov, O., Ivanova Y. and Gerova, M. (2008) SOCl₂/EtOH: Catalytic system for synthesis of chalcones, *Catalysis Communications*, 9(2):315–316

Pilatova M., Varinska L., Perjesi P., Sarissky M., Mirossay L., Solar P., Ostro A. and Mojzis J. (2010) *In vitro* antiproliferative and antiangiogenic effects of synthetic chalcone analogues, *Toxicology in Vitro*, 24(5):1347–1355

Plank M J. and Sleeman B D. (2003) Tumour-Induced Angiogenesis: A Review, *Journal of Theoretical Medicine*, 5(3–4):137–153

- Plate K H., Breier G., Weich H A. Risau W. (1992) Vascular endothelial growth factor is a potential tumour angiogenesis factor in human gliomas *in vivo*, *Nature*, 359(6398):845–848
- Pouyssegur J., Dayan F. and Mazure N. M. (2006) Hypoxia signalling in cancer and approaches to enforce tumour regression, *Nature*, 441(7092):437–443
- Prior B M. Yang H T. and Terjung R L. (2004) What makes vessels grow with exercise training? *Journal of Applied Physiology*, 97(3):1119-1128
- Qian B Z. and Pollard J W. (2010) Macrophage Diversity Enhances Tumor Progression and Metastasis, *Cell*, 141(1):39–51
- Rand A A., Barnych B., Morisseau C., Cajka T., Lee K S S., Panigraphy D. and Hammock B D. (2017) Cyclooxygenase-derived proangiogenic metabolites of epoxyeicosatrienoic acids, *Proceedings of the National Academy of Sciences of the United States of America*, 114(17):4370–4375
- Rapisarda A. and Melillo G. (2012) Role of the VEGF/VEGFR Axis in Cancer Biology and Therapy. 1st edition, *Advances in Cancer Research*.
- Ratty A K. and Das N P. (1988) Effects of flavonoids on nonenzymatic lipid peroxidation: Structure-activity relationship, *Biochemical Medicine and Metabolic Biology*, 39(1):69–79
- Reddy G V., Maitraie D., Narsaiah B., Rambabu Y. and Shanthan Rao P. (2001) MICROWAVE ASSISTED KNOEVENAGEL CONDENSATION: A FACILE METHOD FOR THE SYNTHESIS OF CHALCONES, *Synthetic Communications*, 31(18):2881–2884

- Ricciotti E. and FitzGerald G A. (2011) Prostaglandins and inflammation, *Arteriosclerosis, thrombosis, and vascular biology*, 31(5):986–1000
- Ridgway J., Zhang G., Wu T., Stawicki S., Liang W C., Chanthery Y., Kowalski J., Watts R J., Callahan C., Kasman I., Singh M., Chien M., Tan C., Hongo J A., De Sauvage F., Plowman G. and Yan M. (2006) Inhibition of Dll4 signalling inhibits tumour growth by deregulating angiogenesis, *Nature*, 444(7122):1083–1087
- Riss T L., Moravec R A., Niles A L., Duellman S., Benink H A., Worzella T J., and Minor L. (2004). Cell Viability Assays. Assay Guidance Manual. Bethesda. Eli Lilly & Company and the National Center for Advancing Translational Sciences.
- Rizvi S U., Siddiqui H L., Nisar M., Khan N. and Khan I. (2012) Discovery and molecular docking of quinolyl-thienyl chalcones as anti-angiogenic agents targeting VEGFR-2 tyrosine kinase, *Bioorganic and Medicinal Chemistry Letters*, 22(2):942–944
- Robinson E S., Khankin E V., Karumanchi S A. and Humphreys B D. (2010) Hypertension induced by vascular endothelial growth factor signaling pathway inhibition: mechanisms and potential use as a biomarker, *Seminars in nephrology*, 30(6):591–601
- Rodrigues T., Reker D., Schneider P. and Scheider G. (2016) Counting on natural products for drug design, *Nature Chemistry*, 8(6):531-541
- Roukos D H. (2009) Genome-wide association studies: how predictable is a person's cancer risk? *Expert Review of Anticancer Therapy*, 9(4):389–392
- Rudolph K L., Chang S., Lee H W., Blasco M., Gottlieb G J., Greider C. and DePinho R A. (1999) Longevity, Stress Response, and Cancer in Aging Telomerase-Deficient Mice, *Cell*, 96(5):701–712

de Sá Alves F R., Barreiro E J. and Fraga C A M. (2009) From nature to drug discovery: the indole scaffold as a “privileged structure”, *Mini reviews in medicinal chemistry*, 9(7):782–93

Saharinen P., Eklund L. and Alitalo K. (2017) Therapeutic targeting of the angiotensin–TIE pathway, *Nature Reviews Drug Discovery*, 16(9):636–661

Samant R S. and Shevde L A. (2011) Recent advances in anti-angiogenic therapy of cancer, *Oncotarget*, 2(3):122–34

Sandler A., Gray R., Perry M C., Brahmer J., Schiller J H., Dowlati A., Lelenbaum R. and Johnson D H. (2006) Paclitaxel-carboplatin alone or with bevacizumab for non-small-cell lung cancer, *The New England journal of medicine*, 355(24):2542–2550

El Sayed K A. (2005) Natural products as angiogenesis modulators, *Mini Reviews in Medicinal Chemistry*, 5(11):971–993

Schenone M., Dančik V., Wagner B K. and Clemons P A. (2013) Target identification and mechanism of action in chemical biology and drug discovery, *Nature chemical biology*, 9(4):232–40

Scholz A., Harter P N., Cremer S., Yalcin B H., Gurnik S., Yamaji M., Di Tacchio M., Sommer K., Baumgarten P., Bahr O., Steinbach J P., Trojan J., Glas M., Herrlinger U., Krex D., Meinhardt M., Weyerbrock A., Timmer M., Goldbrunner R., Deckert M., Braun C., Schittenhelm J., Frueh J T., Ullrich E., Mittelbronn M., Plate K H. and Reiss Y. (2016) Endothelial cell-derived angiotensin-2 is a therapeutic target in treatment-naïve and bevacizumab-resistant glioblastoma, *EMBO Molecular Medicine*, 8(1):39–57

- Selepe M., and Van Heerden F. (2013) Application of the Suzuki-Miyaura Reaction in the Synthesis of Flavonoids. *Molecules*, 18(4):4739–4765
- Sfiligoi C., De Luca A., Cascone I., Sorbello V., Fuso L., Ponzzone R., Biglia N., Audero E., Arisio R., Bussolino F., Sismondi P. and De Bortoli M. (2003) Angiopoietin-2 expression in breast cancer correlates with lymph node invasion and short survival, *International Journal of Cancer*, 103(4):466–474
- Sharma N., Dobhal M., Joshi Y. and Chahar M. (2011) Flavonoids: A versatile source of anticancer drugs, *Pharmacognosy reviews*, 5(9):1–12
- Sharma R N., Xavier F P., Vasu K K., Chaturvedi S C. and Pancholi S S. (2009) Synthesis of 4-benzyl-1,3-thiazole derivatives as potential anti-inflammatory agents: An analogue-based drug design approach, *Journal of Enzyme Inhibition and Medicinal Chemistry*, 24(3):890–897
- Shay J W. and Bacchetti S. (1997) A survey of telomerase activity in human cancer, *European Journal of Cancer*, 33(5):787–791
- Sherr C J. and McCormick F. (2002) The RB and p53 pathways in cancer, *Cancer Cell*, 2(2):103–112
- Shi S., Chen L. and Huang G. (2013) Antiangiogenic therapy improves the antitumor effect of adoptive cell immunotherapy by normalizing tumor vasculature, *Medical Oncology*, 30(4):698
- Shibuya M. (2006) Vascular endothelial growth factor receptor-1 (VEGFR-1/Flt-1): a dual regulator for angiogenesis, *Angiogenesis*, 9(4):225–230

Shibuya M. (2011) Vascular Endothelial Growth Factor (VEGF) and Its Receptor (VEGFR) Signaling in Angiogenesis: A Crucial Target for Anti- and Pro-Angiogenic Therapies, *Genes & cancer*, 2(12):1097–105

Shu Y-Z. (1998) Recent Natural Products Based Drug Development: A Pharmaceutical Industry Perspective, *Journal of Natural Products*, 61(8):1053–1071

Siegel A B., Cohen E I., Ocean A., Lehrer D., Goldenberg A., Knox J J., Chen H., Clark-Garvey S., Weinberg A., Mandeli J., Christos P., Mazumdar M., Popa E., Brown R S Jr., Rafii S. and Schwartz J D. (2008) Phase II trial evaluating the clinical and biologic effects of bevacizumab in unresectable hepatocellular carcinoma, *Journal of Clinical Oncology*, 26(18):2992–2998

Sirerol J A., Rodriguez M L., Mena S., Asensi M A., Estrela J M. and Ortega A L. (2016) Role of Natural Stilbenes in the Prevention of Cancer, *Oxidative Medicine and Cellular Longevity*, 2016:1–15

Skipper P L., Kim M Y., Sun H.-L P., Wogan, G N. and Tannenbaum S R. (2010) Monocyclic aromatic amines as potential human carcinogens: old is new again. *Carcinogenesis*, 31(1):50–58

Smith M., and March J. (2007). *March's advanced organic chemistry: reactions, mechanisms, and structure*. Sixth Edition. New Jersey. John Wiley & Sons.

Smyth E M., Grosser T., Wang M., Yu Y. FitzGerald G A. (2009) Prostanoids in health and disease, *Journal of lipid research*, 50:423-428

Soutter A D., Nguyen M., Watanabe H and Folkman J. (1993) Basic fibroblast growth factor secreted by an animal tumor is detectable in urine, *Cancer Research*, 53(21):5297–5299

Srinivasan R., Zabuawala T., Huang H., Zhang J., Gulati P., Fernandez S., Karlo J C., Landreth G E. Leone G. Ostrowski M C. (2009) Erk1 and Erk2 Regulate Endothelial Cell Proliferation and Migration during Mouse Embryonic Angiogenesis, *PLoS ONE*, 4(12): 8283

Stacker S A. and Achen M G., Jussila L., Balwin M e. Alitalo K.(2009) Lymphangiogenesis in cancer metastasis. *Nature reviews, Cancer*, 2(8):573-83

Staton C A., Stribbling S M., Tazzyman S., Hughes R., Brown N J. and Lewis C E. (2004) Current methods for assaying angiogenesis *in vitro* and *in vivo*, *International Journal of Experimental.Pathology*, 85(5):233–248.

Staton C A., Lewis C. and Bicknell R. (2007) *Angiogenesis Assays: A Critical Appraisal of Current Techniques*. Chichester, England: Wiley-Blackwell.

Stoyanov E V., Champavier Y., Simon A. Basly J P. (2002) Efficient liquid-phase synthesis of 2'-hydroxychalcones, *Bioorganic and Medicinal Chemistry Letters*, 12(19):2685–2687

Su M., Huang J., Liiu S., Zioa Y., Qin X., Liu J., Pi C., Luo T., Li J., Chen X. and Luo Z. (2016) The anti-angiogenic effect and novel mechanisms of action of Combretastatin A-4, *Scientific Reports*, 6(1):28139

Swinney D C. and Anthony J. (2011) How were new medicines discovered? *Nature Reviews Drug Discovery*, 10(7):507–519

- Talmadge J E. and Fidler I J. (2010) AACR centennial series: The biology of cancer metastasis: Historical perspective, *Cancer Research*, 70(14):5649–5669
- Tan W F., Lin L P., Li M H., Zhang Y X., Tong Y G., Xiao D. and Ding J (2003) Quercetin, a dietary-derived flavonoid, possesses antiangiogenic potential, *European Journal of Pharmacology*, 459(2–3):255–262
- Tari L., Vo N., Liang S., Patel J., Baral C. and Cai J. (2012) Identifying novel drug indications through automated reasoning, *PloS one*, 7(7):40946
- Torres-Santos E C., Moreira D L., Kaplan M A., Meirelles M N. and Rossi-Bergmann B. (1999) Selective effect of 2',6'-dihydroxy-4'-methoxychalcone isolated from *Piper aduncum* on *Leishmania amazonensis*, *Antimicrobial agents and chemotherapy*, 43(5):1234–41
- Tsuji M., Kawano S., Tsuji S., Sawaoka H., Hori M. and DuBois R N. (1998) Cyclooxygenase Regulates Angiogenesis Induced by Colon Cancer Cells, *Cell*, 93(5):705–716
- Turner N. and Grose R. (2010) Fibroblast growth factor signalling: from development to cancer, *Nature Reviews Cancer*, 10(2):116–129
- Varinska L., Van Wijhe M., Belleri M., Mitola S., Perjesi P., Presta M., Koolwijk P., Ivanova L. and Mojzis J. (2012) Anti-angiogenic activity of the flavonoid precursor 4-hydroxychalcone, *European Journal of Pharmacology*, 691(1–3):125–133
- Vasudev N S. and Reynolds A R. (2014) Anti-angiogenic therapy for cancer: Current progress, unresolved questions and future directions, *Angiogenesis*, 17(3):471–494

- Verheul H M W. and Pinedo H M. (2007) Possible molecular mechanisms involved in the toxicity of angiogenesis inhibition, *Nature reviews. Cancer*, 7:475–485
- Vilar S., Cozza G. and Moro S. (2008) Medicinal Chemistry and the Molecular Operating Environment (MOE): Application of QSAR and Molecular Docking to Drug Discovery, *Current Topics in Medicinal Chemistry*, 8(18):1555–1572
- Vinay D S., Ryan E P., Pawalec G., Talib W H., Stagg J., Elkord E., Lichtor T., Decker W K., Whelan R L., Kumara H M C S., Signori E., Honoki K., Georgakilas A G., Amin A., Helderich W G., Boosani C S., Guha G., Cirioo M R., Chen S., Mohammed S I., Azmi A S., Keith W N., Bilsland A., Bhakta D., Halicka D., Fujii H., Aquilano K., Ashraf S S., Nowsheen S., Yang X., Choi B K., Kwon B S. (2015) Immune evasion in cancer: Mechanistic basis and therapeutic strategies, *Seminars in Cancer Biology*, 35:185–198
- Visser K E., De, Eichten A. and Coussens L M. (2006) Paradoxical roles of the immune system during cancer development, *Nature reviews. Cancer*, 6:24–37
- Vogelstein B. and Kinzler K W. (2004) Cancer genes and the pathways they control, *Nature Medicine*, 10(8):789–799
- Vosseler S., Mirancea N., Bohlen P., Mueller M M. and Fusenig N E. (2005) Angiogenesis inhibition by vascular endothelial growth factor receptor-2 blockade reduces stromal matrix metalloproteinase expression, normalizes stromal, *Cancer Research*, 65(4):1294-1305
- Wang X., Bullock A J., Zhang L., Wei L., Yu D., Mahagaokar K., Alsop D C., Mier J W., Atkins M B., Coxan A., Oliner J. and Bhatt R S. (2014) The role of angiopoietins as potential therapeutic targets in renal cell carcinoma, *Translational Oncology*, 7(2):188–195

Wang, Z. Daniel Z. (2009) *Comprehensive organic name reactions and reagents*. Hoboken, New Jersey: John Wiley and Sons.

Weidner N., Semple J P., Welch W R and Folkman J. (1991) Tumor angiogenesis and metastasis--correlation in invasive breast carcinoma, *The New England journal of medicine*, 324(1):1-8

Weinberg, R. (2013) *The biology of cancer*. New York: Garland Science

Weinstein I B. and Joe A K. (2006) Mechanisms of Disease: oncogene addiction—a rationale for molecular targeting in cancer therapy, *Nature Clinical Practice Oncology*, 3(8):448-457

Wells A., Grahovac L., Wheeler S., Ma B. and Lauffenburger D. (2013) Targeting tumor cell motility as a strategy against invasion and metastasis, *Trends in pharmacological sciences*, 34(5):283-9

White E. (2012) Deconvoluting the context-dependent role for autophagy in cancer, *Nature Reviews Cancer*, 12(6):401-410

White E. (2015) The role for autophagy in cancer, *The Journal of Clinical Investigation*, 125(1):42-46

WHO (2018) *Cancer* [Online] WHO. Available from: <http://www.who.int/news-room/fact-sheets/detail/cancer> [Accessed: 03/07/18]

Williams D H. and Fleming I. (1995) *Spectroscopic Methods in Organic Chemistry*. Berkshire: McGraw-Hill.

Winkler F., Kozin S V., Tong R T., Chae S S., Booth M F., Garkavtsev I., Xu L., Hicklin D J., Fukumura D., di Tomaso E., Munn L L. and Jain R K. (2004) Kinetics of vascular

- normalization by VEGFR2 blockade governs brain tumor response to radiation: Role of oxygenation, angiopoietin-1, and matrix metalloproteinases, *Cancer Cell*, 6(6):553–563
- Witmer A N., van Blijswijk B C., Dai J., Hofman P., Partanen T A., Vrensen G F., Schlingemann R O. (2001) VEGFR-3 in adult angiogenesis, *The Journal of Pathology*, 195(4):490–497
- Woods J A., Hadfield J A., Pettit G R., Fox B W. and McGown A T. (1995) The interaction with tubulin of a series of stilbenes based on combretastatin A-4, *British journal of cancer*, 71(4):705–11
- Wu P., Nielsen T E. and Clausen M H. (2016) Small-molecule kinase inhibitors: an analysis of FDA-approved drugs, *Drug Discovery Today*, 21:5–10
- Wu X.-F., Neumann H., Spannenberg A., Schulz T., Jiao H., and Beller M. (2010) Development of a General Palladium-Catalyzed Carbonylative Heck Reaction of Aryl Halides, *Journal of the American Chemical Society*, 132(41):14596–14602
- Wuts P G M. (1991) Greene's Protective Groups in Organic Synthesis. Chichester: Wiley and Sons.
- Xu C., Chen G., and Huang X. (1995) CHALCONES BY THE WITTIG REACTION OF A STABLE YLIDE WITH ALDEHYDES UNDER MICROWAVE IRRADIATION. *Organic Preparations and Procedures International*, 27(5):559–561
- Xu X., Wu L., Zhou X., Zhou N., Zhuang Q., Yang J., Dai J., Wang H., Chen S. and Mao W. (2017) Cryptotanshinone inhibits VEGF-induced angiogenesis by targeting the VEGFR2 signaling pathway, *Microvascular Research*, 111:25–31

- Yancopoulos, G D., Davis S., Gale N W., Rudge J S., Wiegand S J. and Holash J. (2000) Vascular-specific growth factors and blood vessel formation, *Nature*, 407(6801):242-248
- Yang, C. S. et al. (2001) Inhibition of carcinogenesis by dietary polyphenolic compounds, *Annual Review of Nutrition*, 21(1):381–406
- Yaswen P., MacKenzie K L., Keith W N., Hentosh P., Rodier F., Zhu J., Firestone G L., Matheu A., Carnero A., Bilsland A., Sundin T., Honoki K., Fujii H., Georgakilas A G., Amedei A., Amin A., Helferich B., Boosani C S., Guha G., Ciriolo M R., Chen S., Mohammed S I., Azmi A S., Bhakta D., Halicka D., Niccolai E., Aquilano K., Ashraf S S., Nowsheen S. and Yang X. (2015) Therapeutic targeting of replicative immortality, *Seminars in cancer biology*, 35:104–128
- Yu H. and Jove R. (2004) The STATs of cancer — new molecular targets come of age, *Nature Reviews Cancer*, 4(2):97–105
- Yusof I., Shah F., Hashimoto T., Segall M D. and Greene N. (2014) Finding the rules for successful drug optimisation, *Drug Discovery Today*, 19(5):680–687
- Zhang E-H., Wang R F., Guo S Z. and Liu B. (2013) An Update on Antitumor Activity of Naturally Occurring Chalcones, *Evidence-Based Complementary and Alternative Medicine*, ID 815621
- Zheng J. and Ramirez V D. (1999) Piceatannol, a Stilbene Phytochemical, Inhibits Mitochondrial F₀F₁-ATPase Activity by Targeting the F₁ Complex, *Biochemical and Biophysical Research Communications*, 261(2)499–503

Zhishen J., Mengchen T. and Jianming, W. (1999) The determination of flavonoid contents in mulberry and their scavenging effects on superoxide radicals, *Food Chemistry*, 64(4):555–559

Zhong Z-F., Hoi P M., Wu G S., Xu Z T., Tan W., Chen X P., Cui L., Wu T. and Wang Y T. (2012) Anti-angiogenic effect of furanodiene on HUVECs *in vitro* and on zebrafish *in vivo*, *Journal of Ethnopharmacology*, 141(2):721–727

